7

Fatigue Failure Resulting from Variable Loading

Chapter Outline

In Chap. 6 we considered the analysis and design of parts subjected to static loading. The behavior of machine parts is entirely different when they are subjected to time-varying loading. In this chapter we shall examine how parts fail under variable loading and how to proportion them to successfully resist such conditions.

7–1 Introduction to Fatigue in Metals

In most testing of those properties of materials that relate to the stress-strain diagram, the load is applied gradually, to give sufficient time for the strain to fully develop. Furthermore, the specimen is tested to destruction, and so the stresses are applied only once. Testing of this kind is applicable, then, to what are known as *static conditions;* such conditions closely approximate the actual conditions to which many structural and machine members are subjected.

The condition frequently arises, however, in which the stresses vary or they fluctuate between levels. For example, a particular fiber on the surface of a rotating shaft subjected to the action of bending loads undergoes both tension and compression for each revolution of the shaft. If the shaft is part of an electric motor rotating at 1725 rev/min, the fiber is stressed in tension and compression 1725 times each minute. If, in addition, the shaft is also axially loaded (as it would be, for example, by a helical or worm gear), an axial component of stress is superposed upon the bending component. In this case, some stress is always present in any one fiber, but now the *level* of stress is fluctuating. These and other kinds of loading occurring in machine members produce stresses that are called *variable, repeated, alternating,* or *fluctuating* stresses.

Often, machine members are found to have failed under the action of repeated or fluctuating stresses; yet the most careful analysis reveals that the actual maximum stresses were well below the ultimate strength of the material, and quite frequently even below the yield strength. The most distinguishing characteristic of these failures is that the stresses have been repeated a very large number of times. Hence the failure is called a *fatigue failure*.

When machine parts fail statically, they usually develop a very large deflection, because the stress has exceeded the yield strength, and the part is replaced before fracture actually occurs. Thus many static failures give visible warning in advance. But a fatigue failure gives no warning! It is sudden and total, and hence dangerous. It is relatively simple to design against a static failure, because our knowledge is comprehensive. Fatigue is a much more complicated phenomenon, only partially understood, and the engineer seeking competence must acquire as much knowledge of the subject as possible.

A fatigue failure has an appearance similar to a brittle fracture, as the fracture surfaces are flat and perpendicular to the stress axis with the absence of necking. The fracture features of a fatigue failure, however, are quite different from a static brittle fracture arising from three stages of development. *Stage I* is the initiation of one or more microcracks due to cyclic plastic deformation followed by crystallographic propagation extending from two to five grains about the origin. Stage I cracks are not normally discernible to the naked eye. *Stage II* progresses from microcracks to macrocracks forming parallel plateau-like fracture surfaces separated by longitudinal ridges. The plateaus are generally smooth and normal to the direction of maximum tensile stress. These surfaces can be wavy dark and light bands referred to as *beach marks* or *clamshell marks,* as seen in Fig. 7–1. During cyclic loading, these cracked surfaces open and close, rubbing together, and the beach mark appearance depends on the changes in the level or frequency of loading and the corrosive nature of the environment. *Stage III* occurs during the final stress cycle when the remaining material cannot support the loads, resulting in a sudden,

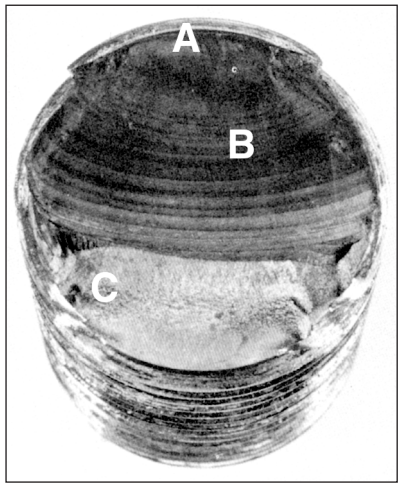

Figure 7–1

Fatigue failure of a bolt due to repeated unidirectional bending. The failure started at the thread root at *A*, propagated across most of the cross section shown by the beach marks at *B*, before final fast fracture at *C*. *(From* ASM Handbook, Vol. 12: Fractography, *ASM International, Materials Park, OH 44073-0002, fig 50, p. 120. Reprinted by permission of ASM International®, www.asminternational.org.)*

fast fracture. A stage III fracture can be brittle, ductile, or a combination of both. Quite often the beach marks, if they exist, and possible patterns in the stage III fracture called *chevron lines,* point toward the origins of the initial cracks.

There is a good deal to be learned from the fracture patterns of a fatigue failure.[1] Figure 7–2 shows representations of failure surfaces of various part geometries under differing load conditions and levels of stress concentration. Note that, in the case of rotational bending, even the direction of rotation influences the failure pattern.

Fatigue failure is due to crack formation and propagation. A fatigue crack will typically initiate at a discontinuity in the material where the cyclic stress is a maximum. Discontinuities can arise because of:

- Design of rapid changes in cross section, keyways, holes, etc. where stress concentrations occur as discussed in Secs. 4–14 and 6–2.
- Elements that roll and/or slide against each other (bearings, gears, cams, etc.) under high contact pressure, developing concentrated subsurface contact stresses (Sec. 4–20) that can cause surface pitting or spalling after many cycles of the load.
- Carelessness in locations of stamp marks, tool marks, scratches, and burrs; poor joint design; improper assembly; and other fabrication faults.
- Composition of the material itself as processed by rolling, forging, casting, extrusion, drawing, heat treatment, etc. Microscopic and submicroscopic surface and subsurface discontinuities arise, such as inclusions of foreign material, alloy segregation, voids, hard precipitated particles, and crystal discontinuities.

Various conditions that can accelerate crack initiation include residual tensile stresses, elevated temperatures, temperature cycling, a corrosive environment, and high-frequency cycling.

The rate and direction of fatigue crack propagation is primarily controlled by localized stresses and by the structure of the material at the crack. However, as with crack formation, other factors may exert a significant influence, such as environment, temperature, and frequency. As stated earlier, cracks will grow along planes normal to the

[1]See the ASM Handbook, *Fractography,* ASM International, Metals Park, Ohio, vol. 12, 9th ed., 1987.

Figure 7–2

Schematics of fatigue fracture surfaces produced in smooth and notched components with round and rectangular cross sections under various loading conditions and nominal stress levels. *(From ASM Handbook, Vol. 11: Failure Analysis and Prevention, ASM International, Materials Park, OH 44073-0002, fig 18, p. 111. Reprinted by permission of ASM International®, www.asminternational.org.)*

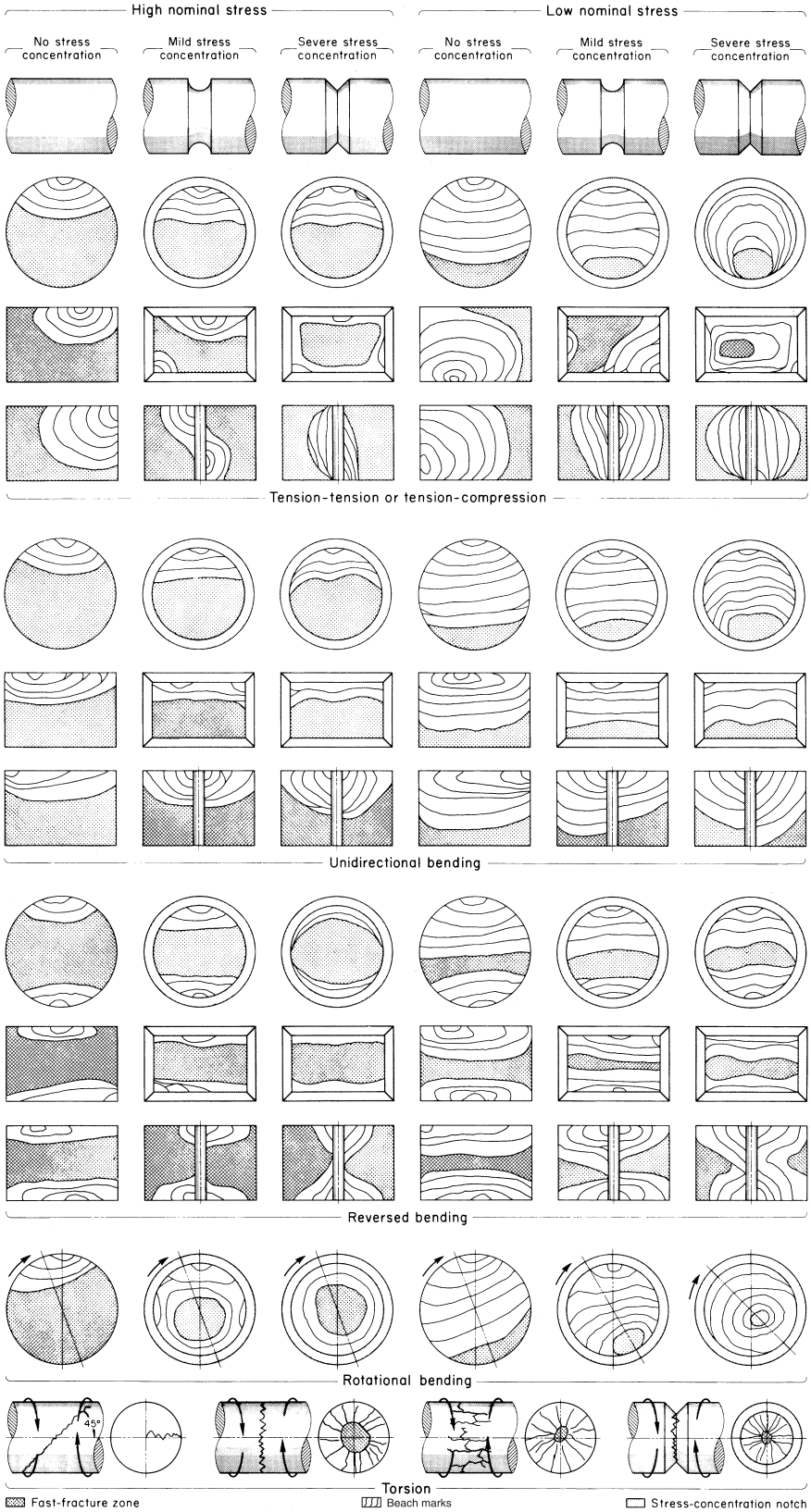

maximum tensile stresses. The crack growth process can be explained by fracture mechanics (see Sec. 7–6).

A major reference source in the study of fatigue failure is the 21-volume ASM *Metals Handbook*. Figures 7–1 to 7–8, reproduced with permission from ASM International, are but a minuscule sample of examples of fatigue failures for a great variety of conditions included in the handbook. Comparing Fig. 7–3 with Fig. 7–2, we see that failure occurred by rotating bending stresses, with the direction of rotation being clockwise with respect to the view and with a mild stress concentration and low nominal stress.

Figure 7–3

Fatigue fracture of an AISI 4320 drive shaft. The fatigue failure initiated at the end of the keyway at points *B* and progressed to final rupture at *C*. The final rupture zone is small, indicating that loads were low. *(From* ASM Handbook, Vol. 11: Failure Analysis and Prevention, *ASM International, Materials Park, OH 44073-0002, fig 18, p. 111. Reprinted by permission of ASM International®, www.asminternational.org.)*

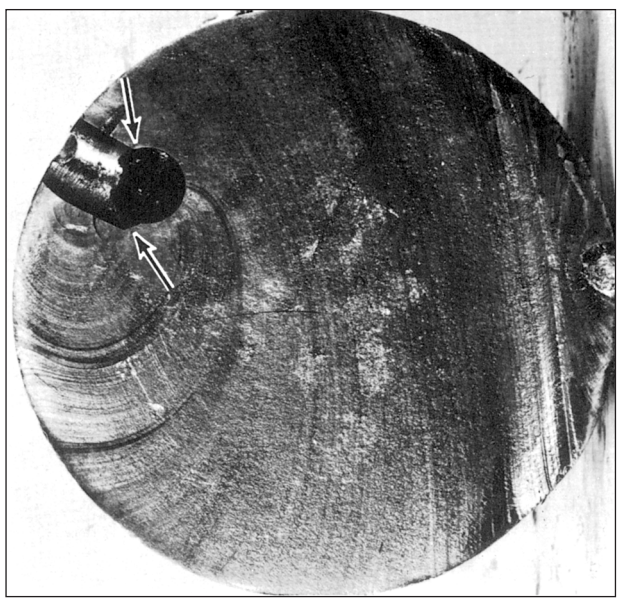

Figure 7–4

Fatigue fracture surface of an AISI 8640 pin. Sharp corners of the mismatched grease holes provided stress concentrations that initiated two fatigue cracks indicated by the arrows. *(From* ASM Handbook, Vol. 12: Fractography, *ASM International, Materials Park, OH 44073-0002, fig 520, p. 331. Reprinted by permission of ASM International®, www.asminternational.org.)*

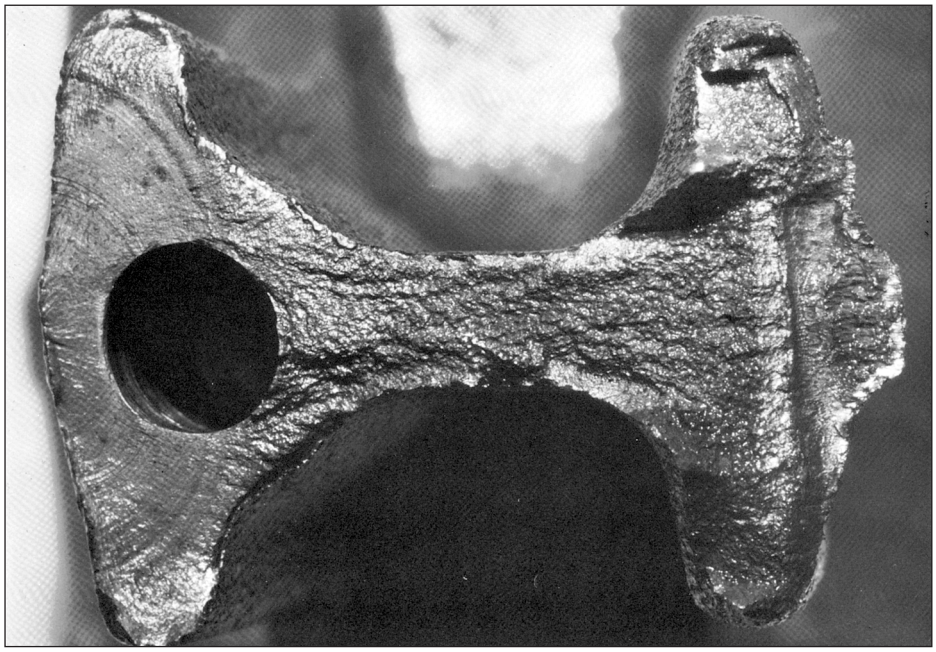

Figure 7–5

Fatigue fracture surface of a forged connecting rod of AISI 8640 steel. The fatigue crack origin is at the left edge, at the flash line of the forging, but no unusual roughness of the flash trim was indicated. The fatigue crack progressed halfway around the oil hole at the left, indicated by the beach marks, before final fast fracture occurred. Note the pronounced shear lip in the final fracture at the right edge. *(From* ASM Handbook, Vol. 12: Fractography, *ASM International, Materials Park, OH 44073-0002, fig 523, p. 332. Reprinted by permission of ASM International®, www.asminternational.org.)*

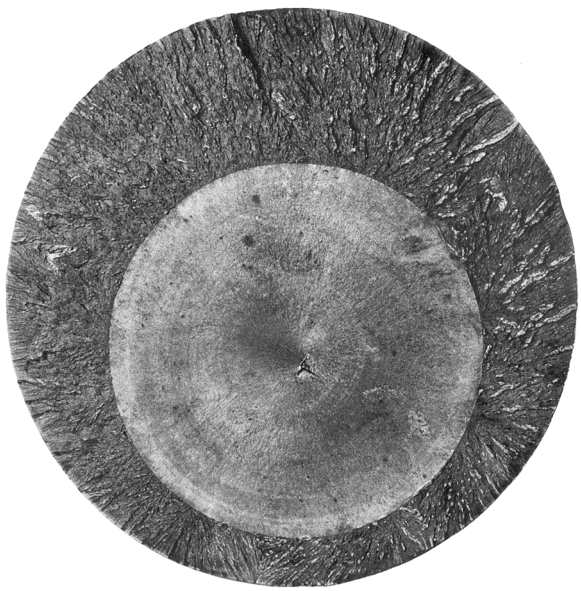

Figure 7–6

Fatigue fracture surface of a 200-mm (8-in) diameter piston rod of an alloy steel steam hammer used for forging. This is an example of a fatigue fracture caused by pure tension where surface stress concentrations are absent and a crack may initiate anywhere in the cross section. In this instance, the initial crack formed at a forging flake slightly below center, grew outward symmetrically, and ultimately produced a brittle fracture without warning. *(From* ASM Handbook, Vol. 12: Fractography, *ASM International, Materials Park, OH 44073-0002, fig 570, p. 342. Reprinted by permission of ASM International®, www.asminternational.org.)*

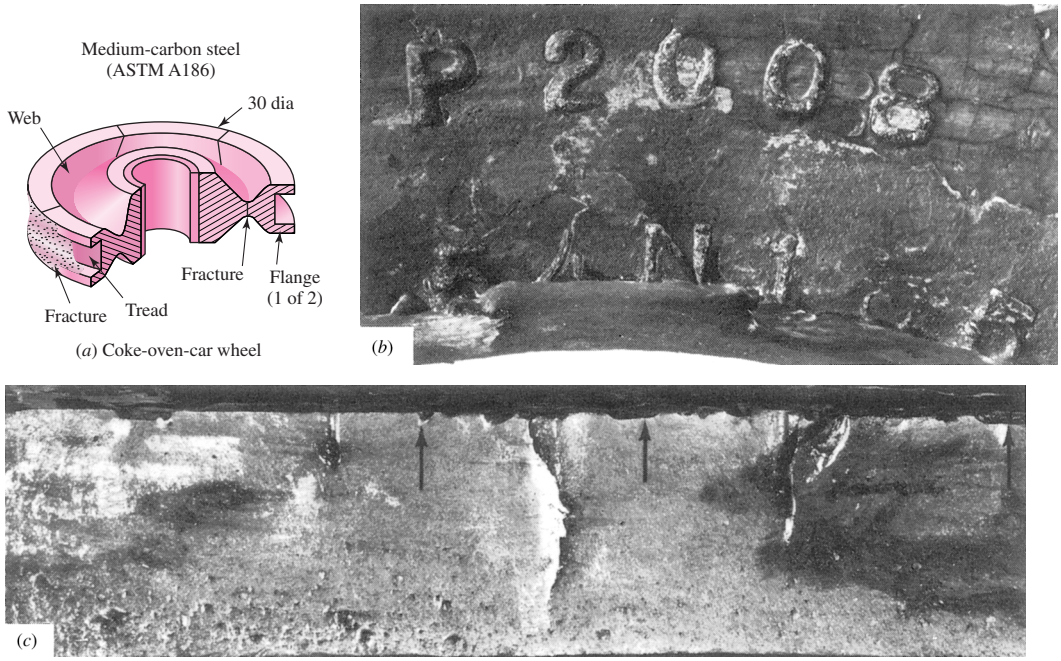

Figure 7–7

Fatigue failure of an ASTM A186 steel double-flange trailer wheel caused by stamp marks. (*a*) Coke-oven car wheel showing position of stamp marks and fractures in the rib and web. (*b*) Stamp mark showing heavy impression and fracture extending along the base of the lower row of numbers. (*c*) Notches, indicated by arrows, created from the heavily indented stamp marks from which cracks initiated along the top at the fracture surface. *(From* ASM Handbook, Vol. 11: Failure Analysis and Prevention, *ASM International, Materials Park, OH 44073-0002, fig 51, p. 130. Reprinted by permission of ASM International®, www.asminternational.org.)*

Figure 7–8

Aluminum alloy 7075-T73 landing-gear torque-arm assembly redesign to eliminate fatigue fracture at a lubrication hole. (*a*) Arm configuration, original and improved design (dimensions given in inches). (*b*) Fracture surface where arrows indicate multiple crack origins. *(From* ASM Handbook, Vol. 11: Failure Analysis and Prevention, *ASM International, Materials Park, OH 44073-0002, fig 23, p. 114. Reprinted by permission of ASM International®, www.asminternational.org.)*

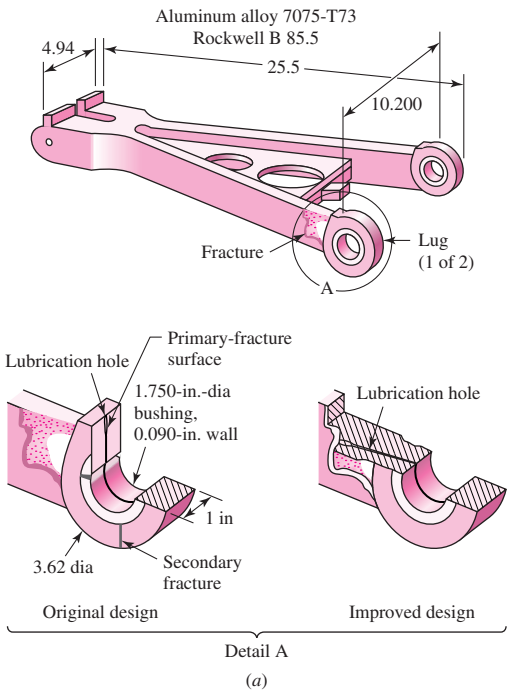

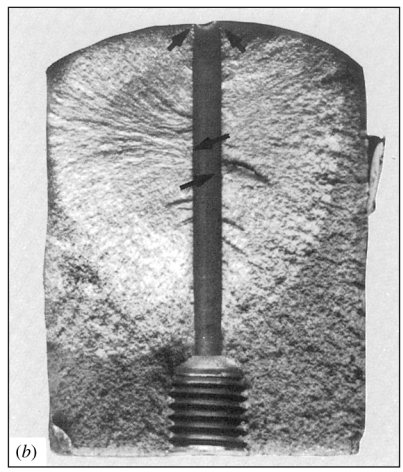

7–2 Approach to Fatigue Failure in Analysis and Design

As noted in the previous section, there are a great many factors to be considered, even for very simple load cases. The methods of fatigue failure analysis represent a combination of engineering and science. Often science fails to provide the complete answers that are needed. But the airplane must still be made to fly—safely. And the automobile must be manufactured with a reliability that will ensure a long and troublefree life and at the same time produce profits for the stockholders of the industry. Thus, while science has not yet completely explained the complete mechanism of fatigue, the engineer must still design things that will not fail. In a sense this is a classic example of the true meaning of engineering as contrasted with science. Engineers use science to solve their problems if the science is available. But available or not, the problem must be solved, and whatever form the solution takes under these conditions is called *engineering*.

In this chapter, we will take a structured approach in the design against fatigue failure. As with static failure, we will attempt to relate to test results performed on simply loaded specimens. However, because of the complex nature of fatigue, there is much more to account for. From this point, we will proceed methodically, and in stages. In an attempt to provide some insight as to what follows in this chapter, a brief description of the remaining sections will be given here.

Fatigue-Life Methods (Secs. 7–3 to 7–6)

Three major approaches used in design and analysis to predict when, if ever, a cyclically loaded machine component will fail in fatigue over a period of time are presented. The premises of each approach are quite different but each adds to our understanding of the mechanisms associated with fatigue. The application, advantages, and disadvantages of each method are indicated. Beyond Sec. 7–6, only one of the methods, the stress-life method, will be pursued for further design applications.

Fatigue Strength and the Endurance Limit (Secs. 7–7 and 7–8)

The strength-life (S-N) diagram provides the fatigue strength S_f versus cycle life N of a material. The results are generated from tests using a simple loading of standard laboratory-controlled specimens. The loading often is that of sinusoidally reversing pure bending. The laboratory-controlled specimens are polished without geometric stress concentration at the region of minimum area.

For steel and iron, the S-N diagram becomes horizontal at some point. The strength at this point is called the *endurance limit* S'_e and occurs somewhere between 10^6 and 10^7 cycles. The prime mark on S'_e refers to the endurance limit of the *controlled laboratory specimen*. For nonferrous materials that do not exhibit an endurance limit, a fatigue strength at a specific number of cycles, S'_f, may be given, where again, the prime denotes the fatigue strength of the laboratory-controlled specimen.

The strength data are based on many controlled conditions that will not be the same as that for an actual machine part. What follows are practices used to account for the differences between the loading and physical conditions of the specimen and the actual machine part.

Endurance Limit Modifying Factors (Sec. 7–9)

Modifying factors are defined and used to account for differences between the specimen and the actual machine part with regard to surface conditions, size, loading, temperature, reliability, and miscellaneous factors. Loading is still considered to be simple and reversing.

Stress Concentration and Notch Sensitivity (Sec. 7–10)

The actual part may have a geometric stress concentration by which the fatigue behavior depends on the static stress concentration factor and the component material's sensitivity to fatigue damage.

Fluctuating Stresses (Secs. 7–11 to 7–13)

These sections account for simple stress states from fluctuating load conditions that are not purely sinusoidally reversing axial, bending, or torsional stresses.

Combinations of Loading Modes (Sec. 7–14)

Here a procedure based on the distortion-energy theory is presented for analyzing combined fluctuating stress states, such as combined bending and torsion. Here it is assumed that the levels of the fluctuating stresses are not time varying.

Varying, Fluctuating Stresses; Cumulative Fatigue Damage (Sec. 7–15)

The fluctuating stress levels on a machine part may be time varying. Methods are provided to assess the fatigue damage on a cumulative basis.

Remaining Sections

The remaining two sections of the chapter pertain to the special topics of surface fatigue strength and stochastic analysis.

7–3 Fatigue-Life Methods

The three major fatigue life methods used in design and analysis are the *stress-life method,* the *strain-life method,* and the *linear-elastic fracture mechanics method*. These methods attempt to predict the life in number of cycles to failure, N, for a specific level of loading. Life of $1 \leq N \leq 10^3$ cycles is generally classified as *low-cycle fatigue,* whereas *high-cycle fatigue* is considered to be $N > 10^3$ cycles. The stress-life method, based on stress levels only, is the least accurate approach, especially for low-cycle applications. However, it is the most traditional method, since it is the easiest to implement for a wide range of design applications, has ample supporting data, and represents high-cycle applications adequately.

The strain-life method involves more detailed analysis of the plastic deformation at localized regions where the stresses and strains are considered for life estimates. This method is especially good for low-cycle fatigue applications. In applying this method, several idealizations must be compounded, and so some uncertainties will exist in the results. For this reason, it will be discussed only because of its value in adding to the understanding of the nature of fatigue.

The fracture mechanics method assumes a crack is already present and detected. It is then employed to predict crack growth with respect to stress intensity. It is most practical when applied to large structures in conjunction with computer codes and a periodic inspection program.

7–4 The Stress-Life Method

To determine the strength of materials under the action of fatigue loads, specimens are subjected to repeated or varying forces of specified magnitudes while the cycles or stress reversals are counted to destruction. The most widely used fatigue-testing device is the R. R. Moore high-speed rotating-beam machine. This machine subjects the specimen

to pure bending (no transverse shear) by means of weights. The specimen, shown in Fig. 7–9, is very carefully machined and polished, with a final polishing in an axial direction to avoid circumferential scratches. Other fatigue-testing machines are available for applying fluctuating or reversed axial stresses, torsional stresses, or combined stresses to the test specimens.

To establish the fatigue strength of a material, quite a number of tests are necessary because of the statistical nature of fatigue. For the rotating-beam test, a constant bending load is applied, and the number of revolutions (stress reversals) of the beam required for failure is recorded. The first test is made at a stress that is somewhat under the ultimate strength of the material. The second test is made at a stress that is less than that used in the first. This process is continued, and the results are plotted as an *S-N* diagram (Fig. 7–10). This chart may be plotted on semilog paper or on log-log paper. In the case of ferrous metals and alloys, the graph becomes horizontal after the material has been stressed for a certain number of cycles. Plotting on log paper emphasizes the bend in the curve, which might not be apparent if the results were plotted by using Cartesian coordinates.

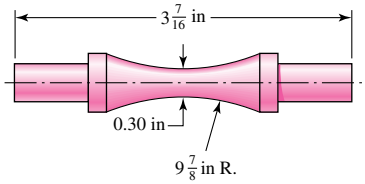

Figure 7–9

Test-specimen geometry for the R. R. Moore rotating-beam machine. The bending moment is uniform over the curved at the highest-stressed portion, a valid test of material, whereas a fracture elsewhere (not at the highest-stress level) is grounds for suspicion of material flaw.

Figure 7–10

An *S-N* diagram plotted from the results of completely reversed axial fatigue tests. Material: UNS G41300 steel, normalized; S_{UT} = 116 kpsi; maximum S_{UT} = 125 kpsi. *(Data from NACA Tech. Note 3866, December 1966.)*

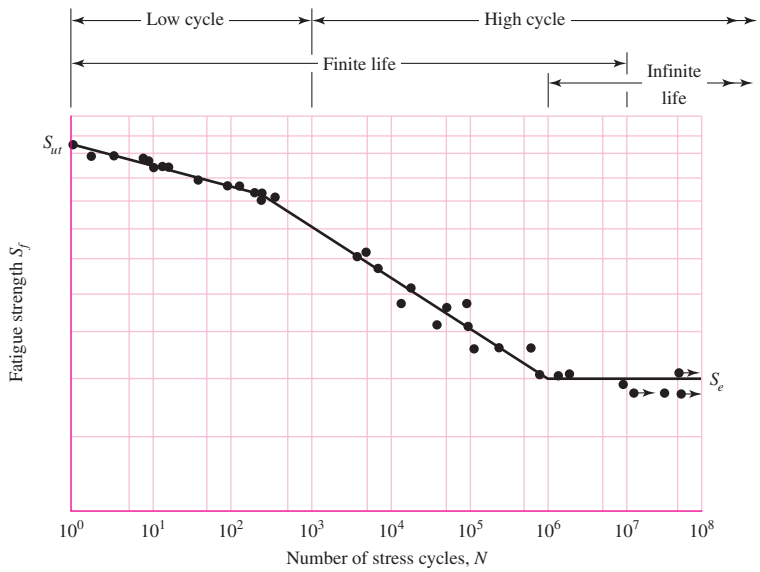

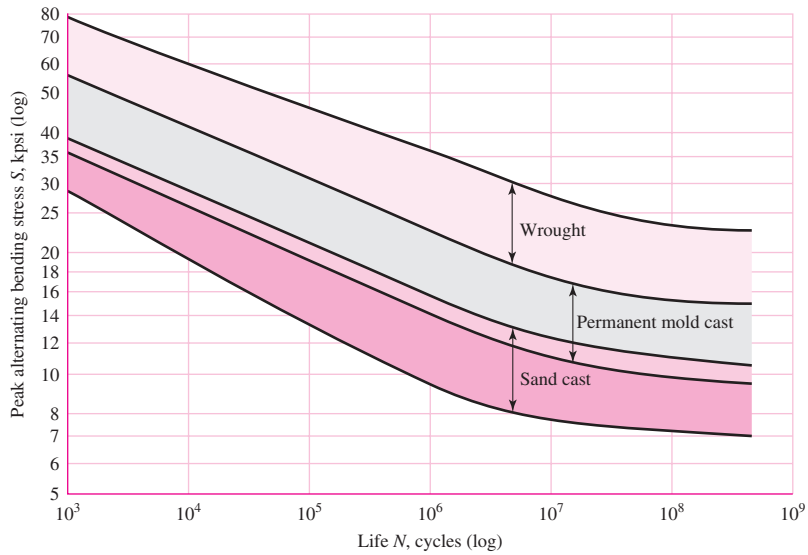

Figure 7–11

S-N bands for representative aluminum alloys, excluding wrought alloys with $S_{ut} < 38$ kpsi. (*From R. C. Juvinall, Engineering Considerations of Stress, Strain and Strength. Copyright © 1967 by The McGraw-Hill Companies, Inc. Reprinted by permission.*)

The ordinate of the *S-N* diagram is called the *fatigue strength* S_f; a statement of this strength value must always be accompanied by a statement of the number of cycles N to which it corresponds.

Soon we shall learn that *S-N* diagrams can be determined either for a test specimen or for an actual mechanical element. Even when the material of the test specimen and that of the mechanical element are identical, there will be significant differences between the diagrams for the two.

In the case of the steels, a knee occurs in the graph, and beyond this knee failure will not occur, no matter how great the number of cycles. The strength corresponding to the knee is called the *endurance limit* S_e, or the fatigue limit. The graph of Fig. 7–10 never does become horizontal for nonferrous metals and alloys, and hence these materials do not have an endurance limit. Figure 7–11 shows scatter bands indicating the *S-N* curves for most common aluminum alloys excluding wrought alloys having a tensile strength below 38 kpsi. Since aluminum does not have an endurance limit, normally the fatigue strength S_f is reported at a specific number of cycles, normally $N = 5(10^8)$ cycles of reversed stress (see Table A–24).

We note that a stress cycle ($N = 1$) constitutes a single application and removal of a load and then another application and removal of the load in the opposite direction. Thus $N = \frac{1}{2}$ means the load is applied once and then removed, which is the case with the simple tension test.

The body of knowledge available on fatigue failure from $N = 1$ to $N = 1000$ cycles is generally classified as *low-cycle fatigue,* as indicated in Fig. 7–10. *High-cycle fatigue,* then, is concerned with failure corresponding to stress cycles greater than 10^3 cycles.

We also distinguish a *finite-life region* and an *infinite-life region* in Fig. 7–10. The boundary between these regions cannot be clearly defined except for a specific material; but it lies somewhere between 10^6 and 10^7 cycles for steels, as shown in Fig. 7–10.

As noted previously, it is always good engineering practice to conduct a testing program on the materials to be employed in design and manufacture. This, in fact, is a requirement, not an option, in guarding against the possibility of a fatigue failure.

Because of this necessity for testing, it would really be unnecessary for us to proceed any further in the study of fatigue failure except for one important reason: the desire to know why fatigue failures occur so that the most effective method or methods can be used to improve fatigue strength. Thus our primary purpose in studying fatigue is to understand why failures occur so that we can guard against them in an optimum manner. For this reason, the analytical design approaches presented in this book, or in any other book, for that matter, do not yield absolutely precise results. The results should be taken as a guide, as something that indicates what is important and what is not important in designing against fatigue failure.

As stated earlier, the stress-life method is the least accurate approach especially for low-cycle applications. However, it is the most traditional method, with much published data available. It is the easiest to implement for a wide range of design applications and represents high-cycle applications adequately. For these reasons the stress-life method will be emphasized in subsequent sections of this chapter. However, care should be exercised when applying the method for low-cycle applications, as the method does not account for the true stress-strain behavior when localized yielding occurs.

7–5 The Strain-Life Method

The best approach yet advanced to explain the nature of fatigue failure is called by some the *strain-life* method. The approach can be used to estimate fatigue strengths, but when it is so used it is necessary to compound several idealizations, and so some uncertainties will exist in the results. For this reason, the method is presented here only because of its value in explaining the nature of fatigue.

A fatigue failure almost always begins at a local discontinuity such as a notch, crack, or other area of stress concentration. When the stress at the discontinuity exceeds the elastic limit, plastic strain occurs. If a fatigue fracture is to occur, there must exist cyclic plastic strains. Thus we shall need to investigate the behavior of materials subject to cyclic deformation.

In 1910, Bairstow verified by experiment Bauschinger's theory that the elastic limits of iron and steel can be changed, either up or down, by the cyclic variations of stress.[2] In general, the elastic limits of annealed steels are likely to increase when subjected to cycles of stress reversals, while cold-drawn steels exhibit a decreasing elastic limit.

Test specimens subjected to reversed bending are not suitable for strain cycling, because of the difficulty of measuring plastic strains. Consequently, most of the research has been done on axial specimens. By using electrical transducers, it is possible to generate signals that are proportional to the stress and strain, respectively. These signals can then be displayed on an oscilloscope or plotted on an *XY* plotter. R. W. Landgraf has investigated the low-cycle fatigue behavior of a large number of very high-strength steels, and during his research he made many cyclic stress-strain plots.[3] Figure 7–12 has been constructed to show the general appearance of these plots for the first few cycles of controlled cyclic strain. In this case the strength decreases with stress repetitions, as evidenced by the fact that the reversals occur at ever-smaller stress levels. As previously noted, other materials may be strengthened, instead, by cyclic stress reversals.

[2]L. Bairstow, "The Elastic Limits of Iron and Steel under Cyclic Variations of Stress," *Philosophical Transactions,* Series A, vol. 210, Royal Society of London, 1910, pp. 35–55.

[3]R. W. Landgraf, *Cyclic Deformation and Fatigue Behavior of Hardened Steels,* Report no. 320, Department of Theoretical and Applied Mechanics, University of Illinois, Urbana, 1968, pp. 84–90.

Figure 7–12

True stress–true strain hysteresis loops showing the first five stress reversals of a cyclic-softening material. The graph is slightly exaggerated for clarity. Note that the slope of the line *AB* is the modulus of elasticity *E*. The stress range is $\Delta\sigma$, $\Delta\varepsilon_p$ is the plastic-strain range, and $\Delta\varepsilon_e$ is the elastic strain range. The total-strain range is $\Delta\varepsilon = \Delta\varepsilon_p + \Delta\varepsilon_e$.

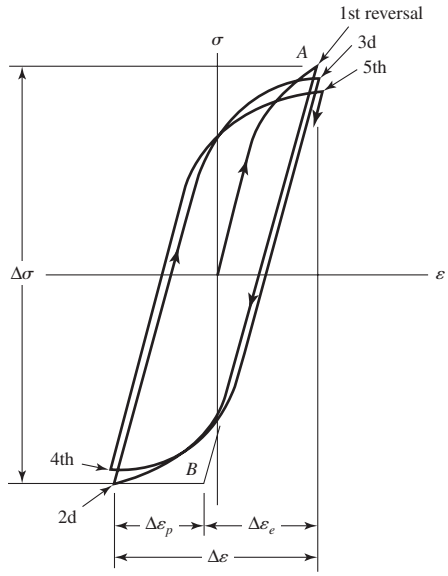

Figure 7–13

Monotonic and cyclic stress-strain results. (*a*) Ausformed H-11 steel, 660 Brinell; (*b*) SAE 4142 steel, 400 Brinell.

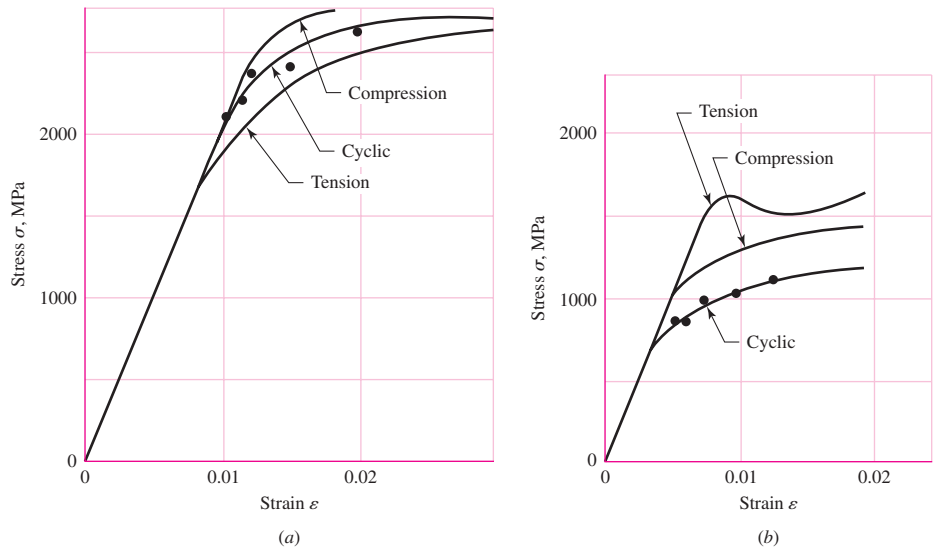

Slightly different results may be obtained if the first reversal occurs in the compressive region; this is probably due to the fatigue-strengthening effect of compression.

Landgraf's paper contains a number of plots that compare the monotonic stress-strain relations in both tension and compression with the cyclic stress-strain curve.[4] Two of these have been redrawn and are shown in Fig. 7–13. The importance of these is that they emphasize the difficulty of attempting to predict the fatigue strength of a material from known values of monotonic yield or ultimate strengths in the low-cycle region.

The SAE Fatigue Design and Evaluation Steering Committee released a report in 1975 in which the life in reversals to failure is related to the strain amplitude $\Delta\varepsilon/2$.[5] The

[4]Ibid., pp. 58–62.

[5]*Technical Report on Fatigue Properties,* SAE J1099, 1975.

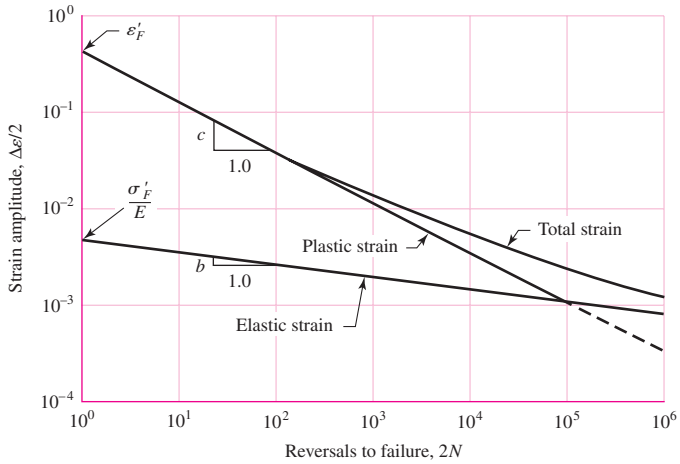

Figure 7–14

A log-log plot showing how the fatigue life is related to the true-strain amplitude for hot-rolled SAE 1020 steel. *(Reprinted with permission from SAE J1099_200208 © 2002 SAE International.)*

report contains a plot of this relationship for SAE 1020 hot-rolled steel; the graph has been reproduced as Fig. 7–14. To explain the graph, we first define the following terms:

- *Fatigue ductility coefficient* ε'_F is the true strain corresponding to fracture in one reversal (point A in Fig. 7–12). The plastic-strain line begins at this point in Fig. 7–14.
- *Fatigue strength coefficient* σ'_F is the true stress corresponding to fracture in one reversal (point A in Fig. 7–12). Note in Fig. 7–14 that the elastic-strain line begins at σ'_F/E.
- *Fatigue ductility exponent* c is the slope of the plastic-strain line in Fig. 7–14 and is the power to which the life $2N$ must be raised to be proportional to the true plastic-strain amplitude. If the number of stress reversals is $2N$, then N is the number of cycles.
- *Fatigue strength exponent* b is the slope of the elastic-strain line, and is the power to which the life $2N$ must be raised to be proportional to the true-stress amplitude.

Now, from Fig. 7–12, we see that the total strain is the sum of the elastic and plastic components. Therefore the total strain amplitude is

$$\frac{\Delta\varepsilon}{2} = \frac{\Delta\varepsilon_e}{2} + \frac{\Delta\varepsilon_p}{2} \tag{a}$$

The equation of the plastic-strain line in Fig. 7–14 is

$$\frac{\Delta\varepsilon_p}{2} = \varepsilon'_F(2N)^c \tag{7–1}$$

The equation of the elastic strain line is

$$\frac{\Delta\varepsilon_e}{2} = \frac{\sigma'_F}{E}(2N)^b \tag{7–2}$$

Therefore, from Eq. (a), we have for the total-strain amplitude

$$\frac{\Delta\varepsilon}{2} = \frac{\sigma'_F}{E}(2N)^b + \varepsilon'_F(2N)^c \tag{7–3}$$

Table 7–1

Cyclic Properties of Some High-Strength Steels *Source:* Data from R. W. Landgraf, *Cyclic Deformation and Fatigue Behavior of Hardened Steels,* Report no. 320, Department of Theoretical and Applied Mechanics, University of Illinois, Urbana, 1968.

AISI Number	Processing	Brinell Hardness H_B	Cyclic Yield Strength S'_y, kpsi	Fatigue Strength Coefficient σ'_F, kpsi	Fatigue Ductility Coefficient ε'_F	Fatigue Strength Exponent b	Fatigue Ductility Exponent c	Fatigue Strain-Hardening Exponent m
1045	Q & T 80°F	705	...	310	...	−0.065	−1.0	0.10
1045	Q & T 360°F	595	250	395	0.07	−0.055	−0.60	0.13
1045	Q & T 500°F	500	185	330	0.25	−0.08	−0.68	0.12
1045	Q & T 600°F	450	140	260	0.35	−0.07	−0.69	0.12
1045	Q & T 720°F	390	110	230	0.45	−0.074	−0.68	0.14
4142	Q & T 80°F	670	300	375	...	−0.075	−1.0	0.05
4142	Q & T 400°F	560	250	385	0.07	−0.076	−0.76	0.11
4142	Q & T 600°F	475	195	315	0.09	−0.081	−0.66	0.14
4142	Q & T 700°F	450	155	290	0.40	−0.080	−0.73	0.12
4142	Q & T 840°F	380	120	265	0.45	−0.080	−0.75	0.14
4142*	Q & D 550°F	475	160	300	0.20	−0.082	−0.77	0.12
4142	Q & D 650°F	450	155	305	0.60	−0.090	−0.76	0.13
4142	Q & D 800°F	400	130	275	0.50	−0.090	−0.75	0.14

*Deformed 14 percent.

which is the Manson-Coffin relationship between fatigue life and total strain.[6] Some values of the coefficients and exponents are listed in Table 7–1. Many more are included in the SAE J1099 report.

Though Eq. (7–3) is a perfectly legitimate equation for obtaining the fatigue life of a part when the strain and other cyclic characteristics are given, it appears to be of little use to the designer. The question of how to determine the total strain at the bottom of a notch or discontinuity has not been answered. There are no tables or charts of strain concentration factors in the literature. It is possible that strain concentration factors will become available in research literature very soon because of the increase in the use of finite-element analysis. Moreover, finite element analysis can of itself approximate the strains that will occur at all points in the subject structure.[7]

7–6 The Linear-Elastic Fracture Mechanics Method

The first phase of fatigue cracking is designated as stage I fatigue. Crystal slip that extends through several contiguous grains, inclusions, and surface imperfections is presumed to play a role. Since most of this is invisible to the observer, we just say that stage I involves

[6] J. F. Tavernelli and L. F. Coffin, Jr., "Experimental Support for Generalized Equation Predicting Low Cycle Fatigue," and S. S. Manson, discussion, *Trans. ASME, J. Basic Eng.,* vol. 84, no. 4, pp. 533–537.

[7] For further discussion of the strain-life method see N. E. Dowling, *Mechanical Behavior of Materials,* 2nd ed., Prentice-Hall, Englewood Cliffs, N.J., 1999, Chap. 14.

several grains. The second phase, that of crack extension, is called stage II fatigue. The advance of the crack (that is, new crack area is created) does produce evidence that can be observed on micrographs from an electron microscope. The growth of the crack is orderly. Final fracture occurs during stage III fatigue, although fatigue is not involved. When the crack is sufficiently long that $K_I = K_{Ic}$ for the stress amplitude involved, then K_{Ic} is the critical stress intensity for the undamaged metal, and there is sudden, catastrophic failure of the remaining cross section in tensile overload (see Sec. 6–13). Stage III fatigue is associated with rapid acceleration of crack growth then fracture.

Crack Growth

Fatigue cracks nucleate and grow when stresses vary and there is some tension in each stress cycle. Consider the stress to be fluctuating between the limits of σ_{min} and σ_{max}, where the stress range is defined as $\Delta\sigma = \sigma_{max} - \sigma_{min}$. From Eq. (6–51) the stress intensity is given by $K_I = \beta\sigma\sqrt{\pi a}$. Thus, for $\Delta\sigma$, the stress intensity range per cycle is

$$\Delta K_I = \beta(\sigma_{max} - \sigma_{min})\sqrt{\pi a} = \beta\Delta\sigma\sqrt{\pi a} \tag{7–4}$$

To develop fatigue strength data, a number of specimens of the same material are tested at various levels of $\Delta\sigma$. Cracks nucleate at or very near a free surface or large discontinuity. Assuming an initial crack length of a_i, crack growth as a function of the number of stress cycles N will depend on $\Delta\sigma$, that is, ΔK_I. For ΔK_I below some threshold value $(\Delta K_I)_{th}$ a crack will not grow. Figure 7–15 represents the crack length a as a function of N for three stress levels $(\Delta\sigma)_3 > (\Delta\sigma)_2 > (\Delta\sigma)_1$, where $(\Delta K_I)_3 > (\Delta K_I)_2 > (\Delta K_I)_1$. Notice the effect of the higher stress range in Fig. 7–15 in the production of longer cracks at a particular cycle count.

When the rate of crack growth per cycle, da/dN in Fig. 7–15, is plotted as shown in Fig. 7–16, the data from all three stress range levels superpose to give a sigmoidal locus. The three stages of crack development are observable, and the stage II data are linear on log-log coordinates, within the domain of linear elastic fracture mechanics (LEFM) validity. A group of similar curves can be generated by changing the stress ratio $R = \sigma_{min}/\sigma_{max}$ of the experiment.

Here we present a simplified procedure for estimating the remaining life of a cyclically stressed part after discovery of a crack. This requires the assumption that plane

Figure 7–15

The increase in crack length a from an initial length of a_i as a function of cycle count for three stress ranges, $(\Delta\sigma)_3 > (\Delta\sigma)_2 > (\Delta\sigma)_1$.

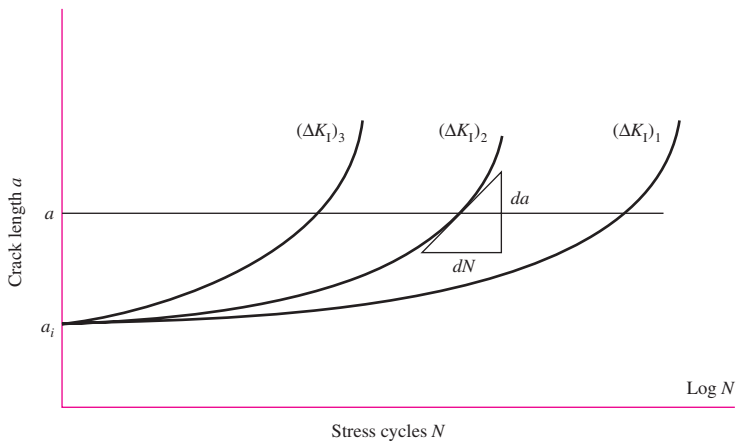

Figure 7–16

When da/dN is measured in Fig. 7–15 and plotted on loglog coordinates, the data for different stress ranges *superpose*, giving rise to a sigmoid curve as shown. $(\Delta K_I)_{th}$ is the threshold value of ΔK_I, below which a crack does not grow. From threshold to rupture an aluminum alloy will spend 85–90 percent of life in region I, 5–8 percent in region II, and 1–2 percent in region III.

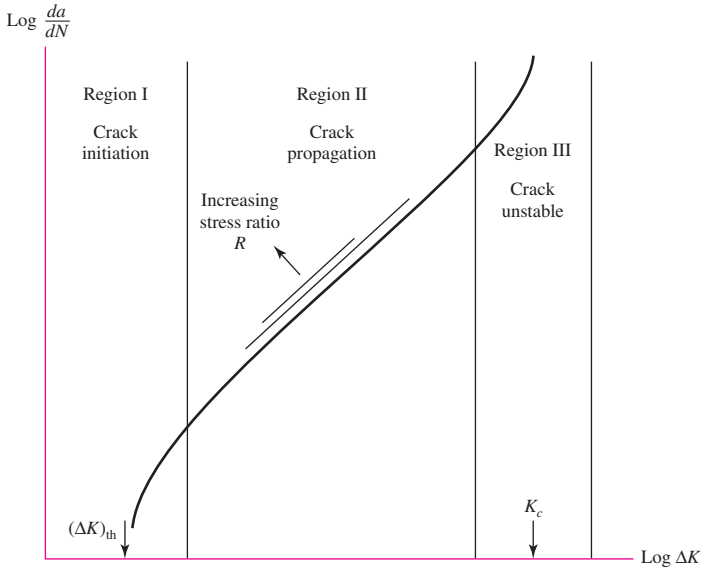

Table 7–2

Conservative Values of Factor C and Exponent m in Eq. (7–5) for Various Forms of Steel ($R \doteq 0$)

Material	C, $\frac{\text{m/cycle}}{(\text{MPa}\sqrt{\text{m}})^m}$	C, $\frac{\text{in/cycle}}{(\text{kpsi}\sqrt{\text{in}})^m}$	m
Ferritic-pearlitic steels	$6.89(10^{-12})$	$3.60(10^{-10})$	3.00
Martensitic steels	$1.36(10^{-10})$	$6.60(10^{-9})$	2.25
Austenitic stainless steels	$5.61(10^{-12})$	$3.00(10^{-10})$	3.25

From J.M. Barsom and S.T. Rolfe, *Fatigue and Fracture Control in Structures, 2nd ed.,* Prentice Hall, Upper Saddle River, NJ, 1987, pp. 288–291, Copyright ASTM International. Reprinted with permission.

strain conditions prevail.[8] Assuming a crack is discovered early in stage II, the crack growth in region II of Fig. 7–16 can be approximated by the *Paris equation,* which is of the form

$$\frac{da}{dN} = C(\Delta K_I)^m \tag{7–5}$$

where C and m are empirical constants and ΔK_I is given by Eq. (7–4). Representative, but conservative, values of C and m for various classes of steels are listed in Table 7–2. Substituting Eq. (7–4) and integrating gives

$$\int_0^{N_f} dN = N_f = \frac{1}{C}\int_{a_i}^{a_f} \frac{da}{(\beta\Delta\sigma\sqrt{\pi a})^m} \tag{7–6}$$

[8]Recommended references are: Dowling, op. cit.; J. A. Collins, *Failure of Materials in Mechanical Design,* John Wiley & Sons, New York, 1981; H. O. Fuchs and R. I. Stephens, *Metal Fatigue in Engineering,* John Wiley & Sons, New York, 1980; and Harold S. Reemsnyder, "Constant Amplitude Fatigue Life Assessment Models," *SAE Trans. 820688,* vol. 91, Nov. 1983.

Here a_i is the initial crack length, a_f is the final crack length corresponding to failure, and N_f is the estimated number of cycles to produce a failure *after* the initial crack is formed. Note that β may vary in the integration variable (e.g., see Figs. 6–35 to 6–40). If this should happen, then Reemsnyder[9] suggests the use of numerical integration employing the algorithm

$$\begin{aligned} \delta a_j &= C(\Delta K_I)_j^m (\delta N)_j \\ a_{j+1} &= a_j + \delta a_j \\ N_{j+1} &= N_j + \delta N_j \\ N_f &= \sum \delta N_j \end{aligned} \tag{7–7}$$

Here δa_j and δN_j are increments of the crack length and the number of cycles. The procedure is to select a value of δN_j, using a_i determine β and compute ΔK_I, determine δa_j, and then find the next value of a. Repeat the procedure until $a = a_f$.

The following example is highly simplified with β constant in order to give some understanding of the procedure. Normally, one uses fatigue crack growth computer programs such as NASA/FLAGRO 2.0 with more comprehensive theoretical models to solve these problems.

[9]Op. cit.

EXAMPLE 7–1 The bar shown in Fig. 7–17 is subjected to a repeated moment $0 \le M \le 1200$ lbf · in. The bar is AISI 4430 steel with $S_{ut} = 185$ kpsi, $S_y = 170$ kpsi, and $K_{Ic} = 74$ kpsi$\sqrt{\text{in}}$. Material tests on various specimens of this material with identical heat treatment indicate worst-case constants of $C = 3.8(10^{-11})(\text{in/cycle})/(\text{kpsi}\sqrt{\text{in}})^m$ and $m = 3.0$. As shown, a nick of size 0.004 in has been discovered on the bottom of the bar. Estimate the number of cycles of life remaining.

Solution The stress range $\Delta\sigma$ is always computed by using the nominal (uncracked) area. Thus

$$\frac{I}{c} = \frac{bh^2}{6} = \frac{0.25(0.5)^2}{6} = 0.0104 \text{ in}^3$$

Therefore, before the crack initiates, the stress range is

$$\Delta\sigma = \frac{\Delta M}{I/c} = \frac{1200}{0.0104} = 115.4(10^3) \text{ psi} = 115.4 \text{ kpsi}$$

which is below the yield strength. As the crack grows, it will eventually become long enough such that the bar will completely yield or undergo a brittle fracture. For the ratio of S_y/S_{ut} it is highly unlikely that the bar will reach complete yield. For brittle fracture,

Figure 7–17

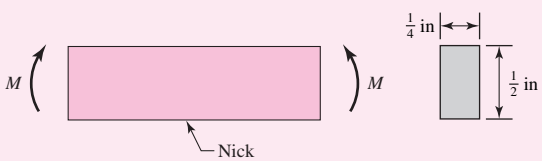

designate the crack length as a_f. If $\beta = 1$, then from Eq. (6–51) with $K_I = K_{Ic}$, we approximate a_f as

$$a_f = \frac{1}{\pi}\left(\frac{K_{Ic}}{\beta\sigma_{max}}\right)^2 \doteq \frac{1}{\pi}\left(\frac{73}{115.4}\right)^2 = 0.127 \text{ in}$$

From Fig. 6–37, we compute the ratio a_f/h as

$$\frac{a_f}{h} = \frac{0.127}{0.5} = 0.254$$

Thus a_f/h varies from near zero to approximately 0.254. From Fig. 6–37, for this range β is nearly constant at approximately 1.07. We will assume it to be so, and re-evaluate a_f as

$$a_f = \frac{1}{\pi}\left(\frac{73}{1.07(115.4)}\right)^2 = 0.111 \text{ in}$$

Thus, from Eq. (7–6), the estimated remaining life is

$$N_f = \frac{1}{C}\int_{a_i}^{a_f} \frac{da}{(\beta\Delta\sigma\sqrt{\pi a})^m} = \frac{1}{3.8(10^{-11})}\int_{0.004}^{0.111} \frac{da}{[1.07(115.4)\sqrt{\pi a}]^3}$$

$$= -\frac{5.02(10^3)}{\sqrt{a}}\Bigg|_{0.004}^{0.111} = 64.3\ (10^3) \text{ cycles}$$

7–7 The Endurance Limit

The determination of endurance limits by fatigue testing is now routine, though a lengthy procedure. Generally, stress testing is preferred to strain testing for endurance limits.

For preliminary and prototype design and for some failure analysis as well, a quick method of estimating endurance limits is needed. There are great quantities of data in the literature on the results of rotating-beam tests and simple tension tests of specimens taken from the same bar or ingot. By plotting these as in Fig. 7–18, it is possible to see whether there is any correlation between the two sets of results. The graph appears to suggest that the endurance limit ranges from about 40 to 60 percent of the tensile strength for steels up to about 212 kpsi (1460 MPa). Beginning at about $S_{ut} = 212$ kpsi (1460 MPa), the scatter appears to increase, but the trend seems to level off, as suggested by the dashed horizontal line at $S'_e = 107$ kpsi (740 MPa).

Another series of tests, this time for various microstructures, is shown in Table 7–3. In this table the endurance limits vary from about 23 to 63 percent of the tensile strength.[10]

Now, it is important to observe that the dispersion of the endurance limit is *not* due to a dispersion in the tensile strengths of the specimen, but rather that the spread occurs even when the tensile strengths of a large number of specimens remain exactly the same. Keep this in mind when choosing factors of safety.

[10]But see H. O. Fuchs and R. I. Stephens, *Metal Fatigue in Engineering,* Wiley, New York, 1980, pp. 69–71, which reports a range of 35 to 60 percent for steels having $S_{ut} < 1400$ MPa and as low as 20 percent for high-strength steels.

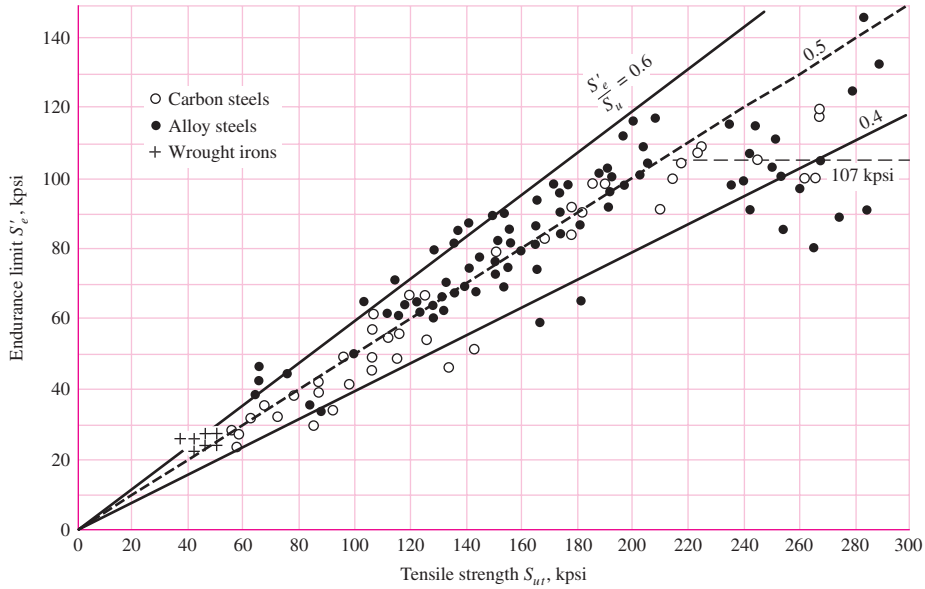

Figure 7–18

Graph of endurance limits versus tensile strengths from actual test results for a large number of wrought irons and steels. Ratios of S'_e/S_{ut} of 0.60, 0.50, and 0.40 are shown by the solid and dashed lines. Note also the horizontal dashed line for $S'_e = 107$ kpsi. Points shown having a tensile strength greater than 214 kpsi have a mean endurance limit of $S'_e = 107$ kpsi and a standard deviation of 13.5 kpsi. *(Collated from data compiled by H. J. Grover, S. A. Gordon, and L. R. Jackson in* Fatigue of Metals and Structures, *Bureau of Naval Weapons Document NAVWEPS 00-25-534, 1960; and from* Fatigue Design Handbook, *SAE, 1968, p. 42.)*

Table 7–3

Endurance-Limit Ratio S'_e/S_{ut} for Various Steel Microstructures

Source: Adapted from L. Sors, *Fatigue Design of Machine Components,* Pergamon Press, Oxford, England, 1971.

	Ferrite		*Pearlite*		*Martensite*	
	Range	**Average**	**Range**	**Average**	**Range**	**Average**
Carbon steel	0.57–0.63	0.60	0.38–0.41	0.40	···	0.25
Alloy steel	···	···	···	···	0.23–0.47	0.35

We wish now to present a method for estimating endurance limits. Note that estimates obtained from quantities of data obtained from many sources probably have a large spread and might deviate significantly from the results of actual laboratory tests of the mechanical properties of specimens obtained through strict purchase-order specifications. Since the area of uncertainty is greater, compensation must be made by employing larger design factors than would be used for static design.

Mischke[11] has analyzed a great deal of actual test data from several sources and concluded that endurance limit can, indeed, be related to tensile strength. For steels, the

[11]Charles R. Mischke, "Prediction of Stochastic Endurance Strength," *Trans. of ASME, Journal of Vibration, Acoustics, Stress, and Reliability in Design,* vol. 109, no. 1, January 1987, pp. 113–122.

relationship is

$$S'_e = \begin{cases} 0.504 S_{ut} \text{ kpsi or MPa} & S_{ut} \le 212 \text{ kpsi } (1460 \text{ MPa}) \\ 107 \text{ kpsi} & S_{ut} > 212 \text{ kpsi} \\ 740 \text{ MPa} & S_{ut} > 1460 \text{ MPa} \end{cases} \tag{7–8}$$

where S_{ut} is the *minimum* tensile strength. The prime mark on S'_e in this equation refers to the *rotating-beam specimen* itself. We wish to reserve the unprimed symbol S_e for the endurance limit of any particular machine element subjected to any kind of loading. Soon we shall learn that the two strengths may be quite different.

The data of Table 7–3 emphasize the difficulty of attempting to provide a single rule for deriving the endurance limit from the tensile strength. The table also shows a part of the cause of this difficulty. Steels treated to give different microstructures have different S'_e/S_{ut} ratios. It appears that the more ductile microstructures have a higher ratio. Martensite has a very brittle nature and is highly susceptible to fatigue-induced cracking; thus the ratio is low. When designs include detailed heat-treating specifications to obtain specific microstructures, it is possible to use an estimate of the endurance limit based on test data for the particular microstructure; such estimates are much more reliable and indeed should be used.

The endurance limits for various classes of cast irons, polished or machined, are given in Table A–24. Aluminum alloys do not have an endurance limit. The fatigue strengths of some aluminum alloys at $5(10^8)$ cycles of reversed stress are given in Table A–24.

7–8 Fatigue Strength

As shown in Fig. 7–10, a region of low-cycle fatigue extends from $N = 1$ to about 10^3 cycles. In this region the fatigue strength S_f is only slightly smaller than the tensile strength S_{ut}. An analytical approach has been given by Mischke[12] for both high-cycle and low-cycle regions, requiring the parameters of the Manson-Coffin equation plus the strain-strengthening exponent m. Engineers often have to work with less information.

Figure 7–10 indicates that the high-cycle fatigue domain extends from 10^3 cycles for steels to the endurance limit life N_e, which is about 10^6 to 10^7 cycles. The purpose of this section is to develop methods of approximation of the S-N diagram in the high-cycle region, when information may be as sparse as the results of a simple tension test. Experience has shown high-cycle fatigue data are rectified by a logarithmic transform to both stress and cycles-to-failure. Engineers can work with Eq. (7–2) in the following way:

$$(S_f)_{10^3 \text{ cycles}} = \sigma'_F (2 \cdot 10^3)^b = f S_{ut}$$

where f is the fraction of S_{ut} represented by $(S_f)_{10^3 \text{ cycles}}$. Solving for f gives

$$f = \frac{\sigma'_F}{S_{ut}} (2 \cdot 10^3)^b \tag{7–9}$$

Now, from Eq. (3–11), $\sigma'_F = \sigma_0 \varepsilon^m$, with $\varepsilon = \varepsilon'_F$. If this true-stress–true-strain equation is not known, the SAE approximation[13] for steels with $H_B \le 500$ may be used:

$$\sigma'_F = S_{ut} + 50 \text{ kpsi} \quad \text{or} \quad \sigma'_F = S_{ut} + 345 \text{ MPa} \tag{7–10}$$

[12] J. E. Shigley and C. R. Mischke, *Standard Handbook of Machine Design,* 2nd ed., McGraw-Hill, New York, 1996, pp. 13.34–13.37.

[13] *Fatigue Design Handbook,* vol. 4, Society of Automotive Engineers, New York, 1958, p. 27.

The exponent b is found from $\sigma_a = S_e = \sigma'_F(2N_e)^b$ as

$$b = -\frac{\log(\sigma'_F/S_e)}{\log(2N_e)} \tag{7–11}$$

Thus the equation $S_f = \sigma'_F(2N)^b$ is known. For example, if $S_{ut} = 105$ kpsi and $S_e = 52.5$ kpsi at 10^6 cycles-to-failure,

$$\sigma'_F = 105 + 50 = 155 \text{ kpsi}$$

$$b = -\frac{\log(155/52.5)}{\log(2 \cdot 10^6)} = -0.0746$$

$$f = \frac{155}{105}(2 \cdot 10^3)^{-0.0746} = 0.837$$

and

$$S_f = 155(2N)^{-0.0746} \tag{a}$$

Empirically, the common curve fit is

$$S_f = aN^b \tag{7–12}$$

where N is cycles to failure and the constants a and b are defined by the points $10^3, (S_f)_{10^3}$ and $10^6, S_e$, with $(S_f)_{10^3} = fS_{ut}$. Substituting these two points in Eq. (7–12) gives

$$a = \frac{(fS_{ut})^2}{S_e} \tag{7–13}$$

$$b = -\frac{1}{3}\log\left(\frac{fS_{ut}}{S_e}\right) \tag{7–14}$$

Continuing the informal example,

$$a = \frac{0.837^2 105^2}{52.5} = 147.1 \text{ kpsi}$$

$$b = -\frac{1}{3}\log\frac{0.837(105)}{52.5} = -0.0746$$

and the resulting equation is

$$S_f = 147.1N^{-0.0746} \tag{b}$$

Note that $2^{-0.0746}(155) = 147.2$, so Eqs. (a) and (b) are really the same. There are popular curve fits with f treated as a constant, normally 0.9, but f varies with S_{ut}. The following table shows the nature of such an approximation:

S_{ut}, kpsi	60	90	120	200
f	0.93	0.86	0.82	0.77

If a completely reversed stress σ_a is given, setting $S_f = \sigma_a$ in Eq. (7–12), the number of cycles-to-failure can be expressed as

$$N = \left(\frac{\sigma_a}{a}\right)^{1/b} \tag{7–15}$$

Low-cycle fatigue is often defined (see Fig. 7–10) as failure that occurs in a range of $1 \le N \le 10^3$ cycles. On a loglog plot such as Fig. 7–10 the failure locus in this range is nearly linear below 10^3 cycles. A straight line between 10^3, $f S_{ut}$ and 1, S_{ut} (transformed) is conservative, and it is given by

$$S_f \ge S_{ut} N^{(\log f)/3} \qquad 1 \le N \le 10^3 \tag{7–16}$$

EXAMPLE 7–2 A 1050 HR steel has an ultimate tensile strength of $S_{ut} = 105$ kpsi and a yield strength of 60 kpsi.
(*a*) Estimate the rotating-beam endurance limit at 10^6 cycles.
(*b*) Estimate the endurance strength for a polished rotating-beam specimen corresponding to 10^4 cycles to failure.
(*c*) Estimate the expected life under a completely reversed stress of 55 kpsi.

Solution (*a*) From Eq. (7–8),

Answer
$$S'_e = 0.504(105) = 52.9 \text{ kpsi}$$

(*b*) From Eq. (7–10),

$$\sigma'_F = 105 + 50 = 155 \text{ kpsi}$$

From Eq. (7–11), with $S_e = S'_e$,

$$b = -\frac{\log(155/52.9)}{\log(2 \cdot 10^6)} = -0.0741$$

From Eq. (7–9),

$$f = \frac{155}{105}(2 \cdot 10^3)^{-0.0741} = 0.840$$

From Eq. (7–13),

$$a = \frac{[(0.840)(105)]^2}{52.9} = 147.1 \text{ kpsi}$$

From Eq. (7–14),

$$b = -\frac{1}{3}\log\left[\frac{0.840(105)}{52.9}\right] = -0.0740$$

$$S_f = 147.2N^{-0.0740}$$

Answer
$$(S_f)_{10^4} = 147.1(10^4)^{-0.0740} = 74.4 \text{ kpsi}$$

(*c*) From Eq. (7–15),

Answer
$$N = \left(\frac{55}{147.1}\right)^{1/-0.0740} = 593\,810 = 5.9(10^5) \text{ cycles}$$

7–9 Endurance Limit Modifying Factors

We have seen that the rotating-beam specimen used in the laboratory to determine endurance limits is prepared very carefully and tested under closely controlled conditions. It is unrealistic to expect the endurance limit of a mechanical or structural member to match the values obtained in the laboratory. Some differences include

- *Material:* composition, basis of failure, variability
- *Manufacturing:* method, heat treatment, fretting corrosion, surface condition, stress concentration
- *Environment:* corrosion, temperature, stress state, relaxation times
- *Design:* size, shape, life, stress state, stress concentration, speed, fretting, galling

Marin[14] identified factors that quantified the effects of surface condition, size, loading, temperature, and miscellaneous items. The question of whether to adjust the endurance limit by subtractive corrections or multiplicative corrections was resolved by an extensive statistical analysis of a 4340 (electric furnace, aircraft quality) steel, in which a correlation coefficient of 0.85 was found for the multiplicative form and 0.40 for the additive form. A Marin equation is therefore written as

$$S_e = k_a k_b k_c k_d k_e k_f S'_e \tag{7–17}$$

where k_a = surface condition modification factor
k_b = size modification factor
k_c = load modification factor
k_d = temperature modification factor
k_e = reliability factor[15]
k_f = miscellaneous-effects modification factor
S'_e = rotary-beam test specimen endurance limit
S_e = endurance limit at the critical location of a machine part in the geometry and condition of use

When endurance tests of parts are not available, estimations are made by applying Marin factors to the endurance limit.

Surface Factor k_a

The surface of a rotating-beam specimen is highly polished, with a final polishing in the axial direction to smooth out any circumferential scratches. The surface modification factor depends on the quality of the finish of the actual part surface and on the tensile strength of the part material. To find quantitative expressions for common finishes of machine parts (ground, machined, or cold-drawn, hot-rolled, and as-forged), the coordinates

[14]Joseph Marin, *Mechanical Behavior of Engineering Materials,* Prentice-Hall, Englewood Cliffs, N.J., 1962, p. 224.

[15]Complete stochastic analysis is presented in Sec. 7–17. Until that point the presentation is one of a deterministic nature. However, we must take care of the known scatter in the fatigue data. This means that we will not carry out a true reliability analysis at this time but will attempt to answer the question: What is the probability that a *known* (assumed) stress will exceed the strength of a randomly selected component made from this material population?

of data points were recaptured from a plot of endurance limit versus ultimate tensile strength of data gathered by Lipson and Noll and reproduced by Horger.[16] The result of regression analysis by Mischke was of the form

$$k_a = aS_{ut}^b \tag{7–18}$$

where S_{ut} is the minimum tensile strength and a and b are to be found in Table 7–4.

Table 7–4

Parameters for Marin Surface Modification Factor, Eq. (7–18)

Surface Finish	Factor a S_{ut}, kpsi	Factor a S_{ut}, MPa	Exponent b
Ground	1.34	1.58	−0.085
Machined or cold-drawn	2.70	4.51	−0.265
Hot-rolled	14.4	57.7	−0.718
As-forged	39.9	272.	−0.995

From C.J. Noll and C. Lipson, "Allowable Working Stresses," *Society for Experimental Stress Analysis,* vol. 3, no. 2, 1946 p. 29. Reproduced by O.J. Horger (eds.) *Metals Engineering Design ASME Handbook,* McGraw-Hill, New York. Copyright © 1953 by The McGraw-Hill Companies, Inc. Reprinted by permission.

EXAMPLE 7–3 A steel has a minimum ultimate strength of 520 MPa and a machined surface. Estimate k_a.

Solution From Table 7–4, $a = 4.51$ and $b = -0.265$. Then, from Eq. (7–18)

$$k_a = 4.51(520)^{-0.265} = 0.860$$

Size Factor k_b

The size factor has been evaluated using 133 sets of data points.[17] The results for bending and torsion may be expressed as

$$k_b = \begin{cases} (d/0.3)^{-0.107} = 0.879d^{-0.107} & 0.11 \le d \le 2 \text{ in} \\ 0.91d^{-0.157} & 2 < d \le 10 \text{ in} \\ (d/7.62)^{-0.107} = 1.24d^{-0.107} & 2.79 \le d \le 51 \text{ mm} \\ 1.51d^{-0.157} & 51 < d \le 254 \text{ mm} \end{cases} \tag{7–19}$$

For axial loading there is no size effect, so

$$k_b = 1 \tag{7–20}$$

but see k_c.

One of the problems that arise in using Eq. (7–19) is what to do when a round bar in bending is not rotating, or when a noncircular cross section is used. For example,

[16] C. J. Noll and C. Lipson, "Allowable Working Stresses," *Society for Experimental Stress Analysis,* vol. 3, no. 2, 1946, p. 29. Reproduced by O. J. Horger (ed.), *Metals Engineering Design ASME Handbook,* McGraw-Hill, New York, 1953, p. 102.

[17] Mischke, op. cit., Table 3.

what is the size factor for a bar 6 mm thick and 40 mm wide? The approach to be used here employs an *effective dimension* d_e obtained by equating the volume of material stressed at and above 95 percent of the maximum stress to the same volume in the rotating-beam specimen.[18] It turns out that when these two volumes are equated, the lengths cancel, and so we need only consider the areas. For a rotating round section, the 95 percent stress area is the area in a ring having an outside diameter d and an inside diameter of $0.95d$. So, designating the 95 percent stress area $A_{0.95\sigma}$, we have

$$A_{0.95\sigma} = \frac{\pi}{4}[d^2 - (0.95d)^2] = 0.0766d^2 \tag{7–21}$$

This equation is also valid for a rotating hollow round. For nonrotating solid or hollow rounds, the 95 percent stress area is twice the area outside of two parallel chords having a spacing of $0.95d$, where d is the diameter. Using an exact computation, this is

$$A_{0.95\sigma} = 0.01046d^2 \tag{7–22}$$

with d_e in Eq. (7–12), setting Eqs. (7–21) and (7–22) equal to each other enables us to solve for the effective diameter. This gives

$$d_e = 0.370d \tag{7–23}$$

as the effective size of a round corresponding to a nonrotating solid or hollow round.

A rectangular section of dimensions $h \times b$ has $A_{0.95\sigma} = 0.05hb$. Using the same approach as before,

$$d_e = 0.808(hb)^{1/2} \tag{7–24}$$

Table 7–5 provides $A_{0.95\sigma}$ areas of common structural shapes undergoing nonrotating bending.

[18]See R. Kuguel, "A Relation between Theoretical Stress Concentration Factor and Fatigue Notch Factor Deduced from the Concept of Highly Stressed Volume," *Proc. ASTM,* vol. 61, 1961, pp. 732–748.

EXAMPLE 7–4 A steel shaft loaded in bending is 32 mm in diameter, abutting a filleted shoulder 38 mm in diameter. The shaft material has a mean ultimate tensile strength of 690 MPa. Estimate the Marin size factor k_b if the shaft is used in

(*a*) A rotating mode.

(*b*) A nonrotating mode.

Solution (*a*) From Eq. (7–19),

Answer
$$k_b = \left(\frac{d}{7.62}\right)^{-0.107} = \left(\frac{32}{7.62}\right)^{-0.107} = 0.858$$

(*b*) From Table 7–5,

$$d_e = 0.37d = 0.37(32) = 11.84 \text{ mm}$$

From Eq. (7–19),

Answer
$$k_b = \left(\frac{11.84}{7.62}\right)^{-0.107} = 0.954$$

Table 7–5

$A_{0.95\sigma}$ Areas of Common Nonrotating Structural Shapes

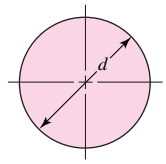	$A_{0.95\sigma} = 0.01046d^2$ $d_e = 0.370d$
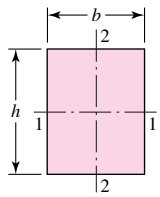	$A_{0.95\sigma} = 0.05hb$ $d_e = 0.808\sqrt{hb}$
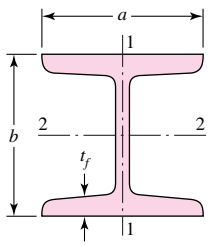	$A_{0.95\sigma} = \begin{cases} 0.10at_f & \text{axis 1-1} \\ 0.05ba \quad t_f > 0.025a & \text{axis 2-2} \end{cases}$
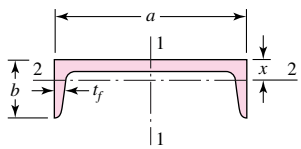	$A_{0.95\sigma} = \begin{cases} 0.05ab & \text{axis 1-1} \\ 0.052xa + 0.1t_f(b-x) & \text{axis 2-2} \end{cases}$

Loading Factor k_c

When fatigue tests are carried out with rotating bending, axial (push-pull), and torsional loading, the endurance limits differ with S_{ut}. This is discussed further in Sec. 7–17. Here, we will specify average values of the load factor as

$$k_c = \begin{cases} 1 & \text{bending} \\ 0.85 & \text{axial} \\ 0.59 & \text{torsion}[19] \end{cases} \tag{7–25}$$

Temperature Factor k_d

When operating temperatures are below room temperature, brittle fracture is a strong possibility and should be investigated first. When the operating temperatures are higher than room temperature, yielding should be investigated first because the yield strength drops off so rapidly with temperature; see Fig. 3–8. Any stress will induce creep in a material operating at high temperatures; so this factor must be considered too. Finally, it may be true that there is no fatigue limit for materials operating at high temperatures. Because of the reduced fatigue resistance, the failure process is, to some extent, dependent on time.

[19]Use this only for pure torsional fatigue loading. When torsion is combined with other stresses, such as bending, $k_c = 1$ and the combined loading is managed by using the effective von Mises stress as in Sec. 6–5. *Note:* For pure torsion, the distortion energy predicts that $(k_c)_{\text{torsion}} = 0.577$.

Table 7–6

Effect of Operating Temperature on the Tensile Strength of Steel.* (S_T = tensile strength at operating temperature; S_{RT} = tensile strength at room temperature; $0.099 \leq \hat{\sigma} \leq 0.110$)

Temperature, °C	S_T/S_{RT}	Temperature, °F	S_T/S_{RT}
20	1.000	70	1.000
50	1.010	100	1.008
100	1.020	200	1.020
150	1.025	300	1.024
200	1.020	400	1.018
250	1.000	500	0.995
300	0.975	600	0.963
350	0.943	700	0.927
400	0.900	800	0.872
450	0.843	900	0.797
500	0.768	1000	0.698
550	0.672	1100	0.567
600	0.549		

Data source: Fig. 3–8.

The limited amount of data available show that the endurance limit for steels increases slightly as the temperature rises and then begins to fall off in the 400 to 700°F range, not unlike the behavior of the tensile strength shown in Fig. 3–8. For this reason it is probably true that the endurance limit is related to tensile strength at elevated temperatures in the same manner as at room temperature.[20] It seems quite logical, therefore, to employ the same relations to predict endurance limit at elevated temperatures as are used at room temperature, at least until more comprehensive data become available. At the very least, this practice will provide a useful standard against which the performance of various materials can be compared.

Table 7–6 has been obtained from Fig. 3–8 by using only the tensile-strength data. Note that the table represents 145 tests of 21 different carbon and alloy steels. A fourth-order polynomial curve fit to the data underlying Fig. 3–8 gives

$$k_d = 0.975 + 0.432(10^{-3})T_F - 0.115(10^{-5})T_F^2 + 0.104(10^{-8})T_F^3 - 0.595(10^{-12})T_F^4 \qquad (7\text{–}26)$$

where $70 \leq T_F \leq 1000$°F.

Two types of problems arise when temperature is a consideration. If the rotating-beam endurance limit is known at room temperature, then use

$$k_d = \frac{S_T}{S_{RT}} \qquad (7\text{–}27)$$

from Table 7–6 or Eq. (7–26) and proceed as usual. If the rotating-beam endurance limit is not given, then compute it using Eq. (7–8) and the temperature-corrected tensile strength obtained by using the factor from Table 7–6. Then use $k_d = 1$.

[20]For more, see Table 2 of ANSI/ASME B106. 1M-1985 shaft standard, and E. A. Brandes (ed.), *Smithell's Metals Reference Book,* 6th ed., Butterworth, London, 1983, pp. 22–134 to 22–136, where endurance limits from 100 to 650°C are tabulated.

EXAMPLE 7–5 A 1035 steel has a tensile strength of 70 kpsi and is to be used for a part that sees 450°F in service. Estimate the Marin temperature modification factor and $(S_e)_{450^\circ}$ if
(*a*) The room-temperature endurance limit by test is $(S'_e)_{70^\circ} = 39.0$ kpsi.
(*b*) Only the tensile strength at room temperature is known.

Solution (*a*) First, from Eq. (7–26),

$$k_d = 0.975 + 0.432(10^{-3})(450) - 0.115(10^{-5})(450^2) + 0.104(10^{-8})(450^3) - 0.595(10^{-12})(450^4) = 1.007$$

Thus,

Answer $$(S_e)_{450^\circ} = k_d(S'_e)_{70^\circ} = 1.007(39.0) = 39.3 \text{ kpsi}$$

(*b*) Interpolating from Table 7–6 gives

$$(S_T/S_{RT})_{450^\circ} = 1.018 + (0.995 - 1.018)\frac{450 - 400}{500 - 400} = 1.007$$

Thus, the tensile strength at 450°F is estimated as

$$(S_{ut})_{450^\circ} = (S_T/S_{RT})_{450^\circ}(S_{ut})_{70^\circ} = 1.007(70) = 70.5 \text{ kpsi}$$

From Eq. (7–8) then,

Answer $$(S_e)_{450^\circ} = 0.504\,(S_{ut})_{450^\circ} = 0.504(70.5) = 35.5 \text{ kpsi}$$

Part *a* gives the better estimate due to actual testing of the particular material.

Reliability Factor k_e

The discussion presented here accounts for the scatter of data such as shown in Fig. 7–18 where the mean endurance limit is shown to be $S'_e/S_{ut} \doteq 0.5$, or as given by Eq. (7–8). Most endurance strength data are reported as mean values. Data presented by Haugen and Wirching[21] show standard deviations of endurance strengths of less than 8 percent. Thus the reliability modification factor to account for this can be written as

$$k_e = 1 - 0.08\,z_a \tag{7–28}$$

where z_a is defined by Eq. (2–16) and values for any desired reliability can be determined from Table A–10. Table 7–7 gives reliability factors for some standard specified reliabilities.

For a more comprehensive approach to reliability, see Sec. 7–17.

Miscellaneous-Effects Factor k_f

Though the factor k_f is intended to account for the reduction in endurance limit due to all other effects, it is really intended as a reminder that these must be accounted for, because actual values of k_f are not always available.

Residual stresses may either improve the endurance limit or affect it adversely. Generally, if the residual stress in the surface of the part is compression, the endurance

[21] E. B. Haugen and P. H. Wirsching, "Probabilistic Design," *Machine Design,* vol. 47, no. 12, 1975, pp. 10–14.

Table 7–7

Reliability Factors k_e Corresponding to 8 Percent Standard Deviation of the Endurance Limit

Reliability, %	Transformation Variate z_a	Reliability Factor k_e
50	0	1.000
90	1.288	0.897
95	1.645	0.868
99	2.326	0.814
99.9	3.091	0.753
99.99	3.719	0.702
99.999	4.265	0.659
99.9999	4.753	0.620

Figure 7–19

The failure of a case-hardened part in bending or torsion. In this example, failure occurs in the core.

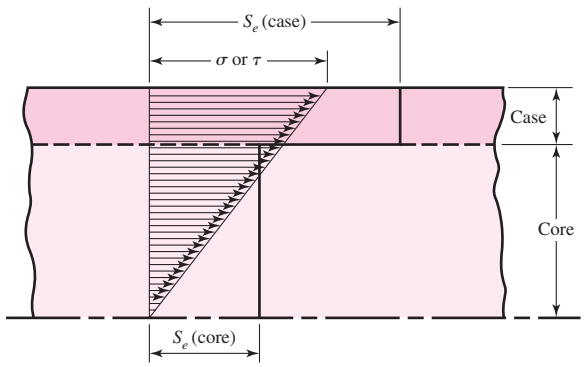

limit is improved. Fatigue failures appear to be tensile failures, or at least to be caused by tensile stress, and so anything that reduces tensile stress will also reduce the possibility of a fatigue failure. Operations such as shot peening, hammering, and cold rolling build compressive stresses into the surface of the part and improve the endurance limit significantly. Of course, the material must not be worked to exhaustion.

The endurance limits of parts that are made from rolled or drawn sheets or bars, as well as parts that are forged, may be affected by the so-called *directional characteristics* of the operation. Rolled or drawn parts, for example, have an endurance limit in the transverse direction that may be 10 to 20 percent less than the endurance limit in the longitudinal direction.

Parts that are case-hardened may fail at the surface or at the maximum core radius, depending upon the stress gradient. Figure 7–19 shows the typical triangular stress distribution of a bar under bending or torsion. Also plotted as a heavy line in this figure are the endurance limits S_e for the case and core. For this example the endurance limit of the core rules the design because the figure shows that the stress σ or τ, whichever applies, at the outer core radius, is appreciably larger than the core endurance limit.

Of course, if stress concentration is also present, the stress gradient is much steeper, and hence failure in the core is unlikely.

Corrosion

It is to be expected that parts that operate in a corrosive atmosphere will have a lowered fatigue resistance. This is, of course, true, and it is due to the roughening or pitting of the surface by the corrosive material. But the problem is not so simple as the one of finding

the endurance limit of a specimen that has been corroded. The reason for this is that the corrosion and the stressing occur at the same time. Basically, this means that in time any part will fail when subjected to repeated stressing in a corrosive atmosphere. There is no fatigue limit. Thus the designer's problem is to attempt to minimize the factors that affect the fatigue life; these are:

- Mean or static stress
- Alternating stress
- Electrolyte concentration
- Dissolved oxygen in electrolyte
- Material properties and composition
- Temperature
- Cyclic frequency
- Fluid flow rate around specimen
- Local crevices

Electrolytic Plating

Metallic coatings, such as chromium plating, nickel plating, or cadmium plating, reduce the endurance limit by as much as 50 percent. In some cases the reduction by coatings has been so severe that it has been necessary to eliminate the plating process. Zinc plating does not affect the fatigue strength. Anodic oxidation of light alloys reduces bending endurance limits by as much as 39 percent but has no effect on the torsional endurance limit.

Metal Spraying

Metal spraying results in surface imperfections that can initiate cracks. Limited tests show reductions of 14 percent in the fatigue strength.

Cyclic Frequency

If, for any reason, the fatigue process becomes time-dependent, then it also becomes frequency-dependent. Under normal conditions, fatigue failure is independent of frequency. But when corrosion or high temperatures, or both, are encountered, the cyclic rate becomes important. The slower the frequency and the higher the temperature, the higher the crack propagation rate and the shorter the life at a given stress level.

Frettage Corrosion

The phenomenon of frettage corrosion is the result of microscopic motions of tightly fitting parts or structures. Bolted joints, bearing-race fits, wheel hubs, and any set of tightly fitted parts are examples. The process involves surface discoloration, pitting, and eventual fatigue. The frettage factor k_f depends upon the material of the mating pairs and ranges from 0.24 to 0.90.

7–10 Stress Concentration and Notch Sensitivity

In Sec. 4–14 it was pointed out that the existence of irregularities or discontinuities, such as holes, grooves, or notches, in a part increases the theoretical stresses significantly in the immediate vicinity of the discontinuity. Equation (4–48) defined a stress concentration factor K_t (or K_{ts}), which is used with the nominal stress to obtain the maximum resulting stress due to the irregularity or defect. It turns out that some materials are not

fully sensitive to the presence of notches and hence, for these, a reduced value of K_t can be used. For these materials, the maximum stress is, in fact,

$$\sigma_{\max} = K_f \sigma_0 \qquad \text{or} \qquad \tau_{\max} = K_{fs} \tau_0 \tag{7–29}$$

where K_f is a reduced value of K_t and σ_0 is the nominal stress. The factor K_f is commonly called a *fatigue stress-concentration factor,* and hence the subscript f. So it is convenient to think of K_f as a stress-concentration factor reduced from K_t because of lessened sensitivity to notches. The resulting factor is defined by the equation

$$K_f = \frac{\text{maximum stress in notched specimen}}{\text{stress in notch-free specimen}} \tag{a}$$

Notch sensitivity q is defined by the equation

$$q = \frac{K_f - 1}{K_t - 1} \qquad \text{or} \qquad q_{\text{shear}} = \frac{K_{fs} - 1}{K_{ts} - 1} \tag{7–30}$$

where q is usually between zero and unity. Equation (7–30) shows that if $q = 0$, then $K_f = 1$, and the material has no sensitivity to notches at all. On the other hand, if $q = 1$, then $K_f = K_t$, and the material has full notch sensitivity. In analysis or design work, find K_t first, from the geometry of the part. Then specify the material, find q, and solve for K_f from the equation

$$K_f = 1 + q(K_t - 1) \qquad \text{or} \qquad K_{fs} = 1 + q_{\text{shear}}(K_{ts} - 1) \tag{7–31}$$

For steels and 2024 aluminum alloys, use Fig. 7–20 to find q for bending and axial loading. For shear loading, use Fig. 7–21. In using these charts it is well to know that the actual test results from which the curves were derived exhibit a large amount of scatter. Because of this scatter it is always safe to use $K_f = K_t$ if there is any doubt about the true value of q. Also, note that q is not far from unity for large notch radii.

The notch sensitivity of the cast irons is very low, varying from 0 to about 0.20, depending upon the tensile strength. To be on the conservative side, it is recommended that the value $q = 0.20$ be used for all grades of cast iron.

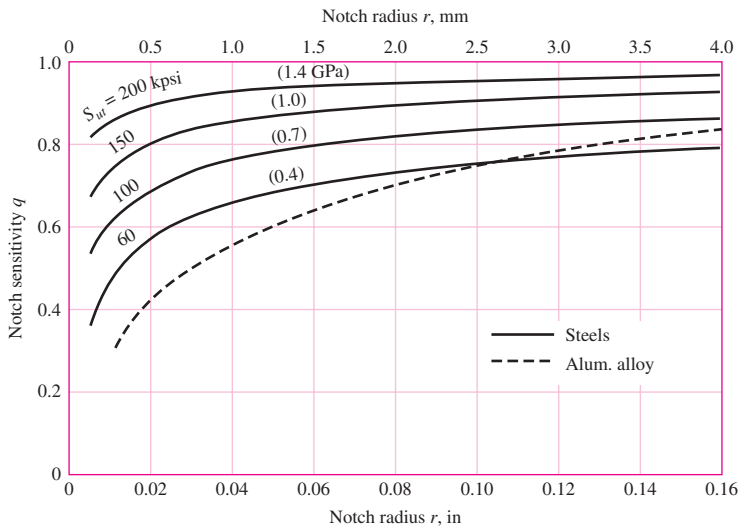

Figure 7–20

Notch-sensitivity charts for steels and UNS A92024-T wrought aluminum alloys subjected to reversed bending or reversed axial loads. For larger notch radii, use the values of q corresponding to the $r = 0.16$-in (4-mm) ordinate. *(From George Sines and J. L. Waisman (eds.), Metal Fatigue, McGraw-Hill, New York. Copyright © 1969 by The McGraw-Hill Companies, Inc. Reprinted by permission.)*

Figure 7–21

Notch-sensitivity curves for materials in reversed torsion. For larger notch radii, use the values of q_{shear} corresponding to $r = 0.16$ in (4 mm).

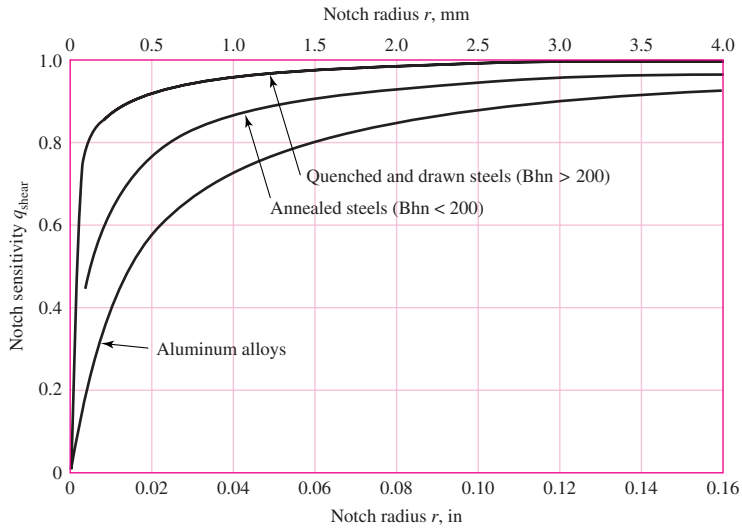

Figure 7–20 has as its basis the *Neuber equation,* which is given by

$$K_f = 1 + \frac{K_t - 1}{1 + \sqrt{a/r}} \tag{7–32}$$

where $\sqrt{a}$ is defined as the *Neuber constant* and is a material constant. Equating Eqs. (7–30) and (7–32) yields the notch sensitivity equation

$$q = \frac{1}{1 + \dfrac{\sqrt{a}}{\sqrt{r}}} \tag{7–33}$$

For steel, with S_{ut} in kpsi, the Neuber constant can be approximated by a third-order polynomial fit of data as

$$\begin{aligned}\sqrt{a} = {} & 0.245\,799 - 0.307\,794(10^{-2})S_{ut} \\ & + 0.150\,874(10^{-4})S_{ut}^2 - 0.266\,978(10^{-7})S_{ut}^3\end{aligned} \tag{7–34}$$

To use Eq. (7–32) or (7–33) for torsion for low-alloy steels, increase the ultimate strength by 20 kpsi in Eq. (7–34) and apply this value of $\sqrt{a}$.

A distinction in the configuration of the notch is accounted for in the modified Neuber equation (after Heywood), where the fatigue stress-concentration factor K_f is given as

$$K_f = \frac{K_t}{1 + \dfrac{2(K_t - 1)}{K_t}\dfrac{\sqrt{a}}{\sqrt{r}}} \tag{7–35}$$

where Table 7–8 gives values of $\sqrt{a}$ for steels for transverse holes, shoulders, and grooves.

Table 7–8

Heywood's Parameter $\sqrt{a}$ for Steels

Feature	$\sqrt{a}\,(\sqrt{\text{in}})$, S_{ut} in kpsi	$\sqrt{a}\,(\sqrt{\text{mm}})$, S_{ut} in MPa
Transverse hole	$5/S_{ut}$	$174/S_{ut}$
Shoulder	$4/S_{ut}$	$139/S_{ut}$
Groove	$3/S_{ut}$	$104/S_{ut}$

EXAMPLE 7–6 A steel shaft in bending has an ultimate strength of 690 MPa and a shoulder with a fillet radius of 3 mm connecting a 32-mm diameter with a 38-mm diameter. Estimate K_f using:
(*a*) Figure 7–20.
(*b*) Equations (7–32) and (7–34).
(*c*) Equation (7–35).

Solution From Fig. A–15–9, using $D/d = 38/32 = 1.1875, r/d = 3/32 = 0.093\,75$, we read the graph to find $K_t \doteq 1.65$.
(*a*) From Fig. 7–20, for $S_{ut} = 690$ MPa and $r = 3$ mm, $q \doteq 0.84$. Thus, from Eq. (7–31)

$$K_f = 1 + q(K_t - 1) \doteq 1 + 0.84(1.65 - 1) = 1.55$$

(*b*) From Eq. (7–34) with $S_{ut} = 690$ MPa $= 100$ kpsi, $\sqrt{a} = 0.062\sqrt{\text{in}} = 0.312\sqrt{\text{mm}}$. Substituting this into Eq. (7–32) with $r = 3$ mm gives

$$K_f = 1 + \frac{K_t - 1}{1 + \sqrt{a/r}} \doteq 1 + \frac{1.65 - 1}{1 + \dfrac{0.312}{\sqrt{3}}} = 1.55$$

(*c*) From Table 7–8,

$$\sqrt{a} = \frac{139}{S_{ut}} = \frac{139}{690} = 0.2015\ \sqrt{\text{mm}}$$

From Eq. (7–35),

$$K_f = \frac{K_t}{1 + \dfrac{2(K_t - 1)}{K_t}\dfrac{\sqrt{a}}{\sqrt{r}}} = \frac{1.65}{1 + \dfrac{2(1.65 - 1)}{1.65}\dfrac{0.2015}{\sqrt{3}}} = 1.51$$

which is 2.5 percent lower than in parts *a* and *b*.

For simple loading, it is acceptable to reduce the endurance limit by either dividing the unnotched specimen endurance limit by K_f or multiplying the reversing stress by K_f. However, in dealing with combined stress problems that may involve more than one value of fatigue-concentration factor, the stresses are multiplied by K_f.

EXAMPLE 7–7 Consider an unnotched specimen with an endurance limit of 55 kpsi. If the specimen was notched such that $K_f = 1.6$, what would be the factor of safety against failure for $N > 10^6$ cycles at a reversing stress of 30 kpsi?
(*a*) Solve by reducing S'_e.
(*b*) Solve by increasing the applied stress.

Solution (*a*) The endurance limit of the notched specimen is given by

$$S_e = \frac{S'_e}{K_f} = \frac{55}{1.6} = 34.4\ \text{kpsi}$$

and the factor of safety is

$$n = \frac{S_e}{\sigma_a} = \frac{34.4}{30} = 1.15$$

(*b*) The maximum stress can be written as

$$(\sigma_a)_{\max} = K_f \sigma_a = 1.6(30) = 48.0 \text{ kpsi}$$

and the factor of safety is

$$n = \frac{S'_e}{K_f \sigma_a} = \frac{55}{48} = 1.15$$

When cycles to failure, N_f, are less than 10^6 there is experimental evidence that the fatigue stress-concentration factor $(K_f)_{N_f}$ is less than K_f. Studies have shown that as N_f approaches 10^3 cycles, $(K_f)_{N_f}$ for high-strength (usually low-ductility) metals approaches K_f, whereas for low-strength (usually ductile) metals $(K_f)_{N_f}$ approaches unity. A conservative approach is to keep K_f constant within the range $10^3 \le N \le 10^6$. To account for a reduction in K_f, Shigley and Mischke[22] suggest defining a notch sensitivity at 10^3 cycles, q_{10^3}, given by

$$q_{10^3} = \frac{(K_f)_{10^3} - 1}{K_f - 1} = -0.18 + 0.43(10^{-2})S_{ut} - 0.45(10^{-5})S_{ut}^2 \qquad (7\text{–}36)$$

where S_{ut} is in kpsi, $S_{ut} < 330$ kpsi, and K_f is the fatigue stress-concentration factor for 10^6 cycles. Solving for $(K_f)_{10^3}$ yields

$$(K_f)_{10^3} = 1 - (K_f - 1)\left[0.18 - 0.43(10^{-2})S_{ut} + 0.45(10^{-5})S_{ut}^2\right] \qquad (7\text{–}37)$$

Assuming a straight-line loglog *S-N* plot for the notched specimen from $f S_{ut}/(K_f)_{10^3}$, 10^3 to S'_e/K_f, 10^6 gives for $S_f/(K_f)_N$, N

$$(K_f)_N = \frac{(K_f)_{10^3}^2}{K_f} N^{(1/3)\log[K_f/(K_f)_{10^3}]} \qquad (7\text{–}38)$$

[22] J. E. Shigley and C. R. Mischke, *Mechanical Engineering Design,* 6th ed., McGraw-Hill, New York, 2001, p. 386–387.

EXAMPLE 7–8 Using the results of Ex. 7–6, find the value of $(K_f)_{10^5}$.

Solution From Ex. 7–6, $K_f = 1.51$ (part c), $S_{ut} = 690/6.89 = 100$ kpsi. From Eq. (7–37),

$$\begin{aligned}(K_f)_{10^3} &= 1 - (K_f - 1)\left[0.18 - 0.43(10^{-2})S_{ut} + 0.45(10^{-5})S_{ut}^2\right] \\ &= 1 - (1.51 - 1)[0.18 - 0.43(10^{-2})100 + 0.45(10^{-5})100^2] \\ &= 1.105\end{aligned}$$

From Eq. (7–38),

Answer
$$(K_f)_{10^3} = \frac{1.105^2}{1.51} 10^{5(1/3)\log(1.51/1.105)} = 1.36$$

Up to this point, examples illustrated each factor in Marin's equation and stress concentrations alone. Let us consider a number of factors occurring simultaneously.

EXAMPLE 7–9 A 1015 hot-rolled steel bar has been machined to a diameter of 1 in. It is to be placed in reversed axial loading for 70 000 cycles to failure in an operating environment of 550°F. Using ASTM minimum properties, and a reliability of 99 percent, estimate the endurance limit and fatigue strength at 70 000 cycles.

Solution From Table A–20, $S_{ut} = 50$ kpsi at 70°F. Since the rotating-beam specimen endurance limit is not known at room temperature, we determine the ultimate strength at the elevated temperature first, using Table 7–6. From Table 7–6,

$$\left(\frac{S_T}{S_{RT}}\right)_{550^\circ} = \frac{0.995 + 0.963}{2} = 0.979$$

The ultimate strength at 550°F is then

$$(S_{ut})_{550^\circ} = (S_T/S_{RT})_{550^\circ}\,(S_{ut})_{70^\circ} = 0.979(50) = 49.0 \text{ kpsi}$$

The rotating-beam specimen endurance limit at 550°F is then estimated from Eq. (7–8) as

$$S'_e = 0.504(49) = 24.7 \text{ kpsi}$$

Next, we determine the Marin factors. For the machined surface, Eq. (7–18) with Table 7–4 gives

$$k_a = aS_{ut}^b = 2.70(49^{-0.265}) = 0.963$$

For axial loading, from Eq. (7–20), the size factor $k_b = 1$, and the loading factor is $k_c = 0.85$, from Eq. (7–25). The temperature factor $k_d = 1$, since we accounted for the temperature in modifying the ultimate strength and consequently the endurance limit. For 99 percent reliability, from Table 7–7, $k_e = 0.814$. Finally, since no other conditions were given, the miscellaneous factor is $k_f = 1$. The endurance limit for the part is estimated by Eq. (7–17) as

Answer
$$\begin{aligned} S_e &= k_a k_b k_c k_d k_e k_f S'_e \\ &= 0.963(1)(0.85)(1)(0.814)(1)24.7 = 16.5 \text{ kpsi} \end{aligned}$$

For the fatigue strength at 70 000 cycles we need to construct the *S-N* equation. From Sec. 7–8, Eq. (7–10),

$$\sigma'_F = 49 + 50 = 99 \text{ kpsi}$$

From Eq. (7–11),

$$b = -\frac{\log(\sigma'_F/S_e)}{\log(2N_e)} = -\frac{\log(99/16.5)}{\log(2 \cdot 10^6)} = -0.1235$$

Equation (7–9) then gives

$$f = \frac{\sigma'_F}{S_{ut}}(2 \cdot 10^3)^b = \frac{99}{49}(2 \cdot 10^3)^{-0.1235} = 0.790$$

From Eq. (7–13),

$$a = \frac{(f S_{ut})^2}{S_e} = \frac{[0.790(49)]^2}{16.5} = 90.8 \text{ kpsi}$$

Finally, Eq. (7–12) gives

Answer

$$S_f = aN^b = 90.8(70\,000)^{-0.1235} = 22.9 \text{ kpsi}$$

EXAMPLE 7–10

Figure 7–22*a* shows a rotating axle simply supported in ball bearings at *A* and *D* and loaded by a nonrotating force *F* of 6.8 kN. Using ASTM "minimum" strengths, estimate the life of the part.

Solution

From Fig. 7–22*b* we learn that failure will probably occur at *B* rather than at *C* or at the point of maximum moment. Point *B* has a smaller cross section, a higher bending moment, and a higher stress-concentration factor than *C*, and the location of maximum moment has a larger size and no stress-concentration factor.

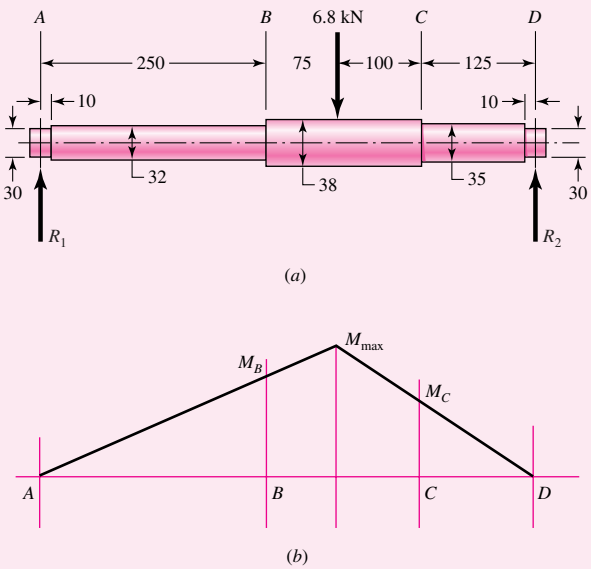

Figure 7–22

(*a*) Shaft drawing showing all dimensions in millimeters; all fillets 3-mm radius. The shaft rotates and the load is stationary; material is machined from AISI 1050 cold-drawn steel. (*b*) Bending-moment diagram.

We shall solve the problem by first estimating the strength at point B, since the strength will be different elsewhere, and comparing this strength with the stress at the same point.

From Table A–20 we find $S_{ut} = 690$ MPa and $S_y = 580$ MPa. The endurance limit S'_e is estimated as

$$S'_e = 0.504(690) = 347.8 \text{ MPa}$$

From Eq. (7–18) and Table 7–4,

$$k_a = 4.51(690)^{-0.265} = 0.798$$

From Eq. (7–19),

$$k_b = (32/7.62)^{-0.107} = 0.858$$

Since $k_c = k_d = k_e = k_f = 1$,

$$S_e = 0.798(0.858)347.8 = 238 \text{ MPa}$$

To find the geometric stress-concentration factor K_t we enter Fig. A–15–9 with $D/d = 38/32 = 1.1875$ and $r/d = 3/32 = 0.093\,75$ and read $K_t \doteq 1.65$. From Table 7–8, $\sqrt{a} = 139/690 = 0.201\ \sqrt{\text{mm}}$. From Eq. (7–35),

$$K_f = \frac{K_t}{1 + \dfrac{2(K_t - 1)}{K_t}\dfrac{\sqrt{a}}{\sqrt{r}}} \doteq \frac{1.65}{1 + \dfrac{2(1.65 - 1)}{1.65}\dfrac{0.201}{\sqrt{3}}} = 1.51$$

This stress-concentration factor applies to 10^6 cycles or more.

The next step is to estimate the bending stress at point B. The bending moment is

$$M_B = R_1 x = \frac{225F}{550}250 = \frac{225(6.8)}{550}250 = 695 \text{ N} \cdot \text{m}$$

Just to the left of B the section modulus is $I/c = \pi d^3/32 = \pi 3.2^3/32 = 3.22$ cm^3. The reversing bending stress is, assuming infinite life,

$$\sigma = K_f \frac{M_B}{I/c} = 1.51\frac{695}{3.22} = 325.9 \text{ MPa}$$

This stress is greater than S_e and less than S_y. This means we have both finite life and no yielding on the first cycle. There are two approaches we may take at this point. The first, conservative, approach is to assume that K_f is constant regardless of N. The second approach is to use Eq. (7–38). We will see that for this problem, approach 1 is far easier.

Approach 1. From Eq. (7–10),

$$\sigma'_F = S_{ut} + 345 = 690 + 345 = 1035 \text{ MPa}$$

From Eq. (7–11),

$$b = -\frac{\log(\sigma'_F/S_e)}{\log(2N_e)} = -\frac{\log(1035/238)}{\log(2 \cdot 10^6)} = -0.1013$$

From Eq. (7–9),

$$f = \frac{\sigma'_F}{S_{ut}}(2 \cdot 10^3)^b = \frac{1035}{690}(2 \cdot 10^3)^{-0.1013} = 0.695$$

From Eq. (7–13),

$$a = \frac{(fS_{ut})^2}{S_e} = \frac{[0.695(690)]^2}{238} = 966.3 \text{ MPa}$$

Answer (Approach 1)

From Eq. (7–15),

$$N = \left(\frac{\sigma_a}{a}\right)^{1/b} = \left(\frac{325.9}{966.3}\right)^{-1/0.1013} = 45.7(10^3) \text{ cycles}$$

Approach 2. Using Eq. (7–38) requires a value of N, which is unknown. Because we don't know K_N, instead of applying the fatigue stress-concentration factor to stress σ we will reduce the strengths in the S-N diagram by the factor. Note that this approach is not advisable for combined stress problems. The nominal stress is

$$\sigma_{\text{nom}} = \frac{M_B}{I/c} = \frac{695}{3.22} = 215.8 \text{ MPa}$$

From Eq. (7–37), with $S_{ut} = 690/6.9 = 100$ kpsi,

$$\begin{aligned}(K_f)_{10^3} &= 1 - (K_f - 1)\left[0.18 - 0.43(10^{-2})S_{ut} + 0.45(10^{-5})S_{ut}^2\right] \\ &= 1 - (1.51 - 1)[0.18 - 0.43(10^{-2})100 + 0.45(10^{-5})100^2] \\ &= 1.105\end{aligned}$$

The S-N equation incorporating the fatigue stress-concentration factor can be written as $N = (\sigma_a/a')^{1/b'}$, where in form similar to that of Eqs. (7–13) and (7–14),

$$a' = \frac{[f S_{ut}/(K_f)_{10^3}]^2}{S_e/K_f} = a\frac{K_f}{(K_f)_{10^3}^2} = 966.3\frac{1.51}{1.105^2} = 1195 \text{ MPa}$$

$$b' = -\frac{1}{3}\log\left[\frac{f S_{ut}/(K_f)_{10^3}}{S_e/K_f}\right] = b - \frac{1}{3}\log\frac{K_f}{(K_f)_{10^3}}$$

$$= -0.1013 - \frac{1}{3}\log\frac{1.51}{1.105} = -0.147$$

where use of a and b from approach 1 was used. The number of cycles can now be determined from Eq. (7–15) as

Answer (Approach 2)

$$N = \left(\frac{\sigma_a}{a'}\right)^{1/b'} = \left(\frac{215.8}{1195}\right)^{-1/0.147} = 113.9(10^3) \text{ cycles}$$

We see that approach 1 is indeed more conservative than approach 2, by a factor of 2.5. This is the effect of a logarithmic scale. Approach 2 predicts a fatigue stress-concentration factor according to Eq. (7–38) of

$$\begin{aligned}(K_f)_{113.9(10^3)} &= \frac{(K_f)_{10^3}^2}{K_f} N^{(1/3)\log[K_f/(K_f)_{10^3}]} \\ &= \frac{1.105^2}{1.51}[113.9(10^3)]^{(1/3)\log(1.51/1.105)} = 1.37\end{aligned}$$

Without any further knowledge of the behavior of the material given, one might select the solution of approach 1. However, if it is known that K_f approaches unity for 10^3 cycles for this material, then approach 2 would be appropriate.

7–11 Characterizing Fluctuating Stresses

Fluctuating stresses in machinery often take the form of a sinusoidal pattern because of the nature of some rotating machinery. However, other patterns, some quite irregular, do occur. It has been found that in periodic patterns exhibiting a single maximum and a single minimum of force, the shape of the wave is not important, but the peaks on both the high side (maximum) and the low side (minimum) are important. Thus $F_{\max}$ and $F_{\min}$ in a cycle of force can be used to characterize the force pattern. It is also true that ranging above and below some baseline can be equally effective in characterizing the force pattern. If the largest force is $F_{\max}$ and the smallest force is $F_{\min}$, then a steady component and an alternating component can be constructed as follows:

$$F_m = \frac{F_{\max} + F_{\min}}{2} \qquad F_a = \left| \frac{F_{\max} - F_{\min}}{2} \right|$$

where F_m is the midrange component of force, and F_a is the amplitude component of force.

Figure 7–23 illustrates some of the various stress-time traces that occur. The components of stress, some of which are shown in Fig. 7–23*d*, are

$\sigma_{\min}$ = minimum stress
$\sigma_{\max}$ = maximum stress
σ_a = amplitude component
σ_m = midrange component
σ_r = range of stress
σ_s = static or steady stress

Figure 7–23

Some stress-time relations: (*a*) fluctuating stress with high-frequency ripple; (*b* and *c*) nonsinusoidal fluctuating stress; (*d*) sinusoidal fluctuating stress; (*e*) repeated stress; (*f*) completely reversed sinusoidal stress.

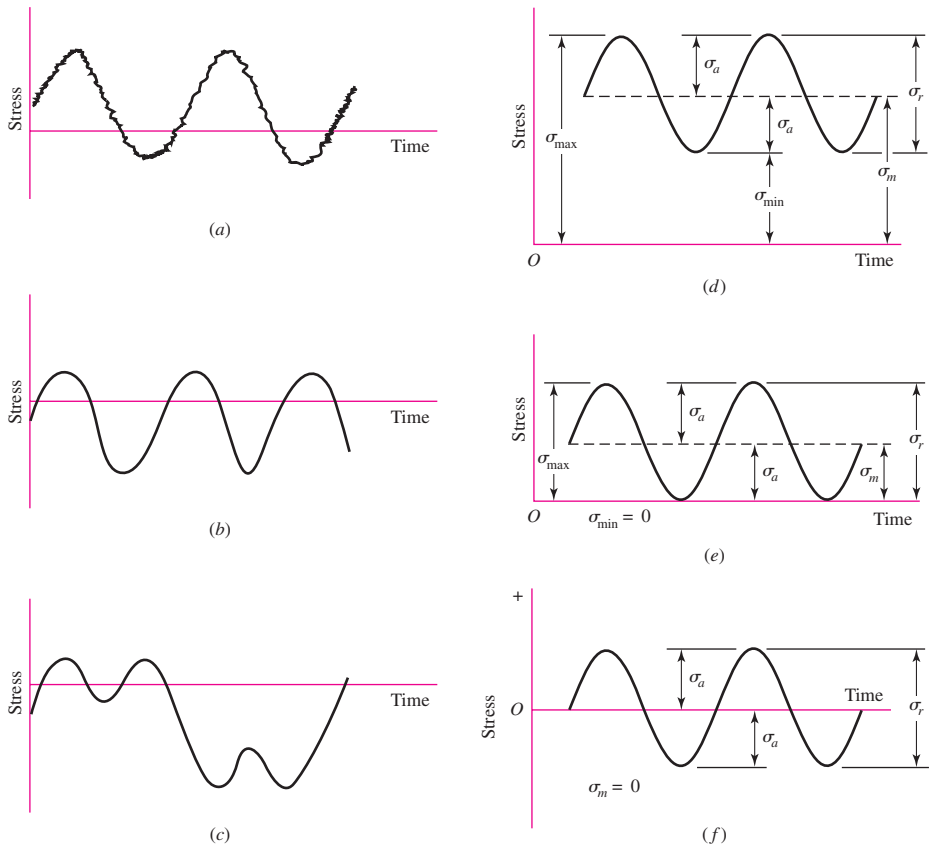

The steady, or static, stress is *not* the same as the midrange stress; in fact, it may have any value between $\sigma_{\min}$ and $\sigma_{\max}$. The steady stress exists because of a fixed load or preload applied to the part, and it is usually independent of the varying portion of the load. A helical compression spring, for example, is always loaded into a space shorter than the free length of the spring. The stress created by this initial compression is called the steady, or static, component of the stress. It is not the same as the midrange stress.

We shall have occasion to apply the subscripts of these components to shear stresses as well as normal stresses.

The following relations are evident from Fig. 7–23:

$$\sigma_m = \frac{\sigma_{\max} + \sigma_{\min}}{2}$$
$$\sigma_a = \left| \frac{\sigma_{\max} - \sigma_{\min}}{2} \right| \tag{7–39}$$

In addition to Eq. (7–39), the *stress ratio*

$$R = \frac{\sigma_{\min}}{\sigma_{\max}} \tag{7–40}$$

and the stress ratio

$$A = \frac{\sigma_a}{\sigma_m} \tag{7–41}$$

are also defined and used in connection with fluctuating stresses.

Equations (7–39) utilize symbols σ_a and σ_m as the stress components at the location under scrutiny. This means, in the absence of a notch, σ_a and σ_m are equal to the nominal stresses σ_{ao} and σ_{mo} induced by loads F_a and F_m, respectively; in the presence of a notch they are $K_f\sigma_{ao}$ and $K_f\sigma_{mo}$, respectively, as long as the material remains without plastic strain. In other words, the fatigue stress concentration factor K_f is applied to *both* components.

When the steady stress component is high enough to induce localized notch yielding, the designer has a problem. The first-cycle local yielding produces plastic strain and strain-strengthening. This is occurring at the location where fatigue crack nucleation and growth are most likely. The material properties (S_y and S_{ut}) are new and difficult to quantify. The prudent engineer controls the concept, material and condition of use, and geometry so that no plastic strain occurs. There are discussions concerning possible ways of quantifying what is occurring under localized and general yielding in the presence of a notch, referred to as the *nominal mean stress* method, *residual stress* method, and the like.[23] The nominal mean stress method (set $\sigma_a = K_f\sigma_{ao}$ and $\sigma_m = \sigma_{mo}$) gives roughly comparable results to the residual stress method, but both are *approximations*.

There is the method of Dowling[24] for ductile material, which, for materials with a pronounced yield point and approximated by an elastic–perfectly plastic behavior

[23]R. C. Juvinall, *Stress, Strain, and Strength,* McGraw-Hill, New York, 1967, articles 14.9–14.12; R. C. Juvinall and K. M. Marshek, *Fundamentals of Machine Component Design,* Wiley, New York, 1991, Sec. 8.11; M. E. Dowling, *Mechanical Behavior of Materials,* 2nd ed., Prentice Hall, Englewood Cliffs, N.J., 1999, Secs. 10.3–10.5.

[24]Dowling, op. cit., p. 437–438.

model, quantitatively expresses the steady stress component stress-concentration factor K_{fm} as

$$\begin{aligned} K_{fm} &= K_f & K_f|\sigma_{\max,o}| &< S_y \\ K_{fm} &= \frac{S_y - K_f\sigma_{ao}}{|\sigma_{mo}|} & K_f|\sigma_{\max,o}| &> S_y \\ K_{fm} &= 0 & K_f|\sigma_{\max,o} - \sigma_{\min,o}| &> 2S_y \end{aligned} \tag{7–42}$$

For the purposes of this book, for ductile materials in fatigue,

- Avoid localized plastic strain at a notch. Set $\sigma_a = K_f\sigma_{a,o}$ and $\sigma_m = K_f\sigma_{mo}$.
- When plastic strain at a notch cannot be avoided, use Eqs. (7–42); or conservatively, set $\sigma_a = K_f\sigma_{ao}$ and use $K_{mf} = 1$, that is, $\sigma_m = \sigma_{mo}$.

7–12 Fatigue Failure Criteria for Fluctuating Stress

Now that we have defined the various components of stress associated with a part subjected to fluctuating stress, we want to vary both the midrange stress and the stress amplitude, or alternating component, to learn something about the fatigue resistance of parts when subjected to such situations. Three methods of plotting the results of such tests are in general use and are shown in Figs. 7–24, 7–25, and 7–26.

The *modified Goodman diagram* of Fig. 7–24 has the midrange stress plotted along the abscissa and all other components of stress plotted on the ordinate, with tension in the positive direction. The endurance limit, fatigue strength, or finite-life strength, whichever applies, is plotted on the ordinate above and below the origin. The midrange-stress line is a 45° line from the origin to the tensile strength of the part. The modified Goodman diagram consists of the lines constructed to S_e (or S_f) above and below the

Figure 7–24

Modified Goodman diagram showing all the strengths and the limiting values of all the stress components for a particular midrange stress.

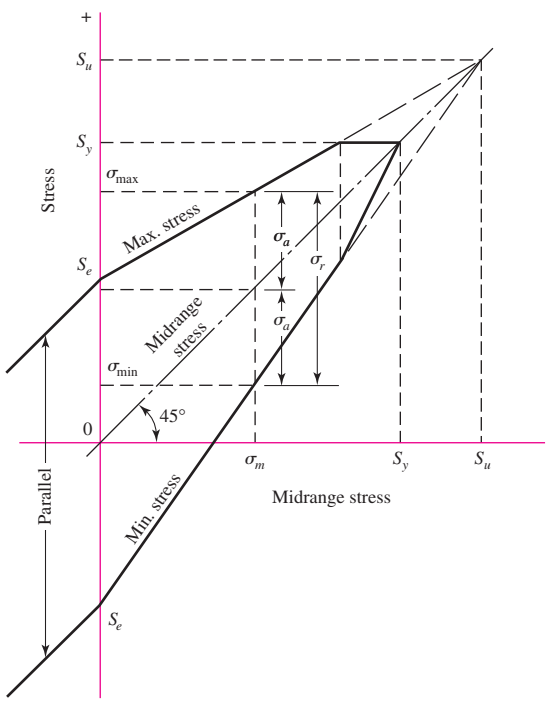

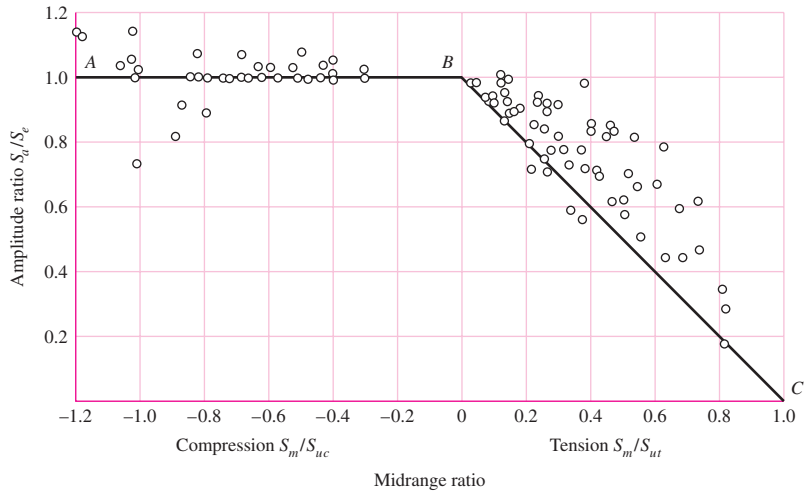

Figure 7–25

Plot of fatigue failures for midrange stresses in both tensile and compressive regions. Normalizing the data by using the ratio of steady strength component to tensile strength S_m/S_{ut}, steady strength component to compressive strength S_m/S_{uc}, and strength amplitude component to endurance limit S_a/S'_e enables a plot of experimental results for a variety of steels. *[Data source: Thomas J. Dolan, "Stress Range," Sec. 6.2 in O. J. Horger (ed.),* ASME Handbook—Metals Engineering Design, *McGraw-Hill, New York, 1953.]*

Figure 7–26

Master fatigue diagram created for AISI 4340 steel having $S_{ut} = 158$ and $S_y = 147$ kpsi. The stress components at A are $\sigma_{min} = 20$, $\sigma_{max} = 120$, $\sigma_m = 70$, and $\sigma_a = 50$, all in kpsi. *(Source: H. J. Grover,* Fatigue of Aircraft Structures, *U.S. Government Printing Office, Washington, D.C., 1966, pp. 317, 322. See also J. A. Collins,* Failure of Materials in Mechanical Design, *Wiley, New York, 1981, p. 216.)*

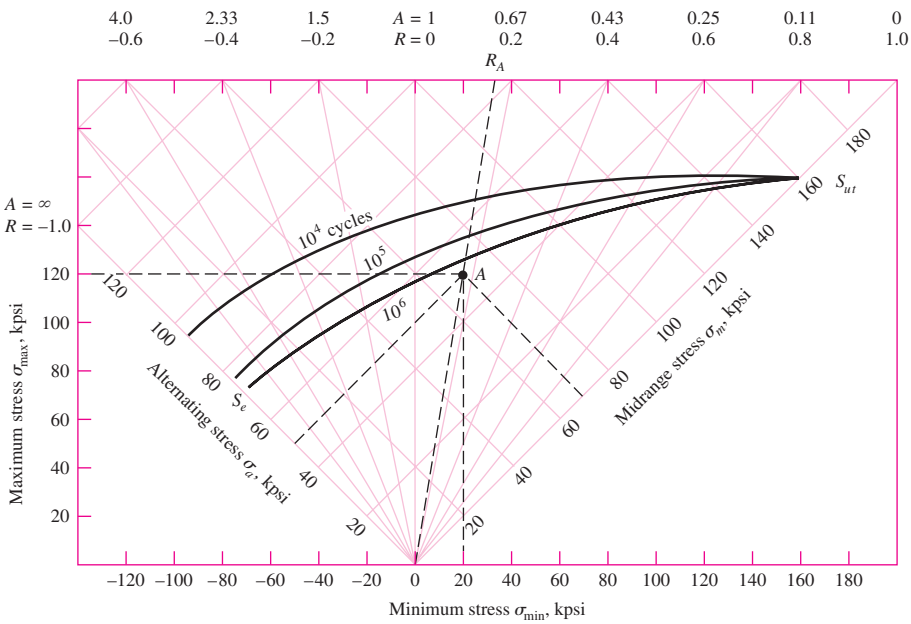

origin. Note that the yield strength is also plotted on both axes, because yielding would be the criterion of failure if σ_{max} exceeded S_y.

Another way to display test results is shown in Fig. 7–25. Here the abscissa represents the ratio of the midrange strength S_m to the ultimate strength, with tension plotted to the right and compression to the left. The ordinate is the ratio of the alternating strength to the endurance limit. The line BC then represents the modified Goodman

Figure 7–27

Fatigue diagram showing various criteria of failure. For each criterion, points on or "above" the respective line indicate failure. Some point A on the Goodman line, for example, gives the strength S_m as the limiting value of σ_m corresponding to the strength S_a, which, paired with σ_m, is the limiting value of σ_a.

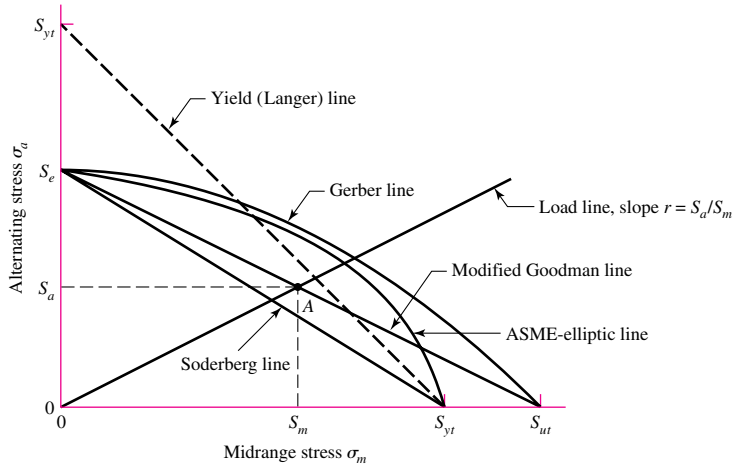

criterion of failure. Note that the existence of midrange stress in the compressive region has little effect on the endurance limit.

The very clever diagram of Fig. 7–26 is unique in that it displays four of the stress components as well as the two stress ratios. A curve representing the endurance limit for values of R beginning at $R = -1$ and ending with $R = 1$ begins at S_e on the σ_a axis and ends at S_{ut} on the σ_m axis. Constant-life curves for $N = 10^5$ and $N = 10^4$ cycles have been drawn too. Any stress state, such as the one at A, can be described by the minimum and maximum components, or by the midrange and alternating components. And safety is indicated whenever the point described by the stress components lies below the constant-life line.

When the midrange stress is compression, failure occurs whenever $\sigma_a = S_e$ or whenever $\sigma_{\max} = S_{yc}$, as indicated by the left-hand side of Fig. 7–25. Neither a fatigue diagram nor any other failure criteria need be developed.

In Fig. 7–27, the tensile side of Fig. 7–25 has been redrawn in terms of strengths, instead of strength ratios, with the same modified Goodman criterion together with four additional criteria of failure. Such diagrams are often constructed for analysis and design purposes; they are easy to use and the results can be scaled off directly.

The early viewpoint expressed on a $\sigma_a\sigma_m$ diagram was that there existed a locus which divided safe from unsafe combinations of σ_a, σ_m. Ensuing proposals included the parabola of Gerber (1874), the Goodman (1890)[25] (straight) line, and the Soderberg (1930) (straight) line. As more data were generated it became clear that a fatigue criterion, rather than being a "fence," was more like a zone or band wherein the probability of failure could be estimated. We include the failure criterion of Goodman because

- It is a straight line and the algebra is linear and easy.
- It is easily graphed, every time for every problem.
- It reveals subtleties of insight into fatigue problems.
- Answers can be scaled from the diagrams as a check on the algebra.

We also caution that it is deterministic and the phenomenon is not. It is biased and we cannot quantify the bias. It is not conservative. It is a stepping-stone to understanding; it is history; and to read the work of other engineers and to have meaningful oral exchanges with them, it is necessary that you understand the Goodman approach should it arise.

[25]It is difficult to date Goodman's work because it went through several modifications and was never published.

Either the fatigue limit S_e or the finite-life strength S_f is plotted on the ordinate of Fig. 7–27. These values will have already been corrected using the Marin factors of Eq. (7–17). Note that the yield strength S_{yt} is plotted on the ordinate too. This serves as a reminder that first-cycle yielding rather than fatigue might be the criterion of failure.

The midrange-stress axis of Fig. 7–27 has the yield strength S_{yt} and the tensile strength S_{ut} plotted along it.

Five criteria of failure are diagrammed in Fig. 7–27: the Soderberg, the modified Goodman, the Gerber, the ASME-elliptic, and yielding. The diagram shows that only the Soderberg criterion guards against any yielding, but is biased low.

Considering the modified Goodman line as a criterion, point A represents a limiting point with an alternating strength S_a and midrange strength S_m. The slope of the load line shown is defined as $r = S_a/S_m$.

The criterion equation for the Soderberg line is

$$\frac{S_a}{S_e} + \frac{S_m}{S_{yt}} = 1 \tag{7–43}$$

Similarly, we find the modified Goodman relation to be

$$\frac{S_a}{S_e} + \frac{S_m}{S_{ut}} = 1 \tag{7–44}$$

Examination of Fig. 7–25 shows that both a parabola and an ellipse have a better opportunity to pass among the midrange tension data and to permit quantification of the probability of failure. The Gerber failure criterion is written as

$$\frac{S_a}{S_e} + \left(\frac{S_m}{S_{ut}}\right)^2 = 1 \tag{7–45}$$

and the ASME-elliptic is written as

$$\left(\frac{S_a}{S_e}\right)^2 + \left(\frac{S_m}{S_y}\right)^2 = 1 \tag{7–46}$$

The *Langer* first-cycle-yielding criterion is used in connection with the fatigue locus:

$$\frac{S_a}{S_{yt}} + \frac{S_m}{S_{yt}} = 1 \tag{7–47}$$

The stresses $n\sigma_a$ and $n\sigma_m$ can replace S_a and S_m, where n is the design factor or factor of safety. Then, Eq. (7–43), the Soderberg line, becomes

$$\frac{\sigma_a}{S_e} + \frac{\sigma_m}{S_y} = \frac{1}{n} \tag{7–48}$$

Equation (7–44), the modified Goodman line, becomes

$$\frac{\sigma_a}{S_e} + \frac{\sigma_m}{S_{ut}} = \frac{1}{n} \tag{7–49}$$

Equation (7–45), the Gerber line, becomes

$$\frac{n\sigma_a}{S_e} + \left(\frac{n\sigma_m}{S_{ut}}\right)^2 = 1 \tag{7–50}$$

Equation (7–46), the ASME-elliptic line, becomes

$$\left(\frac{n\sigma_a}{S_e}\right)^2 + \left(\frac{n\sigma_m}{S_y}\right)^2 = 1 \tag{7–51}$$

We will emphasize the Gerber and ASME-elliptic for fatigue failure criterion and the Langer for first-cycle yielding. However, conservative designers often use the modified

Goodman criterion, so we will continue to include it in our discussions. The failure criteria are used in conjunction with a load line, $r = S_a/S_m = \sigma_a/\sigma_m$. Principal intersections are tabulated in Tables 7–9 to 7–11. Formal expressions for fatigue factor of safety are given in the lower panel of Tables 7–9 to 7–11.

Some examples will help solidify the ideas just discussed.

Table 7–9

Amplitude and Steady Coordinates of Strength and Important Intersections in First Quadrant for Modified Goodman and Langer Failure Criteria

Intersecting Equations	Intersection Coordinates
$\dfrac{S_a}{S_e} + \dfrac{S_m}{S_{ut}} = 1$	$S_a = \dfrac{r S_e S_{ut}}{r S_{ut} + S_e}$
Load line $r = \dfrac{S_a}{S_m}$	$S_m = \dfrac{S_a}{r}$
$\dfrac{S_a}{S_y} + \dfrac{S_m}{S_y} = 1$	$S_a = \dfrac{r S_y}{1 + r}$
Load line $r = \dfrac{S_a}{S_m}$	$S_m = \dfrac{S_y}{1 + r}$
$\dfrac{S_a}{S_e} + \dfrac{S_m}{S_{ut}} = 1$	$S_m = \dfrac{(S_y - S_e)\, S_{ut}}{S_{ut} - S_e}$
$\dfrac{S_a}{S_y} + \dfrac{S_m}{S_y} = 1$	$S_a = S_y - S_m,\ r_{\text{crit}} = S_a/S_m$

Fatigue factor of safety

$$n_f = \frac{1}{\dfrac{\sigma_a}{S_e} + \dfrac{\sigma_m}{S_{ut}}}$$

Table 7–10

Amplitude and Steady Coordinates of Strength and Important Intersections in First Quadrant for Gerber and Langer Failure Criteria

Intersecting Equations	Intersection Coordinates
$\dfrac{S_a}{S_e} + \left(\dfrac{S_m}{S_{ut}}\right)^2 = 1$	$S_a = \dfrac{r^2 S_{ut}^2}{2 S_e}\left[-1 + \sqrt{1 + \left(\dfrac{2 S_e}{r S_{ut}}\right)^2}\right]$
Load line $r = \dfrac{S_a}{S_m}$	$S_m = \dfrac{S_a}{r}$
$\dfrac{S_a}{S_y} + \dfrac{S_m}{S_y} = 1$	$S_a = \dfrac{r S_y}{1 + r}$
Load line $r = \dfrac{S_a}{S_m}$	$S_m = \dfrac{S_y}{1 + r}$
$\dfrac{S_a}{S_e} + \left(\dfrac{S_m}{S_{ut}}\right)^2 = 1$	$S_m = \dfrac{S_{ut}^2}{2 S_e}\left[1 - \sqrt{1 + \left(\dfrac{2 S_e}{S_{ut}}\right)^2 \left(1 - \dfrac{S_y}{S_e}\right)}\right]$
$\dfrac{S_a}{S_y} + \dfrac{S_m}{S_y} = 1$	$S_a = S_y - S_m,\ r_{\text{crit}} = S_a/S_m$

Fatigue factor of safety

$$n_f = \frac{1}{2}\left(\frac{S_{ut}}{\sigma_m}\right)^2 \frac{\sigma_a}{S_e}\left[-1 + \sqrt{1 + \left(\frac{2\sigma_m S_e}{S_{ut}\sigma_a}\right)^2}\right] \qquad \sigma_m > 0$$

Table 7–11

Amplitude and Steady Coordinates of Strength and Important Intersections in First Quadrant for ASME-Elliptic and Langer Failure Criteria

Intersecting Equations	Intersection Coordinates
$\left(\frac{S_a}{S_e}\right)^2 + \left(\frac{S_m}{S_y}\right)^2 = 1$	$S_a = \sqrt{\frac{r^2 S_e^2 S_y^2}{S_e^2 + r^2 S_y^2}}$
Load line $r = S_a/S_m$	$S_m = \frac{S_a}{r}$
$\frac{S_a}{S_y} + \frac{S_m}{S_y} = 1$	$S_a = \frac{r S_y}{1 + r}$
Load line $r = S_a/S_m$	$S_m = \frac{S_y}{1 + r}$
$\left(\frac{S_a}{S_e}\right)^2 + \left(\frac{S_m}{S_y}\right)^2 = 1$	$S_a = 0,\ \frac{2 S_y S_e^2}{S_e^2 + S_y^2}$
$\frac{S_a}{S_y} + \frac{S_m}{S_y} = 1$	$S_m = S_y - S_a,\ r_{\text{crit}} = S_a/S_m$
Fatigue factor of safety	
$n_f = \sqrt{\frac{1}{(\sigma_a/S_e)^2 + (\sigma_m/S_y)^2}}$	

EXAMPLE 7–11 A 1.5-in-diameter bar has been machined from an AISI 1050 cold-drawn bar. This part is to withstand a fluctuating tensile load varying from 0 to 16 kip. Because of the ends, and the fillet radius, a fatigue stress-concentration factor K_f is 1.85 for 10^6 or larger life. Find S_a and S_m and the factor of safety guarding against fatigue and first-cycle yielding, using (*a*) the Gerber fatigue line and (*b*) the ASME-elliptic fatigue line.

Solution We begin with some preliminaries. From Table A–20, $S_{ut} = 100$ kpsi and $S_y = 84$ kpsi. Note that $F_a = F_m = 8$ kip. The Marin factors are, deterministically,

$$k_a = 2.70(100)^{-0.265} = 0.797\text{: Eq. (7–18), Table 7–4}$$

$$k_b = 1 \text{ (axial loading, see } k_c)$$

$$k_c = 0.85\text{: Eq. (7–25)}$$

$$k_d = k_e = k_f = 1$$

$$S_e = 0.797(1)0.850(1)(1)(1)0.504(100) = 34.1\,\text{kpsi: Eqs. (7–8), (7–17)}$$

The nominal axial stress components σ_{ao} and σ_{mo} are

$$\sigma_{ao} = \frac{4F_a}{\pi d^2} = \frac{4(8)}{\pi 1.5^2} = 4.53 \text{ kpsi} \qquad \sigma_{mo} = \frac{4F_m}{\pi d^2} = \frac{4(8)}{\pi 1.5^2} = 4.53 \text{ kpsi}$$

Applying K_f to both components σ_{ao} and σ_{mo} constitutes a prescription of no notch yielding:

$$\sigma_a = K_f \sigma_{ao} = 1.85(4.53) = 8.38 \text{ kpsi} = \sigma_m$$

Figure 7–28

Principal points *A*, *B*, *C*, and *D* on the designer's diagram drawn for Gerber, Langer, and load line.

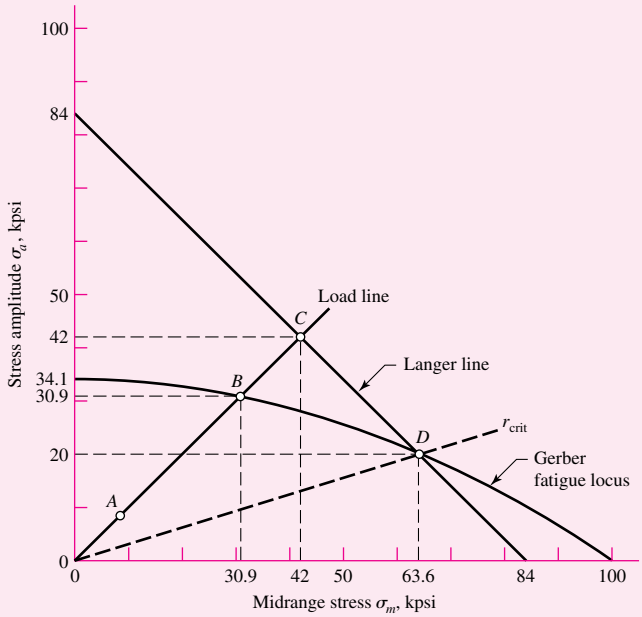

The load line slope is $r = \sigma_a/\sigma_m = 1$.
(*a*) From the first panel of Table 7–10,

$$S_a = \frac{(1)^2 100^2}{2(34.1)} \left\{ -1 + \sqrt{1 + \left[\frac{2(34.1)}{(1)100} \right]^2} \right\} = 30.9 \text{ kpsi}$$

$$S_m = \frac{S_a}{r} = \frac{30.9}{1} = 30.9 \text{ kpsi}$$

In Fig. 7–28 the intersection of the load line and the Gerber line is point *B*. Point *A* on the load line represents the stress components σ_a and σ_m. Point *C* represents the intersection of the load line and the Langer yield line. From Table 7–10,

$$S_a = \frac{r S_y}{1 + r} = \frac{(1)84}{1 + 1} = 42 \text{ kpsi} \qquad S_m = \frac{S_a}{r} = \frac{42}{1} = 42 \text{ kpsi}$$

The load line is the locus of possible stress states. As loading increases, point *A* will move toward point *B* and point *C*. The first encounter is with point *B* on the Gerber line, so the threat to the part is from fatigue. The factor of safety in fatigue n_f is

$$n_f = \frac{OB}{OA} = \frac{(S_a)_{\text{Gerber}}}{\sigma_a} = \frac{30.9}{8.38} = 3.69$$

Alternatively, from the fourth panel of Table 7–10,

$$n_f = \frac{1}{2} \left(\frac{100}{8.38} \right)^2 \left(\frac{8.38}{34.1} \right) \left\{ -1 + \sqrt{1 + \left[\frac{2(8.38)34.1}{100(8.38)} \right]^2} \right\} = 3.68$$

indicating rounding error. The factor of safety guarding against first-cycle yielding is

$$n_y = \frac{OC}{OA} = \frac{(S_a)_{\text{Langer}}}{\sigma_a} = \frac{42.0}{8.38} = 5.01$$

This confirms that there is no local yielding at the fillet. Point D represents the changeover from fatigue failure to first-cycle yielding. The coordinates of point D can be found from the simultaneous solution of Eqs. (7–45) and (7–47), as shown in the third panel of Table 7–10:

$$S_m = \frac{100^2}{2(34.1)}\left[1 - \sqrt{1 + \left(\frac{2(34.1)}{100}\right)^2\left(1 - \frac{84}{34.1}\right)}\right] = 63.8 \text{ kpsi}$$

$$S_a = S_y - S_m = 84 - 63.8 = 20.2 \text{ kpsi}$$

The critical slope of the load line r_{crit} is

$$r_{\text{crit}} = \frac{S_a}{S_m} = \frac{20.2}{63.8} = 0.317$$

The facts that the load line slope is $r = 1$ and $r_{\text{crit}} < r$ confirm that there is a primary threat from fatigue.

(b) From panel 1 of Table 7–11, with $r = 1$, we obtain the coordinates S_a and S_m of point B in Fig. 7–29:

$$S_a = \sqrt{\frac{(1)^2 34.1^2 84^2}{34.1^2 + (1)^2 84^2}} = 31.6 \text{ kpsi} \qquad S_m = \frac{S_a}{r} = \frac{31.6}{1} = 31.6 \text{ kpsi}$$

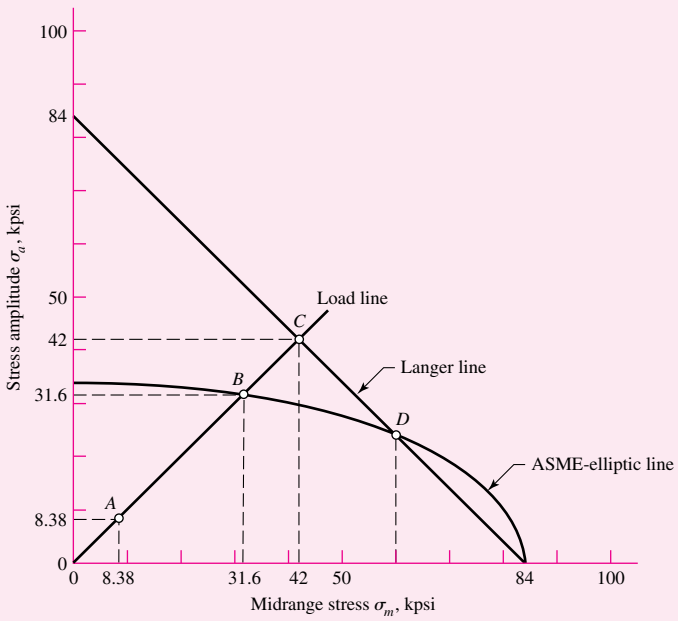

Figure 7–29

Principal points A, B, C, and D on the designer's diagram drawn for ASME-elliptic, Langer, and load lines.

From panel 3 of Table 7–11, the coordinates S_a and S_m of point D in Fig. 7–29 are

$$S_a = \frac{2}{84(1/34.1^2 + 1/84^2)} = 23.8 \text{ kpsi} \qquad S_m = S_y - S_a = 84 - 23.8 = 60.2 \text{ kpsi}$$

$$r_{\text{crit}} = \frac{S_a}{S_m} = \frac{23.8}{60.2} = 0.395$$

Since $r_{\text{crit}} < r$, the primary threat is from fatigue. The factor of safety in fatigue n_f is given by

$$n_f = \frac{S_a}{\sigma_a} = \frac{31.6}{8.38} = 3.77$$

Alternatively, from the fourth panel of Table 7–11,

$$n_f = \sqrt{\frac{1}{(8.38/34.1)^2 + (8.38/84)^2}} = 3.77$$

The factor of safety guarding against first-cycle yielding n_y is

$$n_y = \frac{(S_a)_y}{\sigma_a} = \frac{42}{8.38} = 5.01$$

The ASME-Gerber and the ASME-elliptic fatigue failure criteria are very close to each other and are used interchangeably. The ANSI/ASME Standard B106.1M–1985 uses ASME-elliptic for shafting.

EXAMPLE 7–12 A flat-leaf spring is used to retain an oscillating flat-faced follower in contact with a plate cam. The follower range of motion is 2 in and fixed, so the alternating component of force, bending moment, and stress is fixed, too. The spring is preloaded to adjust to various cam speeds. The preload must be increased to prevent follower float or jump. For lower speeds the preload should be decreased to obtain longer life of cam and follower surfaces. The spring is a steel cantilever 32 in long, 2 in wide, and $\frac{1}{4}$ in thick, as seen in Fig. 7–30*a*. The spring strengths are $S_{ut} = 150$ kpsi, $S_y = 127$ kpsi, and $S_e = 28$ kpsi fully corrected. The total cam motion is 2 in. The designer wishes to preload the spring by deflecting it 2 in for low speed and 5 in for high speed.

(*a*) Plot the Gerber-Langer failure lines with the load line.

(*b*) What are the strength factors of safety corresponding to 2 in and 5 in preload?

(*c*) What are the factors of safety based on preload deflection?

Solution We begin with preliminaries. The second area moment of the cantilever cross section is

$$I = \frac{bh^3}{12} = \frac{2(0.25)^3}{12} = 0.00260 \text{ in}^4$$

Since, from Table A–9, beam 1, force F and deflection y in a cantilever are related by $F = 3EIy/l^3$, then stress σ and deflection y are related by

$$\sigma = \frac{Mc}{I} = \frac{32Fc}{I} = \frac{32(3EIy)}{l^3}\frac{c}{I} = \frac{96Ecy}{l^3} = Ky$$

Figure 7–30

Cam follower retaining spring. (*a*) Geometry; (*b*) designer's fatigue diagram for Ex. 7–12.

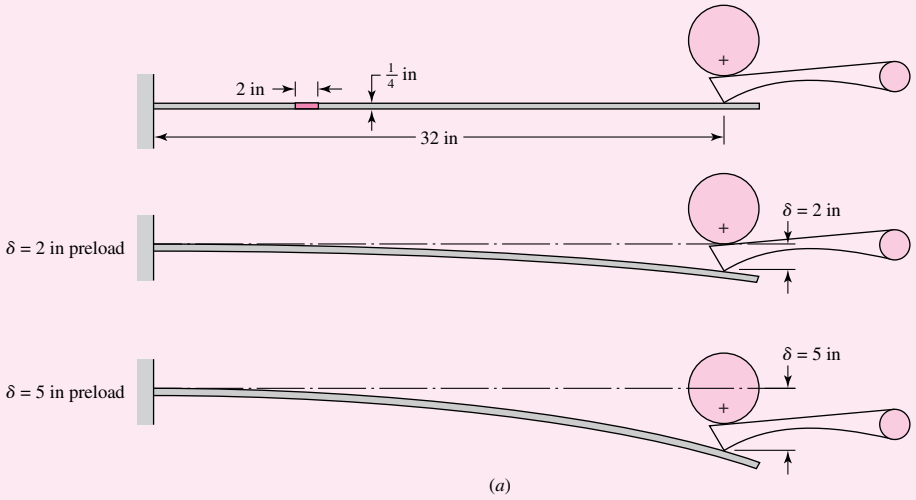

(*a*)

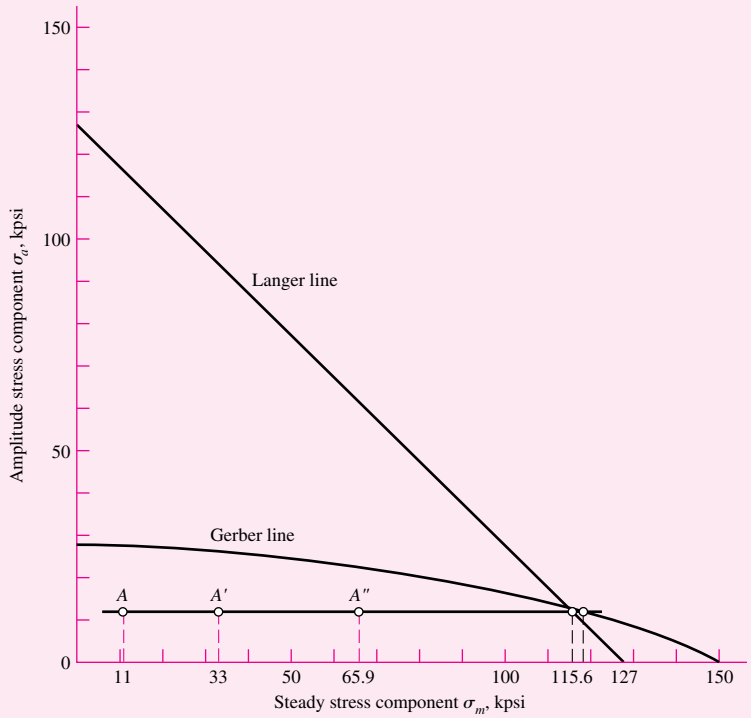

(*b*)

where $$K = \frac{96(30 \cdot 10^6)0.125}{32^3} = 10.99(10^3) \text{ psi/in} = 10.99 \text{ kpsi/in}$$

Now the minimums and maximums of F, y, and σ can be defined by

$$y_{\min} = \delta \qquad y_{\max} = 2 + \delta$$

$$F_{\min} = 3EI\delta/l^3 \qquad F_{\max} = 3EI(2 + \delta)/l^3$$

$$\sigma_{\min} = K\delta \qquad \sigma_{\max} = K(2 + \delta)$$

The stress components are thus

$$\sigma_a = \frac{K(2+\delta) - K\delta}{2} = K$$

$$\sigma_m = \frac{K(2+\delta) + K\delta}{2} = K(1+\delta)$$

For $\delta = 0$,

$$\sigma_{\max} = K(2+\delta) = 10.99(2) = 22 \text{ kpsi} \qquad \sigma_a = (22-0)/2 = 11 \text{ kpsi}$$

$$\sigma_{\min} = K\delta = 0 \text{ kpsi} \qquad \sigma_m = (22+0)/2 = 11 \text{ kpsi}$$

For $\delta = 2$,

$$\sigma_{\max} = K(2+2) = 10.99(4) = 44 \text{ kpsi} \qquad \sigma_a = (44-22)/2 = 11 \text{ kpsi}$$

$$\sigma_{\min} = K\delta = 10.99(2) = 22 \text{ kpsi} \qquad \sigma_m = (44+22)/2 = 33 \text{ kpsi}$$

For $\delta = 5$,

$$\sigma_{\max} = K(2+\delta) = 10.99(2+5) = 76.9 \text{ kpsi} \qquad \sigma_a = (76.9-54.9)/2 = 11 \text{ kpsi}$$

$$\sigma_{\min} = K\delta = 10.99(5) = 54.9 \text{ kpsi} \qquad \sigma_m = (76.9+54.9)/2 = 65.6 \text{ kpsi}$$

(*a*) A plot of the Gerber and Langer criteria is shown in Fig. 7–30*b*. The three preload deflections of 0, 2, and 5 in are shown as points A, A', and A''. Note that since σ_a is constant at 11 kpsi, the load line is horizontal and does not contain the origin. The intersection between the Gerber line and the load line is found from solving Eq. (7–45) for S_m and substituting 11 kpsi for S_a:

$$S_m = S_{ut}\sqrt{1 - \frac{S_a}{S_e}} = 150\sqrt{1 - \frac{11}{28}} = 116.9 \text{ kpsi}$$

The intersection of the Langer line and the load line is found from solving Eq. (7–47) for S_m and substituting 11 kpsi for S_a:

$$S_m = S_y - S_a = 127 - 11 = 116 \text{ kpsi}$$

The threats from fatigue and first-cycle yielding are approximately equal.
(*b*) For $\delta = 2$ in,

$$n_f = \frac{S_m}{\sigma_m} = \frac{116.9}{33} = 3.54 \qquad n_y = \frac{116}{33} = 3.52$$

and for $\delta = 5$ in,

$$n_f = \frac{116.9}{65.9} = 1.77 \qquad n_y = \frac{116}{65.9} = 1.76$$

(*c*) A factor of safety based on preload deflection involves finding the preload deflection associated with failure. Treating fatigue as the threat, Gerber's relation can be expressed as

$$\frac{11}{28} + \left(\frac{K\delta^*}{150}\right)^2 = 1$$

from which

$$\delta^* = \frac{150}{K}\sqrt{1 - \frac{11}{28}} = \frac{150}{11}\sqrt{1 - \frac{11}{28}} = 10.6 \text{ in}$$

For slower speeds the factor of safety can be defined as

Answer

$$n = \frac{\text{loss-of-function preload deflection}}{\text{working preload deflection}} = \frac{\delta^*}{\delta} = \frac{10.6}{2} = 5.3$$

For higher speeds the same definition applies and the factor of safety is

Answer

$$n = \frac{10.6}{5} = 2.12$$

EXAMPLE 7–13

A steel bar undergoes cyclic loading such that $\sigma_{\max} = 60$ kpsi and $\sigma_{\min} = -20$ kpsi. For the material, $S_{ut} = 80$ kpsi, $S_y = 65$ kpsi, a fully corrected endurance limit of $S_e = 40$ kpsi, and $f = 0.9$. Estimate the number of cycles to a fatigue failure using:
(*a*) Modified Goodman criterion.
(*b*) Gerber criterion.

Solution

From the given stresses,

$$\sigma_a = \frac{60 - (-20)}{2} = 40 \text{ kpsi} \qquad \sigma_m = \frac{60 + (-20)}{2} = 20 \text{ kpsi}$$

From the material properties, Eqs. (7–13) to (7–15) give

$$a = \frac{(f S_{ut})^2}{S_e} = \frac{[0.9(80)]^2}{40} = 129.6 \text{ kpsi}$$

$$b = -\frac{1}{3}\log\left(\frac{f S_{ut}}{S_e}\right) = -\frac{1}{3}\log\left[\frac{0.9(80)}{40}\right] = -0.0851$$

$$N = \left(\frac{S_f}{a}\right)^{1/b} = \left(\frac{S_f}{129.6}\right)^{-1/0.0851} \tag{1}$$

where S_f replaced σ_a in Eq. (7–15).
(*a*) For the Goodman criterion with $n = 1$, $S_e = S_f$, Eq. (7–49) gives

$$S_f = \frac{\sigma_a}{1 - \frac{\sigma_m}{S_{ut}}} = \frac{40}{1 - \frac{20}{80}} = 53.3 \text{ kpsi}$$

Substituting this into Eq. (1) yields

Answer

$$N = \left(\frac{53.3}{129.6}\right)^{-1/0.0851} = 3.40(10^4) \text{ cycles}$$

(*b*) For Gerber, similar to part (*a*), from Eq. (7–50),

$$S_f = \frac{\sigma_a}{1 - \left(\frac{\sigma_m}{S_{ut}}\right)^2} = \frac{40}{1 - \left(\frac{20}{80}\right)^2} = 42.7 \text{ kpsi}$$

Again, from Eq. (1),

Answer

$$N = \left(\frac{42.7}{129.6}\right)^{-1/0.0851} = 4.68(10^5) \text{ cycles}$$

Comparing the answers, we see a large difference in the results. Again, the modified Goodman criterion is conservative as compared to Gerber for which the moderate difference in S_f is then magnified by a logarithmic S, N relationship.

For many *brittle* materials, the first quadrant fatigue failure criteria follows a concave upward Smith-Dolan locus represented by

$$\frac{S_a}{S_e} = \frac{1 - S_m/S_{ut}}{1 + S_m/S_{ut}} \tag{7–52}$$

or as a design equation,

$$\frac{n\sigma_a}{S_e} = \frac{1 - n\sigma_m/S_{ut}}{1 + n\sigma_m/S_{ut}} \tag{7–53}$$

For a radial load line of slope r, we substitute S_a/r for S_m in Eq. (7–52) and solve for S_a, obtaining

$$S_a = \frac{rS_{ut} + S_e}{2}\left[-1 + \sqrt{1 + \frac{4rS_{ut}S_e}{(rS_{ut} + S_e)^2}}\right] \tag{7–54}$$

The fatigue diagram for a brittle material differs markedly from that of a ductile material:

- Yielding is not involved since the material may not have a yield strength.
- Characteristically, the compressive ultimate strength exceeds the ultimate tensile strength severalfold.
- First-quadrant fatigue failure locus is concave-upward (Smith-Dolan), for example, and as flat as Goodman. Brittle materials are more sensitive to midrange stress, being lowered, but compressive midrange stresses are beneficial.
- Not enough work has been done on brittle fatigue to discover insightful generalities, so we stay in the first and a bit of the second quadrant.

The most likely domain of designer use is in the range from $-S_{ut} \le \sigma_m \le S_{ut}$. The locus in the first quadrant is Goodman, Smith-Dolan, or something in between. The portion of the second quadrant that is used is represented by a straight line between the points $-S_{ut}$, S_{ut} and 0, S_e, which has the equation

$$S_a = S_e + \left(\frac{S_e}{S_{ut}} - 1\right) S_m \qquad -S_{ut} \le S_m \le 0 \quad \text{(for cast iron)} \tag{7–55}$$

Table A–24 gives properties of gray cast iron. The endurance limit stated is really $k_a k_b S'_e$ and only corrections k_c, k_d, k_e, and k_f need be made. The average k_c for axial and torsional loading is 0.9.

EXAMPLE 7–14 A grade 30 gray cast iron is subjected to a load F applied to a 1 by $\frac{3}{8}$-in cross-section link with a $\frac{1}{4}$-in-diameter hole drilled in the center as depicted in Fig. 7–31*a*. The surfaces are machined. In the neighborhood of the hole, what is the factor of safety guarding against failure under the following conditions:
(*a*) The load $F = 1000$ lbf tensile, steady.
(*b*) The load is 1000 lbf repeatedly applied.
(*c*) The load fluctuates between -1000 lbf and 300 lbf without column action.
Use the Smith-Dolan fatigue locus.

Solution Some preparatory work is needed. From Table A–24, $S_{ut} = 31$ kpsi, $S_{uc} = 109$ kpsi, $k_a k_b S'_e = 14$ kpsi. Since k_c for axial loading is 0.9, then $S_e = (k_a k_b S'_e)k_c = 14(0.9) = 12.6$ kpsi. From Table A–15–1, $A = t(w - d) = 0.375(1 - 0.25) = 0.281$ in^2, $d/w = 0.25/1 = 0.25$, and $K_t = 2.45$. The notch sensitivity for cast iron is 0.20 (see p. 336), so

$$K_f = 1 + q(K_t - 1) = 1 + 0.20(2.45 - 1) = 1.29$$

$$(a)\ \sigma_a = \frac{K_f F_a}{A} = \frac{1.29(0)}{0.281} = 0 \qquad \sigma_m = \frac{K_f F_m}{A} = \frac{1.29(1000)}{0.281}(10^{-3}) = 4.59 \text{ kpsi}$$

and

Answer
$$n = \frac{S_{ut}}{\sigma_m} = \frac{31.0}{4.59} = 6.75$$

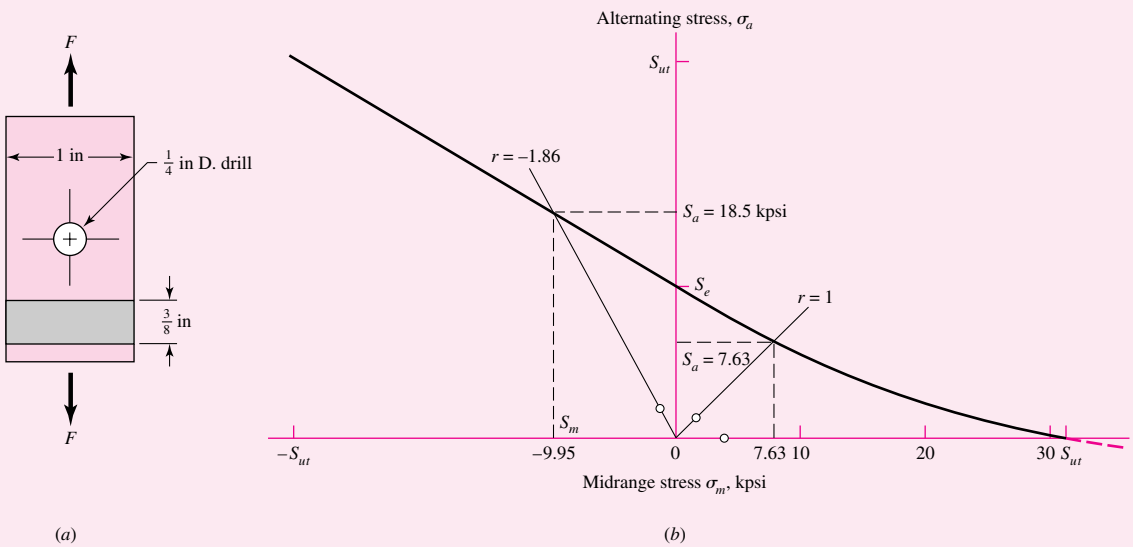

Figure 7–31
The grade 30 cast-iron part in axial fatigue with (*a*) its geometry displayed and (*b*) its designer's fatigue diagram for the circumstances of Ex. 7–14.

(*b*)
$$F_a = F_m = \frac{F}{2} = \frac{1000}{2} = 500 \text{ lbf}$$

$$\sigma_a = \sigma_m = \frac{K_f F_a}{A} = \frac{1.29(500)}{0.281}(10^{-3}) = 2.30 \text{ kpsi}$$

$$r = \frac{\sigma_a}{\sigma_m} = 1$$

From Eq. (7–54),

$$S_a = \frac{(1)31 + 12.6}{2}\left[-1 + \sqrt{1 + \frac{4(1)31(12.6)}{[(1)31 + (12.6)]^2}}\right] = 7.63 \text{ kpsi}$$

Answer
$$n = \frac{S_a}{\sigma_a} = \frac{7.63}{2.30} = 3.32$$

(*c*)
$$F_a = \frac{1}{2}|300 - (-1000)| = 650 \text{ lbf} \qquad \sigma_a = \frac{1.29(650)}{0.281}(10^{-3}) = 3.0 \text{ kpsi}$$

$$F_m = \frac{1}{2}[300 + (-1000)] = -350 \text{ lbf} \qquad \sigma_m = \frac{1.29(-350)}{0.281}(10^{-3}) = -1.61 \text{ kpsi}$$

$$r = \frac{\sigma_a}{\sigma_m} = \frac{3.0}{-1.61} = -1.86$$

From Eq. (7–55), $S_a = S_e + (S_e/S_{ut} - 1)S_m$ and $S_m = S_a/r$. It follows that

$$S_a = \frac{S_e}{1 - \frac{1}{r}\left(\frac{S_e}{S_{ut}} - 1\right)} = \frac{12.6}{1 - \frac{1}{-1.86}\left(\frac{12.6}{31} - 1\right)} = 18.5 \text{ kpsi}$$

Answer
$$n = \frac{S_a}{\sigma_a} = \frac{18.5}{3.0} = 6.17$$

Figure 7–31*b* shows the portion of the designer's fatigue diagram that was constructed.

7–13 Torsional Fatigue Strength under Fluctuating Stresses

Extensive tests by Smith[26] provide some very interesting results on pulsating torsional fatigue. Smith's first result, based on 72 tests, shows that the existence of a torsional steady-stress component not more than the torsional yield strength has no effect on the torsional endurance limit, provided the material is *ductile, polished, notch-free,* and *cylindrical*.

Smith's second result applies to materials with stress concentration, notches, or surface imperfections. In this case, he finds that the torsional fatigue limit decreases monotonically with torsional steady stress. Since the great majority of parts will have

[26]James O. Smith, "The Effect of Range of Stress on the Fatigue Strength of Metals," *Univ. of Ill. Eng. Exp. Sta. Bull*. 334, 1942.

surfaces that are less than perfect, this result indicates Gerber, ASME-elliptic, and other approximations are useful. Joerres[27] of Associated Spring-Barnes Group, confirms Smith's results and recommends the use of the modified Goodman relation for pulsating torsion. In constructing the Goodman diagram, Joerres uses

$$S_{su} = 0.67 S_{ut} \tag{7–56}$$

Also, from Chap. 6, $S_{sy} = 0.577 S_{yt}$ from distortion-energy theory, and the mean load factor k_c is given by Eq. (7–25), or 0.577. This is discussed further in Chap. 10.

7–14 Combinations of Loading Modes

In Sec. 7–9 we learned that a load factor k_c is used to obtain the endurance limit and hence that the result is dependent on whether the loading is axial, bending, or torsion. In this section we want to answer the question, How do we proceed when the loading is a mixture of, say, axial, bending, and torsional loads? In addition to the complication introduced by the fact that a separate endurance limit is associated with each mode of loading, there may also be multiple stress-concentration factors, one also for each mode of loading. Fortunately, the answer turns out to be rather simple. Assuming that all stress components are completely reversing and are always in time phase with each other,

1. For the strength, use the fully corrected endurance limit for bending, S_e.
2. Apply the appropriate fatigue stress-concentration factors to the torsional stress, the bending stress, and the axial stress components.
3. Multiply any alternating axial stress components by the factor $1/k_{c,\text{ax}}$.
4. Enter the resultant stresses into a Mohr's circle analysis and find the principal stresses.
5. Using the results of step 4, find the von Mises alternating stress σ'_a.
6. Compare σ'_a with S_a to find the factor of safety.

If the stress components are not in phase but have the same frequency, the maxima can be found by expressing each component in trigonometric terms, using phase angles, and then finding the sum. If two or more stress components have differing frequencies, the problem is difficult; one solution is to assume that the two (or more) components often reach an in-phase condition, so that their magnitudes are additive.

If midrange stresses are also present, then steps 4 and 5 can be repeated for them and the resulting steady von Mises stress component σ'_m used with σ'_a in forming a Gerber or ASME-elliptic solution. Both the steady and amplitude components are augmented by K_f or K_{fs} stress-concentration factor.

[27]Robert E. Joerres, "Springs," Chap. 24 in Joseph E. Shigley and Charles R. Mischke, *Standard Handbook of Machine Design*, 2nd ed., McGraw-Hill, New York, 1996.

EXAMPLE 7–15 A rotating shaft is made of 42- × 4-mm AISI 1018 cold-drawn steel tubing and has a 6-mm-diameter hole drilled transversely through it. Estimate the factor of safety guarding against fatigue and static failures using the Gerber and Langer failure criteria for the following loading conditions:

(*a*) The shaft is subjected to a completely reversed torque of 120 N · m in phase with a completely reversed bending moment of 150 N · m.

(*b*) The shaft is subjected to a pulsating torque fluctuating from 20 to 160 N · m and a steady bending moment of 150 N · m.

Solution Here we follow the procedure of estimating the strengths and then the stresses, followed by relating the two.

From Table A–20 we find the minimum strengths to be $S_{ut} = 440$ MPa and $S_{yt} = 370$ MPa. The endurance limit of the rotating-beam specimen is $0.504(440) = 222$ MPa. The surface factor, obtained from Eq. (7–18) and Table 7–4, is

$$k_a = 4.51 S_{ut}^{-0.265} = 4.51(440)^{-0.265} = 0.899$$

From Eq. (7–20) the size factor is

$$k_b = \left(\frac{d}{7.62}\right)^{-0.107} = \left(\frac{42}{7.62}\right)^{-0.107} = 0.833$$

The remaining Marin factors are all unity, so the modified endurance strength S_e is

$$S_e = 0.899(0.833)222 = 166 \text{ MPa}$$

(*a*) Theoretical stress-concentration factors are found from Table A–16. Using $a/D = 6/42 = 0.143$ and $d/D = 34/42 = 0.810$, and using linear interpolation, we obtain $A = 0.798$ and $K_t = 2.366$ for bending; and $A = 0.89$ and $K_{ts} = 1.75$ for torsion. Thus, for bending,

$$Z_{\text{net}} = \frac{\pi A}{32D}(D^4 - d^4) = \frac{\pi(0.798)}{32(4.2)}[(4.2)^4 - (3.4)^4] = 3.31 \text{ cm}^3$$

and for torsion

$$J_{\text{net}} = \frac{\pi A}{32}(D^4 - d^4) = \frac{\pi(0.89)}{32}[(4.2)^4 - (3.4)^4] = 15.5 \text{ cm}^4$$

Next, using Figs. 7–20 and 7–21 with a notch radius of 3 mm we find the notch sensitivities to be 0.78 for bending and 0.96 for torsion. The two corresponding fatigue stress-concentration factors are obtained from Eq. (7–31) as

$$K_f = 1 + q(K_t - 1) = 1 + 0.78(2.366 - 1) = 2.07$$

$$K_{fs} = 1 + 0.96(1.75 - 1) = 1.72$$

The bending stress is now found to be

$$\sigma_{xa} = K_f \frac{M}{Z_{\text{net}}} = 2.07 \frac{150}{3.31} = 93.8 \text{ MPa}$$

and the torsional stress is

$$\tau_{xya} = K_{fs} \frac{TD}{2J_{\text{net}}} = 1.72 \frac{120(4.2)}{2(15.5)} = 28.0 \text{ MPa}$$

The von Mises steady-stress component σ'_m is zero. The amplitude component σ'_a is given by

$$\sigma'_a = \left(\sigma_{xa}^2 + 3\tau_{xya}^2\right)^{1/2} = [93.8^2 + 3(28^2)]^{1/2} = 105.6 \text{ MPa}$$

Figure 7–32
Designer's fatigue diagram for Ex. 7–15.

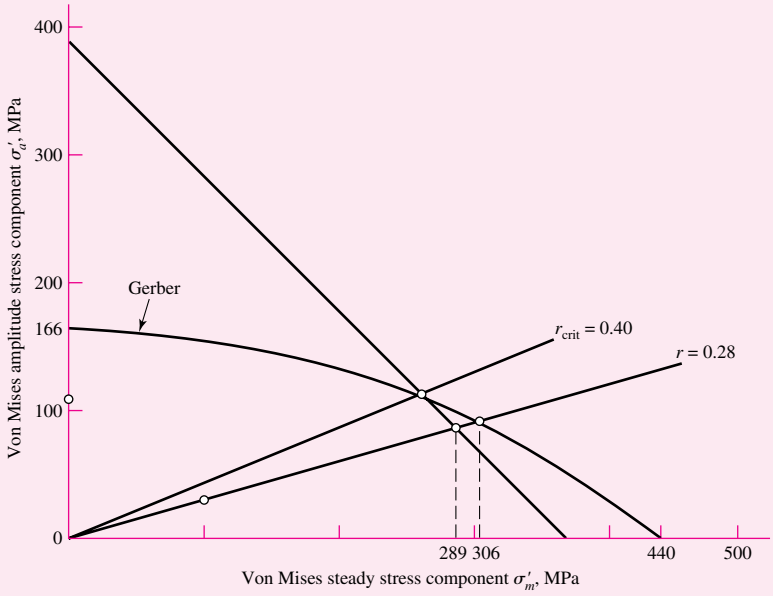

Since $S_e = S_a$, the fatigue factor of safety n_f is

$$n_f = \frac{S_a}{\sigma'_a} = \frac{166}{105.6} = 1.57$$

The first-cycle yield factor of safety is

$$n_y = \frac{S_{yt}}{\sigma'_a} = \frac{370}{105.6} = 3.50$$

There is no localized yielding; the threat is from fatigue. See Fig. 7–32.
(*b*) This part asks us to find the factors of safety when the alternating component is due to pulsating torsion, and a steady component is due to both torsion and bending. We have $T_a = (160 - 20)/2 = 70$ N · m and $T_m = 20 + 70 = 90$ N · m. The corresponding amplitude and steady-stress components are

$$\tau_{xya} = K_{fs}\frac{T_a D}{2J_{\text{net}}} = 1.72\frac{70(4.2)}{2(15.5)} = 16.3 \text{ MPa}$$

$$\tau_{xym} = K_{fs}\frac{T_m D}{2J_{\text{net}}} = 1.72\frac{90(4.2)}{2(15.5)} = 21.0 \text{ MPa}$$

The steady bending stress component σ_{xm} is

$$\sigma_{xm} = K_f\frac{M_m}{Z_{\text{net}}} = 2.07\frac{150}{3.31} = 93.8 \text{ MPa}$$

The von Mises components σ'_a and σ'_m are

$$\sigma'_a = [3(16.3)^2]^{1/2} = 28.2 \text{ MPa}$$

$$\sigma'_m = [93.8^2 + 3(21)^2]^{1/2} = 100.6 \text{ MPa}$$

The slope of the load line is $r = \sigma'_a/\sigma'_m = 28.2/100.6 = 0.28$. From Table 7–10, the strength amplitude component S_a and steady-strength component S_m are

$$S_a = \frac{0.28^2 440^2}{2(166)}\left\{-1 + \sqrt{1 + \left[\frac{2(166)}{0.28(440)}\right]^2}\right\} = 85.7 \text{ MPa}$$

$$S_m = \frac{85.7}{0.28} = 306.1 \text{ MPa}$$

The fatigue factor of safety n_f is

Answer
$$n_f = \frac{S_a}{\sigma'_a} = \frac{85.7}{28.2} = 3.04$$

The first-cycle yield factor of safety n_y is

Answer
$$n_y = \frac{S_y}{\sigma'_a + \sigma'_m} = \frac{370}{28.2 + 100.6} = 2.87$$

There is no notch yielding. The threat is from first-cycle yielding at the notch. See the plot in Fig. 7–32.

7–15 Varying, Fluctuating Stresses; Cumulative Fatigue Damage

Instead of a single fully reversed stress history block composed of n cycles, suppose a machine part, at a critical location, is subjected to

- A fully reversed stress σ_1 for n_1 cycles, σ_2 for n_2 cycles, . . . , or
- A "wiggly" time line of stress exhibiting many and different peaks and valleys.

What stresses are significant, what counts as a cycle, and what is the measure of damage incurred? Consider a fully reversed cycle with stresses varying 60, 80, 40, and 60 kpsi and a second fully reversed cycle −40, −60, −20, and −40 kpsi as depicted in Fig. 7–33*a*. First, it is clear that to impose the pattern of stress in Fig. 7–33*a* on a part it is necessary that the time trace look like the solid line plus the dashed line in Fig. 7–33*a*. Figure 7–33*b* moves the snapshot to exist beginning with 80 kpsi and ending with 80 kpsi. Acknowledging the existence of a single stress-time trace is to discover a "hidden" cycle shown as the dashed line in Fig. 7–33*b*. If there are 100 applications of the all-positive stress cycle, then 100 applications of the all-negative stress cycle, the hidden cycle is applied but once. If the all-positive stress cycle is applied alternately with the all-negative stress cycle, the hidden cycle is applied 100 times.

To ensure that the hidden cycle is not lost, begin on the snapshot with the largest (or smallest) stress and add previous history to the right side, as was done in Fig. 7–33*b*. Characterization of a cycle takes on a max–min–same max (or min–max–same min) form. We identify the hidden cycle first by moving along the dashed-line trace in Fig. 7–33*b* identifying a cycle with an 80-kpsi max, a 60-kpsi min, and returning to 80 kpsi. Mentally deleting the used part of the trace (the dashed line) leaves a 40, 60,

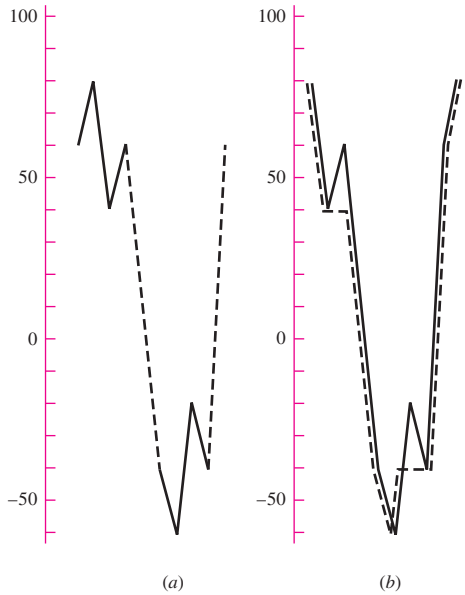

Figure 7–33
Variable stress diagram prepared for assessing cumulative damage.

40 cycle and a −40, −20, −40 cycle. Since failure loci are expressed in terms of stress amplitude component σ_a and steady component σ_m, we use Eq. (7–39) to construct the table below:

Cycle Number	σ_{max}	σ_{min}	σ_a	σ_m
1	80	−60	70	10
2	60	40	10	50
3	−20	−40	10	−30

The most damaging cycle is number 1. It could have been lost.

Methods for counting cycles include:

- Number of tensile peaks to failure.
- All maxima above the waveform mean, all minima below.
- The global maxima between crossings above the mean and the global minima between crossings below the mean.
- All positive slope crossings of levels above the mean, and all negative slope crossings of levels below the mean.
- A modification of the preceding method with only one count made between successive crossings of a level associated with each counting level.
- Each local maxi-min excursion is counted as a half-cycle, and the associated amplitude is half-range.
- The preceding method plus consideration of the local mean.
- Rain-flow counting technique.

The method used here amounts to a variation of the *rain-flow counting technique*.

The *Palmgren-Miner*[28] *cycle-ratio summation rule,* also called *Miner's rule,* is written

$$\sum \frac{n_i}{N_i} = c \tag{7–57}$$

where n_i is the number of cycles at stress level σ_i and N_i is the number of cycles to failure at stress level σ_i. The parameter c has been determined by experiment; it is usually found in the range $0.7 < c < 2.2$ with an average value near unity.

Using the deterministic formulation as a linear damage rule we write

$$D = \sum \frac{n_i}{N_i} \tag{7–58}$$

where D is the accumulated damage. When $D = c = 1$, failure ensues.

[28]A. Palmgren, "Die Lebensdauer von Kugellagern," *ZVDI*, vol. 68, pp. 339–341, 1924; M. A. Miner, "Cumulative Damage in Fatigue," *J. Appl. Mech.,* vol. 12, *Trans. ASME,* vol. 67, pp. A159–A164, 1945.

EXAMPLE 7–16 For the loading of Fig. 7–33 on a part, the following properties at the critical location exist: $S_{ut} = 151$ kpsi, $\sigma_0 = 210$ kpsi, $\varepsilon_f = 0.45$, $m = 0.09$, $S_e = 67.5$ kpsi. Estimate the number of repetitions of the stress-time block in Fig. 7–33 that can be made before failure.

Solution

$$\sigma'_F = \sigma_0 \varepsilon^m = 210(0.45)^{0.09} = 195.4 \text{ kpsi}$$

From Eq. (7–11),

$$b = -\frac{\log(\sigma'_F/S_e)}{\log(2N_e)} = -\frac{\log(195.4/67.5)}{\log(2 \cdot 10^6)} = -0.07326$$

From Eq. (7–9),

$$f = \frac{\sigma'_F}{S_{ut}}(2 \cdot 10^3)^b = \frac{195.4}{151}(2 \cdot 10^3)^{-0.07326} = 0.7415$$

From Eq. (7–13),

$$a = \frac{(f S_{ut})^2}{S_e} = \frac{[0.7415(151)]^2}{67.5} = 186 \text{ kpsi}$$

so

$$S_f = 186N^{-0.07326} \qquad N = \left(\frac{\sigma_a}{186}\right)^{-1/0.07326}$$

We prepare to add two columns to the previous table. Using the Gerber fatigue criterion, Eq. (7–45), with $S_a = S_f$, on the designer's fatigue diagram we can write

$$S_f = \begin{cases} \dfrac{\sigma_a}{1 - (\sigma_m/S_{ut})^2} & \sigma_m > 0 \\ S_e & \sigma_m \le 0 \end{cases} \tag{1}$$

Cycle 1: $r = 70/10 = 7$, and the strength amplitude from Table 7–9 is

$$S_a = \frac{7^2 151^2}{2(67.5)}\left\{-1 + \sqrt{1 + \left[\frac{2(67.5)}{7(151)}\right]^2}\right\} = 67.2 \text{ kpsi}$$

Since $\sigma_a > S_a$, that is, $70 > 67.2$, life is reduced. From Eq. (1),

$$S_f = \frac{70}{1 - (10/151)^2} = 70.3 \text{ kpsi} \qquad N = \left(\frac{70.3}{186}\right)^{-1/0.07326} = 0.586(10^6) \text{ cycles}$$

Cycle 2: $r = 10/50 = 0.2$, and the strength amplitude is

$$S_a = \frac{0.2^2 151^2}{2(67.5)}\left\{-1 + \sqrt{1 + \left[\frac{2(67.5)}{0.2(151)}\right]^2}\right\} = 24.2 \text{ kpsi}$$

Since $\sigma_a < S_a$, that is $10 < 24.2$, then $S_f = S_e$ and indefinite life follows.

Cycle 3: $r = 10/-30 = -0.333$, and since $\sigma_m < 0$, $S_f = S_e$, indefinite life follows.

Cycle Number	S_f, kpsi	N, cycles
1	70.3	$0.58(10^6)$
2	67.5	∞
3	67.5	∞

From Eq. (7–62) the damage per block is

$$D = \sum \frac{n_i}{N_i} = N\left[\frac{1}{0.586(10^6)} + \frac{1}{\infty} + \frac{1}{\infty}\right] = \frac{N}{0.586(10^6)}$$

Answer Setting $D = 1$ yields $N = 0.586(10^6)$ cycles.

To further illustrate the use of the Miner rule, let us choose a steel having the properties $S_{ut} = 80$ kpsi, $S'_{e,0} = 40$ kpsi, and $f = 0.9$, where we have used the designation $S'_{e,0}$ instead of the more usual S'_e to indicate the endurance limit of the *virgin,* or *undamaged, material*. The log S–log N diagram for this material is shown in Fig. 7–34 by the heavy solid line. Now apply, say, a reversed stress $\sigma_1 = 60$ kpsi for $n_1 = 3000$ cycles. Since $\sigma_1 > S'_{e,0}$, the endurance limit will be damaged, and we wish to find the new endurance limit $S'_{e,1}$ of the damaged material using the Miner rule. The equation of the virgin material failure line in Fig. 7–34 in the 10^3 to 10^6 cycle range is

$$S_f = aN^b = 129.6N^{-0.085\,091}$$

The cycles to failure at stress level $\sigma_1 = 60$ kpsi are

$$N_1 = \left(\frac{\sigma_1}{129.6}\right)^{-1/0.085\,091} = \left(\frac{60}{129.6}\right)^{-1/0.085\,091} = 8520 \text{ cycles}$$

Figure 7–34 shows that the material has a life $N_1 = 8520$ cycles at 60 kpsi, and consequently, after the application of σ_1 for 3000 cycles, there are $N_1 - n_1 = 5520$ cycles of

Figure 7–34

Use of the Miner rule to predict the endurance limit of a material that has been overstressed for a finite number of cycles.

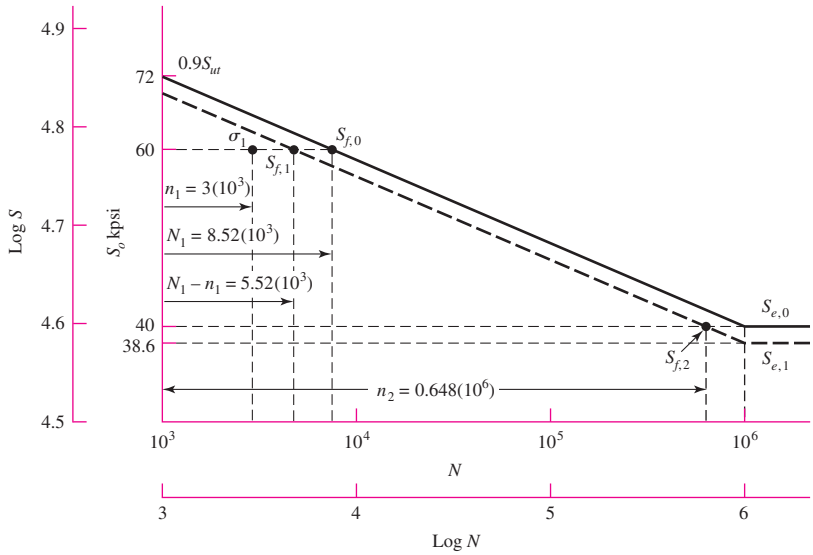

life remaining at σ_1. This locates the finite-life strength $S_{f,1}$ of the damaged material, as shown in Fig. 7–34. To get a second point, we ask the question: With n_1 and N_1 given, how many cycles of stress $\sigma_2 = S'_{e,0}$ can be applied before the damaged material fails? This corresponds to n_2 cycles of stress reversal, and hence, from Eq. (7–57), we have

$$\frac{n_1}{N_1} + \frac{n_2}{N_2} = 1 \tag{a}$$

or

$$n_2 = \left(1 - \frac{n_1}{N_1}\right) N_2 \tag{b}$$

Then

$$n_2 = \left[1 - \frac{3(10)^3}{8.52(10)^3}\right](10^6) = 0.648(10^6) \text{ cycles}$$

This corresponds to the finite-life strength $S_{f,2}$ in Fig. 7–34. A line through $S_{f,1}$ and $S_{f,2}$ is the log S–log N diagram of the damaged material according to the Miner rule. The new endurance limit is $S_{e,1} = 38.5$ kpsi.

We could leave it at this, but a little more investigation can be helpful. We have two points on the new fatigue locus, $N_1 - n_1, \sigma_1$ and n_2, σ_2. It is useful to prove that the slope of the new line is still b. For the equation $S_f = a' N^{b'}$, where the values of a' and b' are established by two points α and β. The equation for b' is

$$b' = \frac{\log \sigma_\alpha / \sigma_\beta}{\log N_\alpha / N_\beta} \tag{c}$$

Examine the denominator of Eq. (*c*):

$$\log \frac{N_\alpha}{N_\beta} = \log \frac{N_1 - n_1}{n_2} = \log \frac{N_1 - n_1}{(1 - n_1/N_1)N_2} = \log \frac{N_1}{N_2}$$
$$= \log \frac{(\sigma_1/a)^{1/b}}{(\sigma_2/a)^{1/b}} = \log \left(\frac{\sigma_1}{\sigma_2}\right)^{1/b} = \frac{1}{b} \log \left(\frac{\sigma_1}{\sigma_2}\right)$$

Substituting this into Eq. (*c*) with $\sigma_\alpha/\sigma_\beta = \sigma_1/\sigma_2$ gives

$$b' = \frac{\log(\sigma_1/\sigma_2)}{(1/b)\log(\sigma_1/\sigma_2)} = b$$

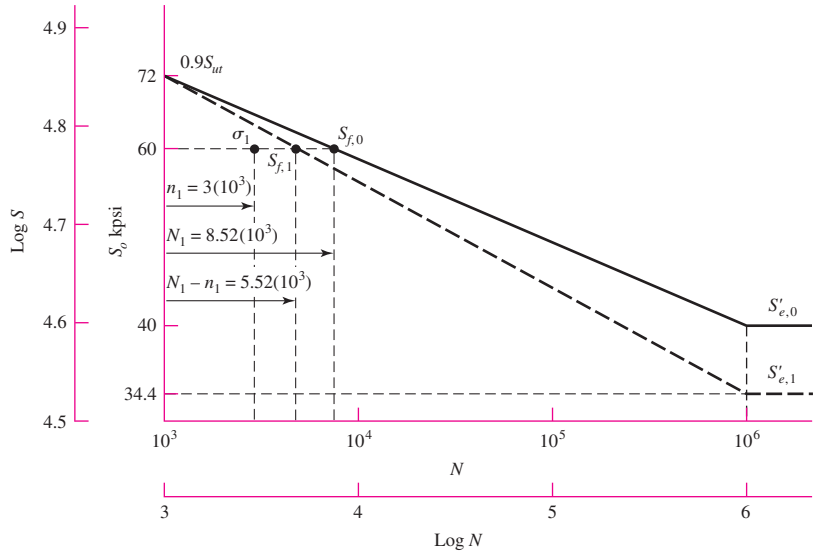

Figure 7–35

Use of the Manson method to predict the endurance limit of a material that has been overstressed for a finite number of cycles.

which means the damaged material line has the same slope as the virgin material line; therefore, the lines are parallel. This information can be helpful in writing a computer program for the Palmgren-Miner hypothesis.

Though the Miner rule is quite generally used, it fails in two ways to agree with experiment. First, note that this theory states that the static strength S_{ut} is damaged, that is, decreased, because of the application of σ_1; see Fig. 7–34 at $N = 10^3$ cycles. Experiments fail to verify this prediction.

The Miner rule, as given by Eq. (7–53), does not account for the order in which the stresses are applied, and hence ignores any stresses less than $S'_{e,0}$. But it can be seen in Fig. 7–34 that a stress σ_3 in the range $S'_{e,1} < \sigma_3 < S'_{e,0}$ would cause damage if applied after the endurance limit had been damaged by the application of σ_1.

Manson's[29] approach overcomes both of the deficiencies noted for the Palmgren-Miner method; historically it is a much more recent approach, and it is just as easy to use. Except for a slight change, we shall use and recommend the Manson method in this book. Manson plotted the S–log N diagram instead of a log S–log N plot as is recommended here. Manson also resorted to experiment to find the point of convergence of the S–log N lines corresponding to the static strength, instead of arbitrarily selecting the intersection of $N = 10^3$ cycles with $S = 0.9S_{ut}$ as is done here. Of course, it is always better to use experiment, but our purpose in this book has been to use the simple test data to learn as much as possible about fatigue failure.

The method of Manson, as presented here, consists in having all log S–log N lines, that is, lines for both the damaged and the virgin material, converge to the same point, $0.9S_{ut}$ at 10^3 cycles. In addition, the log S–log N lines must be constructed in the same historical order in which the stresses occur.

The data from the preceding example are used for illustrative purposes. The results are shown in Fig. 7–35. Note that the strength $S_{f,1}$ corresponding to $N_1 - n_1 = 5.52(10^3)$ cycles is found in the same manner as before. Through this point and through $0.9S_{ut}$ at 10^3 cycles, draw the heavy dashed line to meet $N = 10^6$ cycles and define the

[29]S. S. Manson, A. J. Nachtigall, C. R. Ensign, and J. C. Fresche, "Further Investigation of a Relation for Cumulative Fatigue Damage in Bending," *Trans. ASME, J. Eng. Ind.,* ser. B, vol. 87, No. 1, pp. 25–35, February 1965.

endurance limit $S'_{e,1}$ of the damaged material. In this case the new endurance limit is 34.4 kpsi, somewhat less than that found by the Miner method.

It is now easy to see from Fig. 7–35 that a reversed stress $\sigma = 36$ kpsi, say, would not harm the endurance limit of the virgin material, no matter how many cycles it might be applied. However, if $\sigma = 36$ kpsi should be applied *after* the material was damaged by $\sigma_1 = 60$ kpsi, then additional damage would be done.

Both these rules involve a number of computations, which are repeated every time damage is estimated. For complicated stress-time traces, this might be every cycle. Clearly a computer program is useful to perform the tasks, including scanning the trace and identifying the cycles.

Collins said it well: "In spite of all the problems cited, the Palmgren linear damage rule is frequently used because of its simplicity and the experimental fact that other more complex damage theories do not always yield a significant improvement in failure prediction reliability."[30]

7–16 Surface Fatigue Strength

The surface fatigue mechanism is not definitively understood. The contact-affected zone, in the absence of surface shearing tractions, entertains compressive principal stresses. Rotary fatigue has its cracks grown at or near the surface in the presence of tensile stresses that are associated with crack propagation, to catastrophic failure. There are shear stresses in the zone, which are largest just below the surface. Cracks seem to grow from this stratum until small pieces of material are expelled, leaving pits on the surface. Because engineers had to design durable machinery before the surface fatigue phenomenon was understood in detail, they had taken the posture of conducting tests, observing pits on the surface, and declaring failure at an arbitrary projected area of hole, and they related this to the Hertzian contact pressure. This compressive stress did not produce the failure directly, but whatever the failure mechanism, whatever the stress type that was instrumental in the failure, the contact stress was an *index* to its magnitude.

Buckingham[31] conducted a number of tests relating the fatigue at 10^8 cycles to endurance strength (Hertzian contact pressure). While there is evidence of an endurance limit at about $3(10^7)$ cycles for cast materials, hardened steel rollers showed no endurance limit up to $4(10^8)$ cycles. Subsequent testing on hard steel shows no endurance limit. Hardened steel exhibits such high fatigue strengths that its use in resisting surface fatigue is widespread.

Our studies thus far have dealt with the failure of a machine element by yielding, by fracture, and by fatigue. The endurance limit obtained by the rotating-beam test is frequently called the *flexural endurance limit,* because it is a test of a rotating beam. In this section we shall study a property of *mating materials* called the *surface endurance shear*. The design engineer must frequently solve problems in which two machine elements mate with one another by rolling, sliding, or a combination of rolling and sliding contact. Obvious examples of such combinations are the mating teeth of a pair of gears, a cam and follower, a wheel and rail, and a chain and sprocket. A knowledge of the surface strength of materials is necessary if the designer is to create machines having a long and satisfactory life.

When two surfaces roll or roll and slide against one another with sufficient force, a pitting failure will occur after a certain number of cycles of operation. Authorities are not in complete agreement on the exact mechanism of the pitting; although the subject

[30] J. A. Collins, *Failure of Materials in Mechanical Design,* John Wiley & Sons, New York, 1981, p. 243.

[31] Earle Buckingham, *Analytical Mechanics of Gears,* McGraw-Hill, New York, 1949.

is quite complicated, they do agree that the Hertz stresses, the number of cycles, the surface finish, the hardness, the degree of lubrication, and the temperature all influence the strength. In Sec. 4–20 it was learned that, when two surfaces are pressed together, a maximum shear stress is developed slightly below the contacting surface. It is postulated by some authorities that a surface fatigue failure is initiated by this maximum shear stress and then is propagated rapidly to the surface. The lubricant then enters the crack that is formed and, under pressure, eventually wedges the chip loose.

To determine the surface fatigue strength of mating materials, Buckingham designed a simple machine for testing a pair of contacting rolling surfaces in connection with his investigation of the wear of gear teeth. Buckingham and, later, Talbourdet gathered large numbers of data from many tests so that considerable design information is now available. To make the results useful for designers, Buckingham defined a *load-stress factor,* also called a *wear factor,* which is derived from the Hertz equations. Equations (4–77) and (4–78) for contacting cylinders are found to be

$$b = \sqrt{\frac{2F}{\pi l}\frac{\left(1-\nu_1^2\right)/E_1 + \left(1-\nu_2^2\right)/E_2}{(1/d_1)+(1/d_2)}} \tag{7–59}$$

$$p_{\max} = \frac{2F}{\pi b l} \tag{7–60}$$

where b = half width of rectangular contact area
F = contact force
l = length of cylinders
ν = Poisson's ratio
E = modulus of elasticity
d = cylinder diameter

It is more convenient to use the cylinder radius, so let $2r = d$. If we then designate the length of the cylinders as w (for width of gear, bearing, cam, etc.) instead of l and remove the square root sign, Eq. (7–59) becomes

$$b^2 = \frac{4F}{\pi w}\frac{\left(1-\nu_1^2\right)/E_1 + \left(1-\nu_2^2\right)/E_2}{1/r_1 + 1/r_2} \tag{7–61}$$

We can define a *surface endurance strength* S_C using

$$p_{\max} = \frac{2F}{\pi b w} \tag{7–62}$$

as

$$S_C = \frac{2F}{\pi b w} \tag{7–63}$$

which may also be called *contact strength,* the *contact fatigue strength,* or the *Hertzian endurance strength*. The strength is the contacting pressure which, after a specified number of cycles, will cause failure of the surface. Such failures are often called *wear* because they occur over a very long time. They should not be confused with abrasive wear, however. By substituting the value of b in Eq. (7–61) and substituting the result into Eq. (7–63), we obtain

$$\frac{F}{w}\left(\frac{1}{r_1}+\frac{1}{r_2}\right) = \pi S_C^2\left[\frac{1-\nu_1^2}{E_1}+\frac{1-\nu_2^2}{E_2}\right] = K_1 \tag{7–64}$$

The left expression consists of parameters a designer may seek to control independently. The central expression consists of material properties that come with the material and condition specification. The third expression is the parameter K_1, Buckingham's load-stress factor, determined by a test fixture with values F, w, r_1, r_2 and the number of cycles associated with the first tangible evidence of fatigue. In gear studies a similar K factor is used:

$$K_g = \frac{K_1}{4} \sin \phi \tag{7–65}$$

where ϕ is the tooth pressure angle, and the term $[(1 - \nu_1^2)/E_1 + (1 - \nu_2^2)/E_2]$ is defined as $1/(\pi C_P^2)$, so that

$$S_C = C_P \sqrt{\frac{F}{w}\left(\frac{1}{r_1} + \frac{1}{r_2}\right)} \tag{7–66}$$

Buckingham and others reported K_1 for 10^8 cycles and nothing else. This gives only one point on the $S_C N$ curve. For cast metals this may be sufficient, but for wrought steels, heat-treated, some idea of the slope is useful in meeting design goals of other than 10^8 cycles.

Experiments show that K_1 versus N, K_g versus N, and S_C versus N data are rectified by loglog transformation. This suggests that

$$K_1 = \alpha_1 N^{\beta_1} \qquad K_g = aN^b \qquad S_C = \alpha N^{\beta}$$

The three exponents are given by

$$\beta_1 = \frac{\log(K_1/K_2)}{\log(N_1/N_2)} \qquad b = \frac{\log(K_{g1}/K_{g2})}{\log(N_1/N_2)} \qquad \beta = \frac{\log(S_{C1}/S_{C2})}{\log(N_1/N_2)} \tag{7–67}$$

Data on induction-hardened steel on steel give $(S_C)_{10^7} = 271$ kpsi and $(S_C)_{10^8} = 239$ kpsi, so β, from Eq. (7–67), is

$$\beta = \frac{\log(271/239)}{\log(10^7/10^8)} = -0.055$$

It may be of interest that the American Gear Manufacturers Association (AGMA) uses -0.056 between $10^4 < N < 10^{10}$ if the designer has no data to the contrary beyond 10^7 cycles.

A longstanding correlation in steels between S_C and H_B at 10^8 cycles is

$$(S_C)_{10^8} = \begin{cases} 0.4H_B - 10 \text{ kpsi} \\ 2.76H_B - 70 \text{ MPa} \end{cases} \tag{7–68}$$

AGMA uses

$${}_{0.99}(S_C)_{10^7} = 0.327H_B + 26 \text{ kpsi} \tag{7–69}$$

Equation (7–66) can be used in design to find an allowable surface stress by using a design factor. Since this equation is nonlinear in its stress-load transformation, the designer must decide if loss of function denotes inability to carry the load. If so, then to find the allowable stress, one divides the load F by the design factor n_d:

$$\sigma_C = C_P \sqrt{\frac{F}{w n_d}\left(\frac{1}{r_1} + \frac{1}{r_2}\right)} = \frac{C_P}{\sqrt{n_d}} \sqrt{\frac{F}{w}\left(\frac{1}{r_1} + \frac{1}{r_2}\right)} = \frac{S_C}{\sqrt{n_d}}$$

and $n_d = (S_C/\sigma_C)^2$. If the loss of function is focused on stress, then $n_d = S_C/\sigma_C$. It is recommended that an engineer

- Decide whether loss of function is failure to carry load or stress.
- Define the design factor and factor of safety accordingly.

- Announce what he or she is using and why.
- Be prepared to defend his or her position.

In this way everyone who is party to the communication knows what a design factor (or factor of safety) of 2 means and adjusts, if necessary, the judgmental perspective.

7–17 Stochastic Analysis

As already demonstrated in this chapter, there are a great many factors to consider in a fatigue analysis, much more so than in a static analysis. So far, each factor has been treated in a deterministic manner, and if not obvious, these factors are subject to variability and control the overall reliability of the results. When reliability is important, then fatigue testing must certainly be undertaken. There is no other way. Consequently, the methods of stochastic analysis presented here and in other sections of this book constitute guidelines that enable the designer to obtain a good understanding of the various issues involved and help in the development of a safe and reliable design.

In this section, key stochastic modifications to the deterministic features and equations described in earlier sections are provided in the same order of presentation.

Endurance Limit

To begin, a method for estimating endurance limits, the *tensile strength correlation method,* is presented. The ratio $\boldsymbol{\phi} = \mathbf{S}'_e/\bar{S}_{ut}$ is called the *fatigue ratio*.[32] For ferrous metals, most of which exhibit an endurance limit, the endurance limit is used as a numerator. For materials that do not show an endurance limit, an endurance strength at a specified number of cycles to failure is used and noted. Gough[33] reported the stochastic nature of the fatigue ratio $\boldsymbol{\phi}$ for several classes of metals, and this is shown in Fig. 7–36. The first item to note is that the coefficient of variation is of the order 0.10 to 0.15, and the distribution varies for classes of metals. The second item to note is that Gough's data include materials of no interest to engineers. In the absence of testing, engineers use the correlation that $\boldsymbol{\phi}$ represents to estimate the endurance limit $\mathbf{S}'_e$ from the mean ultimate strength $\bar{S}_{ut}$.

Gough's data are for ensembles of metals, some chosen for metallurgical interest, and include materials that are not commonly selected for machine parts. Mischke[34] analyzed data for 133 common steels and treatments in varying diameters in rotating bending,[35] and the result was

$$\boldsymbol{\phi} = 0.445d^{-0.107}\mathbf{LN}(1, 0.138)$$

where d is the specimen diameter in inches and $\mathbf{LN}(1, 0.138)$ is a unit lognormal variate with a mean of 1 and a standard deviation (and coefficient of variation) of 0.138. For the standard R. R. Moore specimen,

$$\boldsymbol{\phi}_{0.30} = 0.445(0.30)^{-0.107}\mathbf{LN}(1, 0.138) = 0.506\mathbf{LN}(1, 0.138)$$

[32]From this point, since we will be dealing with statistical distributions in terms of means, standard deviations, etc. A key quantity, the ultimate strength, will here be presented by its mean value, $\bar{S}_{ut}$. This means that certain terms that were defined earlier in terms of the minimum value of S_{ut} will change slightly.

[33]In J. A. Pope, *Metal Fatigue,* Chapman and Hall, London, 1959.

[34]Charles R. Mischke, "Prediction of Stochastic Endurance Strength," *Trans. ASME, Journal of Vibration, Acoustics, Stress, and Reliability in Design,* vol. 109, no. 1, January 1987, pp. 113–122.

[35]Data from H. J. Grover, S. A. Gordon, and L. R. Jackson, *Fatigue of Metals and Structures*, Bureau of Naval Weapons, Document NAVWEPS 00-2500435, 1960.

Figure 7–36

The lognormal probability density PDF of the fatigue ratio ϕ_b of Gough.

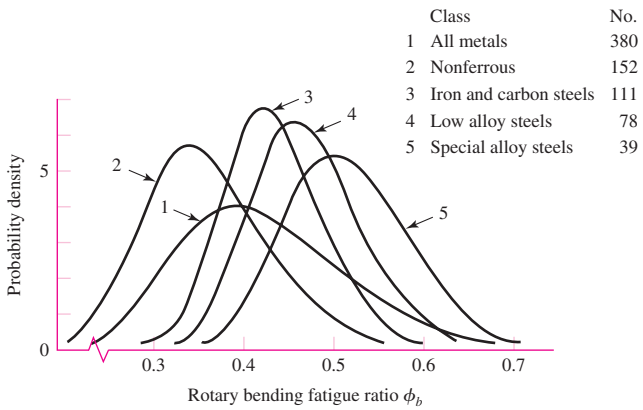

Also, 25 plain carbon and low-alloy steels with $S_{ut} > 212$ kpsi are described by

$$\mathbf{S}'_e = 107\mathbf{LN}(1, 0.139) \text{ kpsi}$$

In summary, for the rotating-beam specimen,

$$\mathbf{S}'_e = \begin{cases} 0.506\bar{S}_{ut}\mathbf{LN}(1, 0.138) \text{ kpsi or MPa} & \bar{S}_{ut} \le 212 \text{ kpsi (1460 MPa)} \\ 107\mathbf{LN}(1, 0.139) \text{ kpsi} & \bar{S}_{ut} > 212 \text{ kpsi} \\ 740\mathbf{LN}(1, 0.139) \text{ MPa} & \bar{S}_{ut} > 1460 \text{ MPa} \end{cases} \tag{7–70}$$

where $\bar{S}_{ut}$ is the *mean* ultimate tensile strength.

Equations (7–70) represent the state of information before an engineer has chosen a material. In choosing, the designer has made a random choice from the ensemble of possibilities, and the statistics can give the odds of disappointment. If the testing is limited to finding an estimate of the ultimate tensile strength mean $\bar{S}_{ut}$ with the chosen material, Eqs. (7–70) are directly helpful. If there is to be rotary-beam fatigue testing, then statistical information on the endurance limit is gathered and there is no need for the correlation above.

Table 7–12 compares approximate mean values of the fatigue ratio $\bar{\phi}_{0.30}$ for several classes of ferrous materials.

Endurance Limit Modifying Factors

A Marin equation can be written as

$$\mathbf{S}_e = \mathbf{k}_a k_b \mathbf{k}_c \mathbf{k}_d \mathbf{k}_f \mathbf{S}'_e \tag{7–71}$$

where the size factor k_b is deterministic and remains unchanged from that given in Sec. 7–9. Also, since we are performing a stochastic analysis, the "reliability factor" k_e is unnecessary here.

The surface factor $\mathbf{k}_a$ cited earlier in deterministic form as Eq. (7–19) is now given in stochastic form by

$$\mathbf{k}_a = a\bar{S}_{ut}^b \mathbf{LN}(1, C) \qquad (\bar{S}_{ut} \text{ in kpsi or MPa}) \tag{7–72}$$

where Table 7–13 gives values of a, b, and C for various surface conditions.

Table 7–12

Comparison of Approximate Values of Mean Fatigue Ratio for Some Classes of Metals

Material Class	$\bar{\phi}_{0.30}$
Wrought steels	0.50
Cast steels	0.40
Powdered steels	0.38
Gray cast iron	0.35
Malleable cast iron	0.40
Normalized nodular cast iron	0.33

Table 7–13

Parameters in Marin Surface Condition Factor

$\mathbf{k}_a = aS_{ut}^b\,\mathbf{LN}(1, C)$				
Surface Finish	a kpsi	a MPa	b	Coefficient of Variation, C
Ground*	1.34	1.58	−0.086	0.120
Machined or Cold-rolled	2.67	4.45	−0.265	0.058
Hot-rolled	14.5	58.1	−0.719	0.110
As-forged	39.8	271	−0.995	0.145

*Due to the wide scatter in ground surface data, an alternate function is $\mathbf{k}_a = 0.878\mathbf{LN}(1, 0.120)$. *Note:* S_{ut} in kpsi or MPa.

EXAMPLE 7–17 A steel has a mean ultimate strength of 520 MPa and a machined surface. Estimate $\mathbf{k}_a$.

Solution From Table 7–13,

$$\mathbf{k}_a = 4.45(520)^{-0.265}\mathbf{LN}(1, 0.058)$$

$$\bar{k}_a = 4.45(520)^{-0.265}(1) = 0.848$$

$$\hat{\sigma}_{ka} = C\bar{k}_a = (0.058)4.45(520)^{-0.265} = 0.049$$

Answer so $\mathbf{k}_a = \mathbf{LN}(0.848, 0.049)$.

The load factor $\mathbf{k}_c$ for axial and torsional loading is given by

$$(\mathbf{k}_c)_{\text{axial}} = 1.23\bar{S}_{ut}^{-0.0778}\mathbf{LN}(1, 0.125) \tag{7–73}$$

$$(\mathbf{k}_c)_{\text{torsion}} = 0.328\bar{S}_{ut}^{0.125}\mathbf{LN}(1, 0.125) \tag{7–74}$$

There are fewer data to study for axial fatigue. Equation (7–73) was deduced from the data of Landgraf and of Grover, Gordon, and Jackson (as cited earlier).

Torsional data are sparser, and Eq. (7–74) is deduced from data in Grover et al. Notice the mild sensitivity to strength in the axial and torsional load factor, so $\mathbf{k}_c$ in these cases is not constant. Average values are shown in the last column of Table 7–14, and as footnotes to Tables 7–15 and 7–16. Table 7–17 shows the influence of material classes on the load factor $\mathbf{k}_c$. Distortion energy theory predicts $(k_c)_{\text{torsion}} = 0.577$ for materials to which the distortion-energy theory applies. For bending, $\mathbf{k}_c = \mathbf{LN}(1, 0)$.

Table 7–14

Parameters in Marin Loading Factor

$k_c = \alpha \bar{S}_{ut}^{\beta}\,\mathrm{LN}(1, C)$					
Mode of Loading	α kpsi	α MPa	β	C	Average k_c
Bending	1	1	0	0	1
Axial	1.23	1.43	−0.078	0.125	0.85
Torsion	0.328	0.258	0.125	0.125	0.59

Table 7–15

Average Marin Loading Factor for Axial Load

$\bar{S}_{ut}$, kpsi	k_c^*
50	0.907
100	0.860
150	0.832
200	0.814

*Average entry 0.85.

Table 7–16

Average Marin Loading Factor for Torsional Load

$\bar{S}_{ut}$, kpsi	k_c^*
50	0.535
100	0.583
150	0.614
200	0.636

*Average entry 0.59.

Table 7–17

Average Marin Torsional Loading Factor k_c for Several Materials

Material	Range	n	$\bar{k}_c$	$\hat{\sigma}_{kc}$
Wrought steels	0.52–0.69	31	0.60	0.03
Wrought Al	0.43–0.74	13	0.55	0.09
Wrought Cu and alloy	0.41–0.67	7	0.56	0.10
Wrought Mg and alloy	0.49–0.60	2	0.54	0.08
Titanium	0.37–0.57	3	0.48	0.12
Cast iron	0.79–1.01	9	0.90	0.07
Cast Al, Mg, and alloy	0.71–0.91	5	0.85	0.09

Source: The table is an extension of P. G. Forrest, *Fatigue of Metals*, Pergamon Press, London, 1962, Table 17, p. 110, with standard deviations estimated from range and sample size using Table A–1 in J. B. Kennedy and A. M. Neville, *Basic Statistical Methods for Engineers and Scientists*, 3rd ed., Harper & Row, New York, 1986, pp. 54–55.

EXAMPLE 7–18 Estimate the Marin loading factor $\mathbf{k}_c$ for a 1–in-diameter bar that is used as follows.
(*a*) In bending. It is made of steel with $\mathbf{S}_{ut} = 100\mathbf{LN}(1, 0.035)$ kpsi, and the designer intends to use the correlation $\mathbf{S}'_e = \boldsymbol{\phi}_{0.30}\bar{S}_{ut}$ to predict $\mathbf{S}'_e$.
(*b*) In bending, but endurance testing gave $\mathbf{S}'_e = 55\mathbf{LN}(1, 0.081)$ kpsi.
(*c*) In push-pull (axial) fatigue, $\mathbf{S}_{ut} = \mathbf{LN}(86.2, 3.92)$ kpsi, and the designer intended to use the correlation $\mathbf{S}'_e = \boldsymbol{\phi}_{0.30}\bar{S}_{ut}$.
(*d*) In torsional fatigue. The material is cast iron, and $\mathbf{S}'_e$ is known by test.

Solution (*a*) Since the bar is in bending,

Answer
$$\mathbf{k}_c = (1, 0)$$

(*b*) Since the test is in bending and use is in bending,

Answer
$$\mathbf{k}_c = (1, 0)$$

(*c*) From Eq. (7–73),

Answer
$$(\mathbf{k}_c)_{ax} = 1.23(86.2)^{-0.0778}\mathbf{LN}(1, 0.125)$$
$$\bar{k}_c = 1.23(86.2)^{-0.0778}(1) = 0.870$$
$$\hat{\sigma}_{kc} = C\bar{k}_c = 0.125(0.870) = 0.109$$

(*d*) From Table 7–17, $\bar{k}_c = 0.90$, $\hat{\sigma}_{kc} = 0.07$, and

Answer
$$C_{kc} = \frac{0.07}{0.90} = 0.08$$

The temperature factor $\mathbf{k}_d$ is

$$\mathbf{k}_d = \bar{k}_d\mathbf{LN}(1, 0.11) \tag{7–75}$$

where $\bar{k}_d = k_d$, given by Eq. (7–26).

Finally, $\mathbf{k}_e$ is, as before, the miscellaneous factor that can come about from a great many considerations, as discussed in Sec. 7–9, where now statistical distributions, possibly from testing, are considered.

Stress Concentration and Notch Sensitivity

Notch sensitivity q was defined by Eq. (2–30). The stochastic equivalent is

$$\mathbf{q} = \frac{\mathbf{K}_f - 1}{K_t - 1} \tag{7–76}$$

where K_t is the theoretical (or geometric) stress-concentration factor, a deterministic quantity. A study of lines 3 and 4 of Table 2–6 will reveal that adding a scalar to (or subtracting one from) a variate $\mathbf{x}$ will affect only the mean. Also, multiplying (or dividing) by a scalar affects both the mean and standard deviation. With this in mind, we can

Table 7–18

Coefficients of Variation C_{Kf} for Steels

Notch Type	Coefficient of Variation C_{Kf}
Transverse hole	0.10
Shoulder	0.11
Groove	0.15

Notes: Heywood's coefficients of variation. Notch sensitivity charts can be avoided using a modified Neuber equation. See Sec. 7–10.

relate the statistical parameters of the fatigue stress-concentration factor $\mathbf{K}_f$ to those of notch sensitivity $\mathbf{q}$. It follows that

$$\mathbf{q} = \mathbf{LN}\left(\frac{\bar{K}_f - 1}{K_t - 1}, \frac{C\bar{K}_f}{K_t - 1}\right)$$

where $C = C_{Kf}$ and

$$\bar{q} = \frac{\bar{K}_f - 1}{K_t - 1}$$

$$\hat{\sigma}_q = \frac{C\bar{K}_f}{K_t - 1} \tag{7–77}$$

$$C_q = \frac{C\bar{K}_f}{\bar{K}_f - 1}$$

The fatigue stress-concentration factor $\mathbf{K}_f$ has been investigated more in England than in the United States. Values of C_{Kf} for transverse holes, shoulders, and grooves are listed in Table 7–18. Once $\mathbf{K}_f$ is described, $\mathbf{q}$ can also be quantified using the set Eqs. (7–77).

The modified Neuber equation (after Heywood) gives the fatigue stress concentration factor as

$$\mathbf{K}_f = \bar{K}_f \mathbf{LN}\left(1, C_{K_f}\right) \tag{7–78}$$

where $\bar{K}_f = K_f$, given by Eq. (7–35).

EXAMPLE 7–19 Estimate $\mathbf{K}_f$ and $\mathbf{q}$ for the steel shaft given in Ex. 7–6.

Solution From Ex. 7–6 and Eq. (7–35), $K_f = 1.51$. From Table 7–18, $C_{K_f} = 0.11$. Thus, from Eq. (7–78),

Answer $$\mathbf{K}_f = 1.51\mathbf{LN}(1, 0.11)$$

From Eq. (7–77), with $K_t = 1.65$ from Ex. 7–6,

$$\bar{q} = \frac{1.51 - 1}{1.65 - 1} = 0.785$$

$$C_q = \frac{C_{K_f}\bar{K}_f}{\bar{K}_f - 1} = \frac{0.11(1.51)}{1.51 - 1} = 0.326$$

$$\hat{\sigma}_q = C_q\bar{q} = 0.326(0.785) = 0.256$$

So,

Answer $$\mathbf{q} = \mathbf{LN}(0.785, 0.256)$$

EXAMPLE 7–20 The bar shown in Fig. 7–37 is machined from a cold-rolled flat having an ultimate strength of $\mathbf{S}_{ut} = \mathbf{LN}(87.6, 5.74)$ kpsi. The axial load shown is completely reversed. The load amplitude is $\mathbf{F}_a = \mathbf{LN}(1000, 120)$ lbf.
(*a*) Estimate the reliability.
(*b*) Reestimate the reliability when a rotating bending endurance test shows that $\mathbf{S}'_e = \mathbf{LN}(40, 2)$ kpsi.

Solution (*a*) From Eq. (7–70), $\mathbf{S}'_e = 0.506\bar{S}_{ut}\mathbf{LN}(1, 0.138) = 0.506(87.6)\mathbf{LN}(1, 0.138)$

$$= 44.3\mathbf{LN}(1, 0.138) \text{ kpsi}$$

From Eq. (7–72) and Table 7–13,

$$\mathbf{k}_a = 2.67\bar{S}_{ut}^{-0.265}\mathbf{LN}(1, 0.058) = 2.67(87.6)^{-0.265}\mathbf{LN}(1, 0.058)$$

$$= 0.816\mathbf{LN}(1, 0.058)$$

$$k_b = 1 \qquad \text{(axial loading)}$$

From Eq. (7–73),

$$\mathbf{k}_c = 1.23\bar{S}_{ut}^{-0.0778}\mathbf{LN}(1, 0.125) = 1.23(87.6)^{-0.0778}\mathbf{LN}(1, 0.125)$$

$$= 0.869\mathbf{LN}(1, 0.125)$$

$$\mathbf{k}_d = \mathbf{k}_f = (1, 0)$$

The endurance strength, from Eq. (7–71), is

$$\mathbf{S}_e = \mathbf{k}_a k_b \mathbf{k}_c \mathbf{k}_d \mathbf{k}_f \mathbf{S}'_e$$

$$\mathbf{S}_e = 0.816\mathbf{LN}(1, 0.058)(1)0.868\mathbf{LN}(1, 0.125)(1)(1)44.3\mathbf{LN}(1, 0.138)$$

The parameters of $\mathbf{S}_e$ are

$$\bar{S}_e = 0.816(0.868)44.3 = 31.4 \text{ kpsi}$$

$$C_{Se} = (0.058^2 + 0.125^2 + 0.138^2)^{1/2} = 0.195$$

so $\mathbf{S}_e = 31.4\mathbf{LN}(1, 0.195)$ kpsi.

In computing the stress, the section at the hole governs. Using the terminology of Table A–15–1 we find $d/w = 0.50$, therefore $K_t = 2.18$. From Tables 7–8 and 7–18, $\sqrt{a} = 5/S_{ut} = 5/87.6 = 0.057$ and $C_{kf} = 0.10$. From Eqs. (7–35) and (7–78) with $r = 0.375$ in,

$$\mathbf{K}_f = \frac{K_t}{1 + \dfrac{2(K_t - 1)}{K_t}\dfrac{\sqrt{a}}{\sqrt{r}}}\mathbf{LN}\left(1, C_{K_f}\right) = \frac{2.18}{1 + \dfrac{2(2.18 - 1)}{2.18}\dfrac{0.057}{\sqrt{0.375}}}\mathbf{LN}(1, 0.10)$$

$$= 1.98\mathbf{LN}(1, 0.10)$$

Figure 7–37

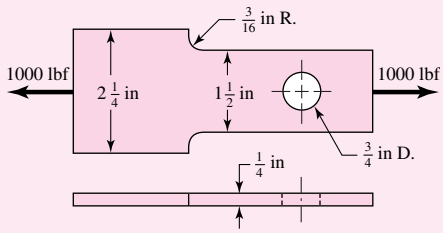

The stress at the hole is

$$\boldsymbol{\sigma} = \mathbf{K}_f \frac{\mathbf{F}}{A} = 1.98\mathbf{LN}(1, 0.10)\frac{1000\mathbf{LN}(1, 0.12)}{0.25(0.75)}$$

$$\bar{\sigma} = 1.98\frac{1000}{0.25(0.75)}10^{-3} = 10.56 \text{ kpsi}$$

$$C_\sigma = (0.10^2 + 0.12^2)^{1/2} = 0.156$$

so stress can be expressed as $\boldsymbol{\sigma} = 10.56\mathbf{LN}(1, 0.156)$ kpsi.

The endurance limit is considerably greater than the load-induced stress, indicating that finite life is not a problem. For interfering lognormal-lognormal distributions, Eq. (6–57) gives

$$z = -\frac{\ln\left(\dfrac{\bar{S}_e}{\bar{\sigma}}\sqrt{\dfrac{1+C_\sigma^2}{1+C_{S_e}^2}}\right)}{\sqrt{\ln\left[\left(1+C_{S_e}^2\right)\left(1+C_\sigma^2\right)\right]}} = -\frac{\ln\left(\dfrac{31.4}{10.56}\sqrt{\dfrac{1+0.156^2}{1+0.195^2}}\right)}{\sqrt{\ln[(1+0.195^2)(1+0.156^2)]}} = -4.36$$

From Table A–10 the probability of failure $p_f = \Phi(-4.36) = .000\,006\,66$, and the reliability is

Answer

$$R = 1 - 0.000\,006\,66 = 0.999\,993\,34$$

(*b*) The rotary endurance tests are described by $\mathbf{S}'_e = 40\mathbf{LN}(1, 0.05)$ kpsi whose mean is *less* than the predicted mean in part *a*. The mean endurance strength $\bar{S}_e$ is

$$\bar{S}_e = 0.816(0.868)40 = 28.3 \text{ kpsi}$$

$$C_{Se} = (0.058^2 + 0.125^2 + 0.05^2)^{1/2} = 0.147$$

so the endurance strength can be expressed as $\mathbf{S}_e = 28.3\mathbf{LN}(1, 0.147)$ kpsi. From Eq. (6–57),

$$z = -\frac{\ln\left(\dfrac{28.3}{10.56}\sqrt{\dfrac{1+0.156^2}{1+0.147^2}}\right)}{\sqrt{\ln[(1+0.147^2)(1+0.156^2)]}} = -4.63$$

Using Table A–10, we see the probability of failure $p_f = \Phi(-4.63) = 0.000\,001\,87$, and

$$R = 1 - 0.000\,001\,87 = 0.999\,998\,13$$

an increase! The reduction in the probability of failure is $(0.000\,001\,87 - 0.000\,006\,66)/0.000\,006\,66 = -0.72$, a reduction of 72 percent. We are analyzing an existing design, so in part (*a*) the factor of safety was $\bar{n} = \bar{S}/\bar{\sigma} = 31.3/10.56 = 2.96$. In part (*b*) $\bar{n} = 28.3/10.56 = 2.68$, a *decrease*. This example gives you the opportunity to see the role of the design factor. Given knowledge of $\bar{S}$, C_S, $\bar{\sigma}$, C_σ, and reliability (through z), the mean factor of safety (as a design factor) separates $\bar{S}$ and $\bar{\sigma}$ so that the reliability goal is achieved. Knowing $\bar{n}$ alone *says nothing about the probability of failure*. Looking at $\bar{n} = 2.96$ and $\bar{n} = 2.68$ says nothing about the respective probabilities of failure. The tests did not reduce $\bar{S}_e$ significantly, but reduced the variation C_S such that the reliability was *increased*.

When a mean design factor (or mean factor of safety) defined as $\bar{S}_e/\bar{\sigma}$ is said to be *silent* on matters of frequency of failures, it means that a scalar factor of safety by itself does not offer any information about probability of failure. Nevertheless, some engineers let the factor of safety speak up, and they can be wrong in their conclusions.

As revealing as Ex. 7–20 is concerning the meaning (and lack of meaning) of a design factor or factor of safety, let us remember that the rotary testing associated with part (*b*) changed *nothing* about the part, but only our knowledge about the part. The mean endurance limit was 40 kpsi all the time, and our adequacy assessment had to move with what was known.

Fluctuating Stresses

Deterministic failure loci that lie among the data are candidates for regression models. Included among these are the Gerber, ASME-elliptic, and, for brittle materials, Smith-Dolan models, which use mean values in their presentation. The Gerber parabola is

$$\frac{\bar{S}_a}{\bar{S}_e} + \left(\frac{\bar{S}_m}{\bar{S}_{ut}}\right)^2 = 1 \tag{7–79}$$

Just as the deterministic failure loci are located by endurance strength and ultimate tensile (or yield) strength, so too are stochastic failure loci located by $\mathbf{S}_e$ and by $\mathbf{S}_{ut}$ or $\mathbf{S}_y$. Figure 7–32 shows how the mean locus of Eq. (7–79) fits a parabola to form the Gerber mean locus. We also need to establish a contour located one standard deviation from the mean. Since stochastic loci are most likely to be used with a radial load line, we will develop the equation using the load line slope $r = \bar{S}_a/\bar{S}_m$. Substituting $\bar{S}_m = \bar{S}_a/r$ in Eq. (7–79) and solving for $\bar{S}_a$ gives

$$\bar{S}_a = \frac{r^2\bar{S}_{ut}^2}{2\bar{S}_e}\left[-1 + \sqrt{1 + \left(\frac{2\bar{S}_e}{r\bar{S}_{ut}}\right)^2}\right] \tag{7–80}$$

Because of the positive correlation between $\mathbf{S}_e$ and $\mathbf{S}_{ut}$, we increment $\bar{S}_e$ by $C_{Se}\bar{S}_e$, $\bar{S}_{ut}$ by $C_{Sut}\bar{S}_{ut}$, and $\bar{S}_a$ by $C_{Sa}\bar{S}_a$, substitute into Eq. (7–80), and solve for C_{Sa} to obtain

$$C_{Sa} = \frac{(1 + C_{Sut})^2}{1 + C_{Se}} \frac{\left\{-1 + \sqrt{1 + \left[\dfrac{2\bar{S}_e(1 + C_{Se})}{r\bar{S}_{ut}(1 + C_{Sut})}\right]^2}\right\}}{\left[-1 + \sqrt{1 + \left(\dfrac{2\bar{S}_e}{r\bar{S}_{ut}}\right)^2}\right]} - 1 \tag{7–81}$$

Equation (7–81) can be viewed as an interpolation formula for C_{Sa}, which falls between C_{Se} and C_{Sut} depending on load line slope r. Note that $\mathbf{S}_a = \bar{S}_a\mathbf{LN}(1, C_{Sa})$.

The ASME-elliptic criterion is expressed in terms of its means as

$$\left(\frac{\bar{S}_a}{\bar{S}_e}\right)^2 + \left(\frac{\bar{S}_m}{\bar{S}_y}\right)^2 = 1 \tag{7–82}$$

Similarly, substituting $\bar{S}_m = \bar{S}_a/r$ into Eq. (7–82) and solving for $\bar{S}_a$ gives

$$\bar{S}_a = \frac{r\bar{S}_y\bar{S}_e}{\sqrt{r^2\bar{S}_y^2 + \bar{S}_e^2}} \tag{7–83}$$

Similarly, we increment $\bar{S}_e$ by $C_{Se}\bar{S}_e$, $\bar{S}_y$ by $C_{Sy}\bar{S}_y$, and $\bar{S}_a$ by $C_{Sa}\bar{S}_a$, substitute into Eq. (7–83), and solve for C_{Sa}:

$$C_{Sa} = (1 + C_{Sy})(1 + C_{Se}) \sqrt{\frac{r^2\bar{S}_y^2 + \bar{S}_e^2}{r^2\bar{S}_y^2(1 + C_{Sy})^2 + \bar{S}_e^2(1 + C_{Se})^2}} - 1 \tag{7–84}$$

Many *brittle* materials follow a Smith-Dolan failure criterion, written deterministically as

$$\frac{n\sigma_a}{S_e} = \frac{1 - n\sigma_m/S_{ut}}{1 + n\sigma_m/S_{ut}} \tag{7–85}$$

Expressed in terms of its means,

$$\frac{\bar{S}_a}{\bar{S}_e} = \frac{1 - \bar{S}_m/\bar{S}_{ut}}{1 + \bar{S}_m/\bar{S}_{ut}} \tag{7–86}$$

For a radial load line slope of r, we substitute $\bar{S}_a/r$ for $\bar{S}_m$ and solve for $\bar{S}_a$, obtaining

$$\bar{S}_a = \frac{r\bar{S}_{ut} + \bar{S}_e}{2}\left[-1 + \sqrt{1 + \frac{4r\bar{S}_{ut}\bar{S}_e}{(r\bar{S}_{ut} + \bar{S}_e)^2}}\right] \tag{7–87}$$

and the expression for C_{Sa} is

$$C_{Sa} = \frac{r\bar{S}_{ut}(1 + C_{Sut}) + \bar{S}_e(1 + C_{Se})}{2\bar{S}_a} \cdot \left\{-1 + \sqrt{1 + \frac{4r\bar{S}_{ut}\bar{S}_e(1 + C_{Se})(1 + C_{Sut})}{[r\bar{S}_{ut}(1 + C_{Sut}) + \bar{S}_e(1 + C_{Se})]^2}}\right\} - 1 \tag{7–88}$$

EXAMPLE 7–21 A rotating shaft experiences a steady torque $\mathbf{T} = 1360\mathbf{LN}(1, 0.05)$ lbf · in, and at a shoulder with a 1.1-in small diameter, a fatigue stress-concentration factor $\mathbf{K}_f = 1.50\mathbf{LN}(1, 0.11)$, $K_{fs} = 1.28\mathbf{LN}(1, 0.11)$, and at that location a bending moment of $\mathbf{M} = 1260\mathbf{LN}(1, 0.05)$ lbf · in. The material of which the shaft is machined is hot-rolled 1035 with $\mathbf{S}_{ut} = 86.2\mathbf{LN}(1, 0.045)$ kpsi and $\mathbf{S}_y = 56.0\mathbf{LN}(1, 0.077)$ kpsi. Estimate the reliability using a stochastic Gerber failure zone.

Solution Establish the endurance strength. From Eqs. (7–70) to (7–72) and Eq. (7–19),

$$\mathbf{S}'_e = 0.506(86.2)\mathbf{LN}(1, 0.138) = 43.6\mathbf{LN}(1, 0.138) \text{ kpsi}$$
$$\mathbf{k}_a = 2.67(86.2)^{-0.265}\mathbf{LN}(1, 0.058) = 0.820\mathbf{LN}(1, 0.058)$$
$$k_b = (1.1/0.30)^{-0.107} = 0.870$$
$$\mathbf{k}_c = \mathbf{k}_d = \mathbf{k}_f = \mathbf{LN}(1, 0)$$
$$\mathbf{S}_e = 0.820\mathbf{LN}(1, 0.058)0.870(43.6)\mathbf{LN}(1, 0.138)$$
$$\bar{S}_e = 0.820(0.870)43.6 = 31.1 \text{ kpsi}$$
$$C_{Se} = (0.058^2 + 0.138^2)^{1/2} = 0.150$$

and so $S_e = 31.1\mathbf{LN}(1, 0.150)$ kpsi.

Stress (in kpsi):

$$\boldsymbol{\sigma}_a = \frac{32\mathbf{K}_f\mathbf{M}_a}{\pi d^3} = \frac{32(1.50)\mathbf{LN}(1, 0.11)1.26\mathbf{LN}(1, 0.05)}{\pi(1.1)^3}$$

$$\bar{\sigma}_a = \frac{32(1.50)1.26}{\pi(1.1)^3} = 14.5 \text{ kpsi}$$

$$C_{\sigma a} = (0.11^2 + 0.05^2)^{1/2} = 0.121$$

$$\boldsymbol{\tau}_m = \frac{16\mathbf{K}_{fs}\mathbf{T}_m}{\pi d^3} = \frac{16(1.28)\mathbf{LN}(1, 0.11)1.36\mathbf{LN}(1, 0.05)}{\pi(1.1)^3}$$

$$\bar{\tau}_m = \frac{16(1.28)1.36}{\pi(1.1)^3} = 6.66 \text{ kpsi}$$

$$C_{\tau m} = (0.11^2 + 0.05^2)^{1/2} = 0.121$$

$$\bar{\sigma}'_a = \left(\bar{\sigma}_a^2 + 3\bar{\tau}_a^2\right)^{1/2} = [14.5^2 + 3(0)^2]^{1/2} = 14.5 \text{ kpsi}$$

$$\bar{\sigma}'_m = \left(\bar{\sigma}_m^2 + 3\bar{\tau}_m^2\right)^{1/2} = [0 + 3(6.66)^2]^{1/2} = 11.54 \text{ kpsi}$$

$$r = \frac{\bar{\sigma}'_a}{\bar{\sigma}'_m} = \frac{14.5}{11.54} = 1.26$$

Strength: From Eqs. (7–80) and (7–81),

$$\bar{S}_a = \frac{1.26^2 86.2^2}{2(31.1)}\left\{-1 + \sqrt{1 + \left[\frac{2(31.1)}{1.26(86.2)}\right]^2}\right\} = 28.9 \text{ kpsi}$$

$$C_{Sa} = \frac{(1 + 0.045)^2}{1 + 0.150}\frac{-1 + \sqrt{1 + \left[\dfrac{2(31.1)(1 + 0.15)}{1.26(86.2)(1 + 0.045)}\right]^2}}{-1 + \sqrt{1 + \left[\dfrac{2(31.1)}{1.26(86.2)}\right]^2}} - 1 = 0.134$$

Reliability: Since $\mathbf{S}_a = 28.9\mathbf{LN}(1, 0.134)$ kpsi and $\boldsymbol{\sigma}'_a = 14.5\mathbf{LN}(1, 0.121)$ kpsi, Eq. (6–58) gives

$$z = -\frac{\ln\left(\dfrac{\bar{S}_a}{\bar{\sigma}}\sqrt{\dfrac{1 + C_\sigma^2}{1 + C_{S_a}^2}}\right)}{\sqrt{\ln\left[\left(1 + C_{S_a}^2\right)\left(1 + C_\sigma^2\right)\right]}} = -\frac{\ln\left(\dfrac{28.9}{14.5}\sqrt{\dfrac{1 + 0.121^2}{1 + 0.134^2}}\right)}{\sqrt{\ln[(1 + 0.134^2)(1 + 0.121^2)]}} = -3.83$$

From Table A–10 the probability of failure is $p_f = 0.000\,065$, and the reliability is, against fatigue,

Answer

$$R = 1 - p_f = 1 - 0.000\,065 = 0.999\,935$$

The chance of first-cycle yielding is estimated by interfering $\mathbf{S}_y$ with $\boldsymbol{\sigma}'_{\max}$. The quantity $\boldsymbol{\sigma}'_{\max}$ is formed from $\boldsymbol{\sigma}'_a + \boldsymbol{\sigma}'_m$. The mean of $\boldsymbol{\sigma}'_{\max}$ is $\bar{\sigma}'_a + \bar{\sigma}'_m = 14.5 + 11.54 = 26.04$ kpsi. The coefficient of variation of the sum is 0.121, since both COVs are 0.121, thus $C_{\sigma\,\max} = 0.121$. We interfere $\mathbf{S}_y = 56\mathbf{LN}(1, 0.077)$ kpsi with

$\sigma'_{\max} = 26.04\mathbf{LN}(1, 0.121)$ kpsi. The corresponding z variable is

$$z = -\frac{\ln\left(\frac{56}{26.04}\sqrt{\frac{1+0.121^2}{1+0.077^2}}\right)}{\sqrt{\ln[(1+0.077^2)(1+0.121^2)]}} = -5.39$$

which represents, from Table A–10, a probability of failure of approximately 0.0^7358 [which represents $3.58(10^{-8})$] of first-cycle yield in the fillet.

The probability of observing a fatigue failure exceeds the probability of a yield failure, something a deterministic analysis does not foresee and in fact could lead one to expect a yield failure should a failure occur. Look at the $\sigma'_a \mathbf{S}_a$ interference and the $\sigma'_{\max}\mathbf{S}_y$ interference and examine the z expressions. These control the relative probabilities. A deterministic analysis is oblivious to this and can mislead. Check your statistics text for events that are not mutually exclusive, but are independent, to quantify the probability of failure:

$$\begin{aligned} p_f &= p(\text{yield}) + p(\text{fatigue}) - p(\text{yield and fatigue}) \\ &= p(\text{yield}) + p(\text{fatigue}) - p(\text{yield})\,p(\text{fatigue}) \\ &= 0.358(10^{-7}) + 0.65(10^{-4}) - 0.358(10^{-7})0.65(10^{-4}) = 0.650(10^{-4}) \\ R &= 1 - 0.650(10^{-4}) = 0.999\,935 \end{aligned}$$

against either or both modes of failure.

Examine Fig. 7–38, which depicts the results of Ex. 7–16. The problem distribution of $\mathbf{S}_e$ was compounded of historical experience with $\mathbf{S}'_e$ and the uncertainty manifestations due to features requiring Marin considerations. The Gerber "failure zone" displays

Figure 7–38

Designer's fatigue diagram for Ex. 7–21.

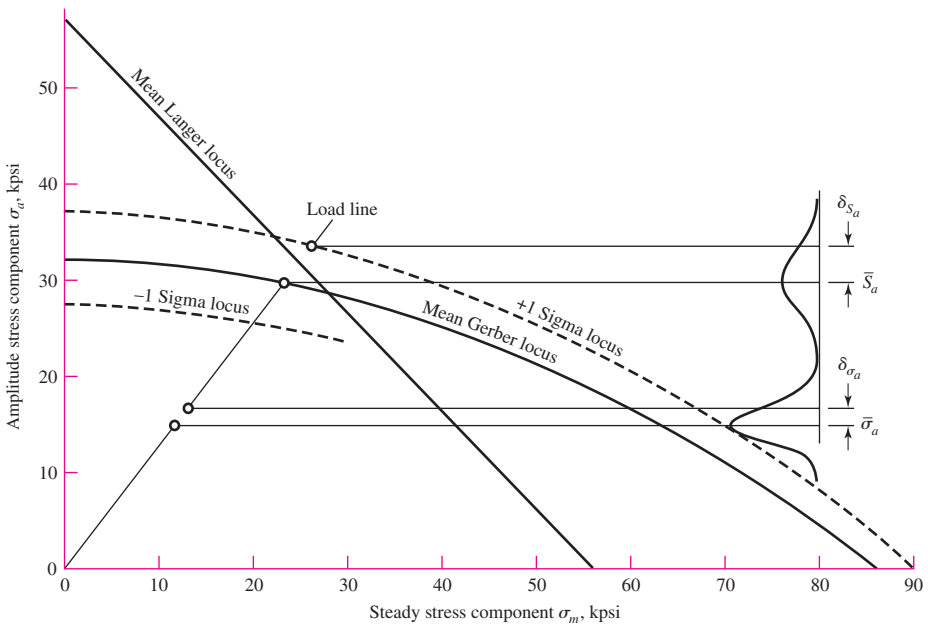

this. The interference with load-induced stress predicts the risk of failure. If additional information is known (R. R. Moore testing, with or without Marin features), the stochastic Gerber can accommodate to the information. Usually, the accommodation to additional test information is movement and contraction of the failure zone. In its own way the stochastic failure model accomplishes more precisely what the deterministic models and conservative postures intend. Additionally, stochastic models can estimate the probability of failure, something a deterministic approach cannot address.

The Design Factor in Fatigue

The designer, in envisioning how to execute the geometry of a part subject to the imposed constraints, can begin making a priori decisions without realizing the impact on the design task. Now is the time to note how these things are related to the reliability goal.

The mean value of the design factor is given by Eq. (6–59),

$$\bar{n} = \exp\left[-z\sqrt{\ln\left(1+C_n^2\right)} + \ln\sqrt{1+C_n^2}\right] \doteq \exp[C_n(-z+C_n/2)] \qquad (6\text{–}59)$$

in which, from Table 2–6 for the quotient $\mathbf{n} = \mathbf{S}/\boldsymbol{\sigma}$,

$$C_n = \sqrt{\frac{C_S^2 + C_\sigma^2}{1+C_\sigma^2}}$$

where C_S is the COV of the significant strength and C_σ is the COV of the significant stress at the critical location. Note that $\bar{n}$ is a function of the reliability goal (through z) and the COVs of the strength and stress. There are no means present, just measures of variability. The nature of C_S in a fatigue situation may be C_{Se} for fully reversed loading, or C_{Sa} otherwise. Also, experience shows $C_{Se} > C_{Sa} > C_{Sut}$, so C_{Se} can be used as a conservative estimate of C_{Sa}. If the loading is bending or axial, the form of σ_a' might be

$$\boldsymbol{\sigma}_a' = \mathbf{K}_f \frac{\mathbf{M}_a c}{I} \qquad \text{or} \qquad \boldsymbol{\sigma}_a' = \mathbf{K}_f \frac{\mathbf{F}}{A}$$

respectively. This makes the COV of $\boldsymbol{\sigma}_a'$, namely $C_{\sigma_a'}$, expressible as

$$C_{\sigma_a'} = \left(C_{Kf}^2 + C_F^2\right)^{1/2}$$

again a function of variabilities. The COV of $\mathbf{S}_e$, namely C_{Se}, is

$$C_{Se} = \left(C_{ka}^2 + C_{kc}^2 + C_{kd}^2 + C_{kf}^2 + C_{Se'}^2\right)^{1/2}$$

again, a function of variabilities. An example will be useful.

EXAMPLE 7–22 A strap to be made from a cold-drawn steel strip workpiece is to carry a fully reversed axial load $\mathbf{F} = \mathbf{LN}(1000, 120)$ lbf as shown in Fig. 7–39. Consideration of adjacent parts established the geometry as shown in the figure, except for the thickness t. Make a decision as to the magnitude of the design factor if the reliability goal is to be 0.999 95, then make a decision as to the workpiece thickness t.

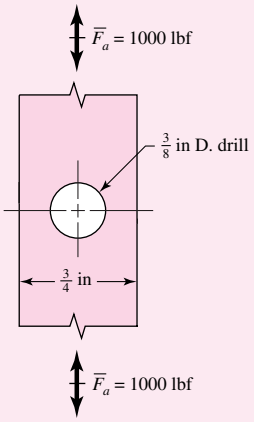

Figure 7–39

A strap with a thickness t is subjected to a fully reversed axial load of 1000 lbf. Example 7–22 considers the thickness necessary to attain a reliability of 0.999 95 against a fatigue failure.

Solution Let us take each a priori decision and note the consequence:

A Priori Decision	Consequence
Use 1018 CD steel	$\bar{S}_{ut} = 87.6$ kpsi, $C_{Sut} = 0.0655$
Function:	
Carry axial load	$C_F = 0.12$, $C_{kc} = 0.125$
$R \geq 0.999\,95$	$z = -3.891$
Machined surfaces	$C_{ka} = 0.058$
Hole critical	$C_{Kf} = 0.10$, $C_{\sigma'_a} = (0.10^2 + 0.12^2)^{1/2} = 0.156$
Ambient temperature	$C_{kd} = 0$
Correlation method	$C_{S'_e} = 0.138$
Hole drilled	$C_{Se} = (0.058^2 + 0.125^2 + 0.138^2)^{1/2} = 0.195$
	$C_n = \sqrt{\dfrac{C_{Se}^2 + C_{\sigma'_a}^2}{1 + C_{\sigma'_a}^2}} = \sqrt{\dfrac{0.195^2 + 0.156^2}{1 + 0.156^2}} = 0.2467$
	$\bar{n} = \exp\left[-(-3.891)\sqrt{\ln(1 + 0.2467^2)} + \ln\sqrt{1 + 0.2467^2}\right]$ $= 2.65$

These eight a priori decisions have quantified the mean design factor as $\bar{n} = 2.65$. Proceeding deterministically hereafter we write

$$\sigma'_a = \frac{\bar{S}_e}{\bar{n}} = \bar{K}_f \frac{\bar{F}}{(w - d)t}$$

from which

$$t = \frac{\bar{K}_f \bar{n} \bar{F}}{(w - d)\bar{S}_e}$$

To evaluate the preceding equation we need $\bar{S}_e$ and $\bar{K}_f$. The Marin factors are

$$\mathbf{k}_a = 2.67\bar{S}_{ut}^{-0.265}\mathbf{LN}(1, 0.058) = 2.67(87.6)^{-0.265}\mathbf{LN}(1, 0.058)$$
$$\bar{k}_a = 0.816$$
$$k_b = 1 \text{ (see } \mathbf{k}_c)$$
$$\mathbf{k}_c = 1.23\bar{S}_{ut}^{-0.078}\mathbf{LN}(1, 0.125) = 0.868\mathbf{LN}(1, 0.125)$$
$$\bar{k}_c = 0.868$$
$$\bar{k}_d = \bar{k}_f = 1$$

and the endurance strength is

$$\bar{S}_e = 0.816(0.868)(1)(1)(1)0.506(87.6) = 31.4 \text{ kpsi}$$

The hole governs. From Table A–15–1 we find $d/w = 0.50$, therefore $K_t = 2.18$. From Table 7–7 $\sqrt{a} = 5/\bar{S}_{ut} = 5/87.6 = 0.057$, $r = 0.375$ in. From Eq. (7–34) the fatigue stress concentration factor is

$$\bar{K}_f = \frac{2.18}{1 + \dfrac{2}{\sqrt{0.375}}\dfrac{2.18 - 1}{2.18}0.057} = 1.98$$

The thickness t can now be determined from $S_e/\bar{n} = \bar{K}_f \bar{F}/A$,

$$t \geq \frac{\bar{K}_f \bar{n} \bar{F}}{(w-d)S_e} = \frac{1.98(2.65)1000}{(0.75-0.375)31\,400} = 0.446 \text{ in}$$

Use $\frac{1}{2}$-in-thick strap for the workpiece. The $\frac{1}{2}$-in thickness attains and, in the rounding to available nominal size, exceeds the reliability goal.

The example demonstrates that, for a given reliability goal, the fatigue design factor that facilitates its attainment is decided by the variabilities of the situation. Furthermore, the necessary design factor is not a constant independent of the way the concept unfolds. Rather, it is a function of a number of seemingly unrelated a priori decisions that are made in giving definition to the concept. The involvement of stochastic methodology can be limited to defining the necessary design factor. In particular, in the example, the design factor is not a function of the design variable t; rather, t follows from the design factor.

PROBLEMS

Problems 7–1 to 7–31 are to be solved by deterministic methods. Problems 7–32 to 7–38 are to be solved by stochastic methods. Problems 7–39 to 7–46 are computer problems.

Deterministic Problems

ANALYSIS **7–1** A $\frac{3}{16}$-in drill rod was heat-treated and ground. The measured hardness was found to be 490 Brinell. Estimate the endurance strength if the rod is used in rotating bending.

ANALYSIS **7–2** Estimate S'_e for the following materials:
(*a*) AISI 1020 CD steel.
(*b*) AISI 1080 HR steel.
(*c*) 2024 T3 aluminum.
(*d*) AISI 4340 steel heat-treated to a tensile strength of 250 kpsi.

ANALYSIS **7–3** Estimate the fatigue strength of a rotating-beam specimen made of AISI 1020 hot-rolled steel corresponding to a life of 12.5 kilocycles of stress reversal. Also, estimate the life of the specimen corresponding to a stress amplitude of 36 kpsi. The known properties are $S_{ut} = 66.2$ kpsi, $\sigma_0 = 115$ kpsi, $m = 0.22$, and $\varepsilon_f = 0.90$.

ANALYSIS **7–4** Derive Eq. (7–16). For the specimen of Prob. 7–3, estimate the strength corresponding to 500 cycles.

ANALYSIS **7–5** For the interval $10^3 \leq N \leq 10^6$ cycles, develop an expression for the fatigue strength $(S'_f)_{ax}$ for the polished specimens of 4130 used to obtain Fig. 7–10. The ultimate strength is $S_{ut} = 125$ kpsi and the endurance limit is $(S'_e)_{ax} = 49$ kpsi.

7–6 Estimate the endurance strength of a 32-mm-diameter rod of AISI 1035 steel having a machined finish and heat-treated to a tensile strength of 710 MPa.

ANALYSIS **7–7** Two steels are being considered for manufacture of as-forged connecting rods. One is AISI 4340 Cr-Mo-Ni steel capable of being heat-treated to a tensile strength of 260 kpsi. The other is a plain carbon steel AISI 1040 with an attainable S_{ut} of 113 kpsi. If each rod is to have a size giving an equivalent diameter d_e of 0.75 in, is there any advantage to using the alloy steel for this fatigue application?

ANALYSIS **7–8** A solid round bar, 25 mm in diameter, has a groove 2.5-mm deep with a 2.5-mm radius machined into it. The bar is made of AISI 1018 CD steel and is subjected to a purely reversing torque of 200 N · m. For the *S-N* curve of this material, let $f = 0.9$.

(*a*) Estimate the number of cycles to failure.
(*b*) If the bar is also placed in an environment with a temperature of 450°C, estimate the number of cycles to failure.

ANALYSIS **7–9** A solid square rod is cantilevered at one end. The rod is 0.8 m long and supports a completely reversing transverse load at the other end of ±1 kN. The material is AISI 1045 hot-rolled steel. If the rod must support this load for 10^4 cycles with a factor of safety of 1.5, what dimension should the square cross section have? Neglect any stress concentrations at the support end and assume that $f = 0.9$.

ANALYSIS **7–10** A rectangular bar is cut from an AISI 1018 cold-drawn steel flat. The bar is 60 mm wide by 10 mm thick and has a 12-mm hole drilled through the center as depicted in Table A–15–1. The bar is concentrically loaded in push-pull fatigue by axial forces F_a, uniformly distributed across the width. Using a design factor of $n_d = 1.8$, estimate the largest force F_a that can be applied ignoring column action.

DESIGN **7–11** Bearing reactions R_1 and R_2 are exerted on the shaft shown in the figure, which rotates at 1150 rev/min and supports a 10-kip bending force. Use a 1095 HR steel. Specify a diameter d using a design factor of $n_d = 1.6$ for a life of 3 min. The surfaces are machined.

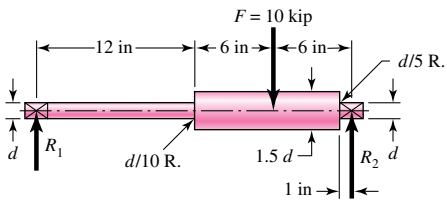

Problem 7–11

ANALYSIS **7–12** A bar of steel has the minimum properties $S_e = 276$ MPa, $S_y = 413$ MPa, and $S_{ut} = 551$ MPa. The bar is subjected to a steady torsional stress of 103 MPa and an alternating bending stress of 172 MPa. Find the factor of safety guarding against a static failure, and either the factor of safety guarding against a fatigue failure or the expected life of the part. For the fatigue analysis use:
(*a*) Modified Goodman criterion.
(*b*) Gerber criterion.
(*c*) ASME-elliptic criterion.

ANALYSIS **7–13** Repeat Prob. 7–12 but with a steady torsional stress of 138 MPa and an alternating bending stress of 69 MPa.

ANALYSIS **7–14** Repeat Prob. 7–12 but with a steady torsional stress of 103 MPa, an alternating torsional stress of 69 MPa, and an alternating bending stress of 83 MPa.

ANALYSIS **7–15** Repeat Prob. 7–12 but with an alternating torsional stress of 207 MPa.

ANALYSIS **7–16** Repeat Prob. 7–12 but with an alternating torsional stress of 103 MPa and a steady bending stress of 103 MPa.

ANALYSIS **7–17** The cold-drawn AISI 1018 steel bar shown in the figure is subjected to a tensile load fluctuating between 800 and 3000 lbf. Estimate the factors of safety n_y and n_f using (*a*) a Gerber fatigue failure criterion as part of the designer's fatigue diagram, and (*b*) a ASME-elliptic fatigue failure criterion as part of the designer's fatigue diagram.

7–18 Repeat Prob. 7–17, with the load fluctuating between −800 and 3000 lbf. Assume no buckling.

ANALYSIS **7–19** Repeat Prob. 7–17, with the load fluctuating between 800 and −3000 lbf. Assume no buckling.

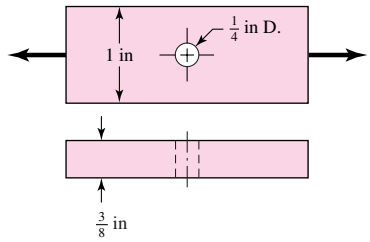

Problem 7–17

ANALYSIS **7–20** The figure shows a formed round-wire cantilever spring subjected to a varying force. The hardness tests made on 25 springs gave a minimum hardness of 380 Brinell. It is apparent from the mounting details that there is no stress concentration. A visual inspection of the springs indicates that the surface finish corresponds closely to a hot-rolled finish. What number of applications is likely to cause failure? Solve using:

(*a*) Modified Goodman criterion.

(*b*) Gerber criterion.

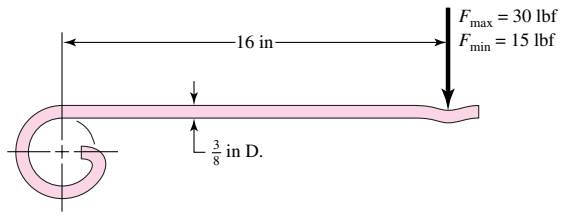

Problem 7–20

ANALYSIS **7–21** The figure is a drawing of a 3- by 18-mm latching spring. A preload is obtained during assembly by shimming under the bolts to obtain an estimated initial deflection of 2 mm. The latching operation itself requires an additional deflection of exactly 4 mm. The material is ground high-carbon steel, bent then hardened and tempered to a minimum hardness of 490 Bhn. The radius of the bend is 3 mm. Estimate the yield strength to be 90 percent of the ultimate strength.

(*a*) Find the maximum and minimum latching forces.

(*b*) Is it likely the spring will fail in fatigue? Use the Gerber criterion.

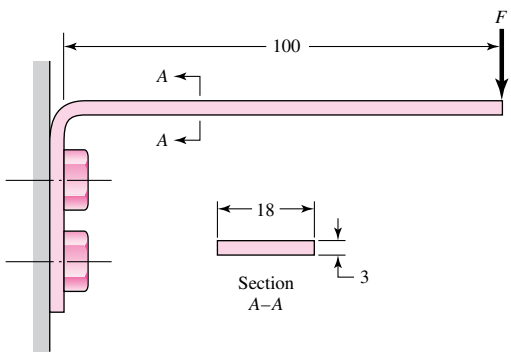

Problem 7–21
Dimensions in millimeters

ANALYSIS **7–22** Repeat Prob. 21, part *b*, using the modified Goodman criterion.

ANALYSIS **7–23** The figure shows the free-body diagram of a connecting-link portion having stress concentration at three sections. The dimensions are $r = 0.25$ in, $d = 0.75$ in, $h = 0.50$ in, $w_1 = 3.75$ in, and $w_2 = 2.5$ in. The forces F fluctuate between a tension of 4 kip and a compression of 16 kip. Neglect column action and find the least factor of safety if the material is cold-drawn AISI 1018 steel.

Problem 7–23

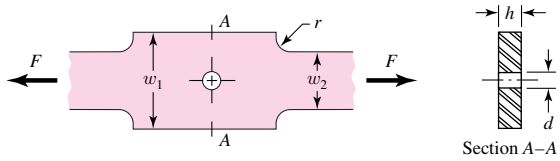

ANALYSIS **7–24** The torsional coupling in the figure is composed of a curved beam of square cross section that is welded to an input shaft and output plate. A torque is applied to the shaft and cycles from zero to T. The cross section of the beam has dimensions of 5 by 5 mm, and the centroidal axis of the beam describes a curve of the form $r = 10\,\theta/\pi$, where r and θ are in mm and radians, respectively ($2\pi \le \theta \le 6\pi$). The curved beam has a machined surface with yield and ultimate strength values of 420 and 770 MPa, respectively.

(a) Determine the maximum allowable value of T such that the coupling will have an infinite life with a factor of safety, $n = 3$, using the modified Goodman criterion.

(b) Repeat part (a) using the Gerber criterion.

(c) Using T found in part (b), determine the factor of safety guarding against yield.

Problem 7–24

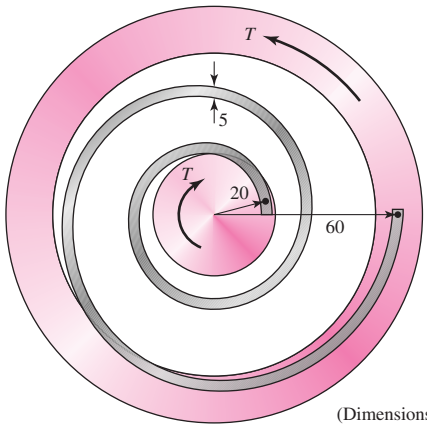

(Dimensions in mm)

ANALYSIS **7–25** Repeat Prob. 7–24 ignoring curvature effects on the bending stress.

ANALYSIS **7–26** In the figure shown, shaft A, made of AISI 1010 hot-rolled steel, is welded to a fixed support and is subjected to loading by equal and opposite forces F via shaft B. A theoretical stress concentration K_{ts} of 1.6 is induced by the 3-mm fillet. The length of shaft A from the fixed support to the connection at shaft B is 1 m. The load F cycles from 0.5 to 2 kN.

Problem 7–26

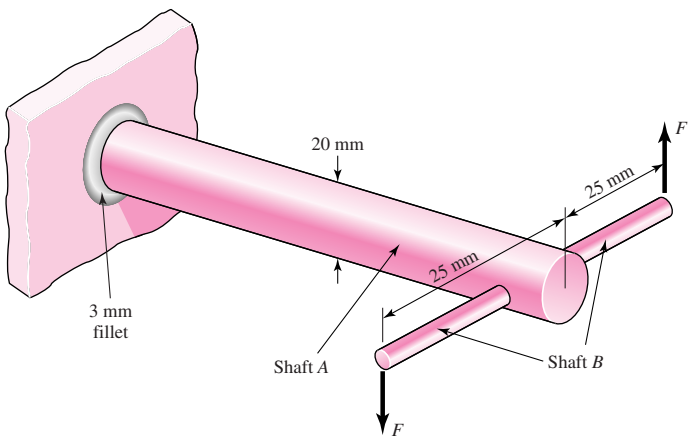

(*a*) For shaft A, find the factor of safety for infinite life using the modified Goodman fatigue failure criterion.

(*b*) Repeat part (*a*) using the Gerber fatigue failure criterion.

ANALYSIS **7–27** A schematic of a clutch-testing machine is shown. The steel shaft rotates at a constant speed ω. An axial load is applied to the shaft and is cycled from zero to P. The torque T induced by the clutch face onto the shaft is given by

$$T = \frac{f P(D + d)}{4}$$

where D and d are defined in the figure and f is the coefficient of friction of the clutch face. The shaft is machined with $S_y = 800$ MPa and $S_{ut} = 1000$ MPa. The theoretical stress concentration factors for the fillet are 3.0 and 1.8 for the axial and torsional loading, respectively.

(*a*) Assume the load variation P is synchronous with shaft rotation. With $f = 0.3$, find the maximum allowable load P such that the shaft will survive a minimum of 10^6 cycles with a factor of safety of 3. Use the modified Goodman criterion. Determine the corresponding factor of safety guarding against yielding.

(*b*) Suppose the shaft is not rotating, but the load P is cycled as shown. With $f = 0.3$, find the maximum allowable load P so that the shaft will survive a minimum of 10^6 cycles with a factor of safety of 3. Use the modified Goodman criterion. Determine the corresponding factor of safety guarding against yielding.

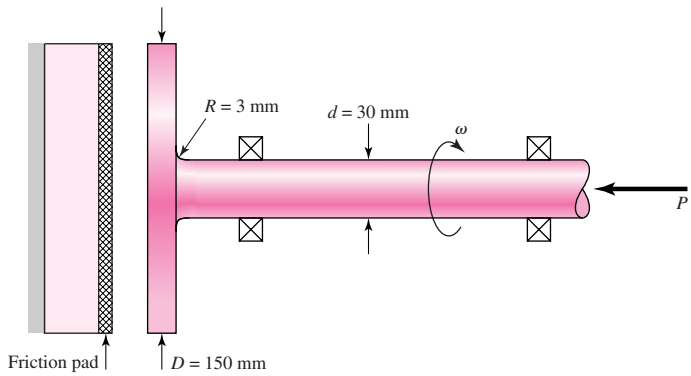

Problem 7–27

ANALYSIS **7–28** For the clutch of Prob. 7–27, the external load P is cycled between 20 kN and 80 kN. Assuming that the shaft is rotating synchronous with the external load cycle, estimate the number of cycles to failure. Use the modified Goodman fatigue failure criteria.

ANALYSIS **7–29** A flat leaf spring has fluctuating stress of $\sigma_{\max} = 420$ MPa and $\sigma_{\min} = 140$ MPa applied for 5 (10^4) cycles. If the load changes to $\sigma_{\max} = 350$ MPa and $\sigma_{\min} = -200$ MPa, how many cycles should the spring survive? The material is AISI 1040 CD and has a fully corrected endurance strength of $S_e = 200$ MPa. Assume that $f = 0.9$.

(*a*) Use Miner's method.

(*b*) Use Manson's method.

ANALYSIS **7–30** A machine part will be cycled at ±48 kpsi for 4 (10^3) cycles. Then the loading will be changed to ±38 kpsi for 6 (10^4) cycles. Finally, the load will be changed to ±32 kpsi. How many cycles of operation can be expected at this stress level? For the part, $S_{ut} = 76$ kpsi, $f = 0.9$, and has a fully corrected endurance strength of $S_e = 30$ kpsi.

(*a*) Use Miner's method.

(*b*) Use Manson's method.

ANALYSIS **7–31** A rotating-beam specimen with an endurance limit of 50 kpsi and an ultimate strength of 100 kpsi is cycled 20 percent of the time at 70 kpsi, 50 percent at 55 kpsi, and 30 percent at 40 kpsi. Let $f = 0.9$ and estimate the number of cycles to failure.

Stochastic Problems

ANALYSIS **7–32** Solve Prob. 7–1 if the hardness of production pieces is found to be $\mathbf{H}_b = 495\mathbf{LN}(1, 0.03)$.

DESIGN **7–33** The situation is similar to that of Prob. 7–10 wherein the imposed completely reversed axial load $F_a = 15\mathbf{LN}(1, 0.20)$ kN is to be carried by the link with a thickness to be specified by you, the designer. Use the 1018 cold-drawn steel of Prob. 7–10 with $\mathbf{S}_{ut} = 440\mathbf{LN}(1, 0.30)$ MPa and $\mathbf{S}_{yt} = 370\mathbf{LN}(1, 0.061)$. The reliability goal must exceed 0.999. Using the correlation method, specify the thickness t.

ANALYSIS **7–34** A solid round steel bar is machined to a diameter of 1.25 in. A groove $\frac{1}{8}$ in deep with a radius of $\frac{1}{8}$ in is cut into the bar. The material has a mean tensile strength of 110 kpsi. A completely reversed bending moment $M = 1400$ lbf · in is applied. Estimate the reliability. The size factor should be based on the gross diameter. The bar rotates.

7–35 Repeat Prob. 7–34, with a completely reversed torsional moment of $T = 1400$ lbf · in applied.

ANALYSIS **7–36** A $1\frac{1}{4}$-in-diameter hot-rolled steel bar has a $\frac{1}{8}$-in diameter hole drilled transversely through it. The bar is nonrotating and is subject to a completely reversed bending moment of $M = 1600$ lbf · in in the same plane as the axis of the transverse hole. The material has a mean tensile strength of 58 kpsi. Estimate the reliability. The size factor should be based on the gross size. Use Table A–16 for K_t.

7–37 Repeat Prob. 7–36, with the bar subject to a completely reversed torsional moment of 2400 lbf · in.

DESIGN **7–38** The plan view of a link is the same as in Prob. 7–23; however, the forces F are completely reversed, the reliability goal is 0.998, and the material properties are $\mathbf{S}_{ut} = 64\mathbf{LN}(1, 0.045)$ kpsi and $\mathbf{S}_y = 54\mathbf{LN}(1, 0.077)$ kpsi. Treat F_a as deterministic, and specify the thickness h.

Computer Problems

ANALYSIS **7–39** A $\frac{1}{4}$ by $1\frac{1}{2}$-in steel bar has a $\frac{3}{4}$-in drilled hole located in the center, much as is shown in Table A–15–1. The bar is subjected to a completely reversed axial load with a deterministic load of 1200 lbf. The material has a mean ultimate tensile strength of $\bar{S}_{ut} = 80$ kpsi.

(a) Estimate the reliability.

(b) Conduct a computer simulation to confirm your answer to part a.

DESIGN **7–40** From your experience with Prob. 7–39 and Ex. 7–20, you observed that for completely reversed axial and bending fatigue, it is possible to

- Observe the COVs associated with a priori design considerations.
- Note the reliability goal.
- Find the mean design factor $\bar{n}_d$ which will permit making a geometric design decision that will attain the goal using deterministic methods in conjunction with $\bar{n}_d$.

Formulate an interactive computer program that will enable the user to find $\bar{n}_d$. While the material properties $\mathbf{S}_{ut}$, $\mathbf{S}_y$, and the load COV must be input by the user, all of the COVs associated with $\boldsymbol{\phi}_{0.30}$, $\mathbf{k}_a$, $\mathbf{k}_c$, $\mathbf{k}_d$, and $\mathbf{K}_f$ can be internal, and answers to questions will allow C_σ and C_S, as well as C_n and $\bar{n}_d$, to be calculated. Later you can add improvements. Test your program with problems you have already solved.

7–41 When using the Gerber fatigue failure criterion in a stochastic problem, Eqs. (7–80) and (7–81) are useful. They are also computationally complicated. It is helpful to have a computer subroutine or procedure that performs these calculations. When writing an executive program, and it is appropriate to find S_a and C_{Sa}, a simple call to the subroutine does this with a minimum of effort. Also, once the subroutine is tested, it is always ready to perform. Write and test such a program.

7–42 Repeat Problem. 7–41 for the ASME-elliptic fatigue failure locus, implementing Eqs. (7–83) and (7–84).

7–43 Repeat Prob. 7–41 for the Smith-Dolan fatigue failure locus, implementing Eqs. (7–87) and (7–88).

7–44 Write and test computer subroutines or procedures that will implement
(*a*) Table 7–4, returning a, b, C, and $\bar{k}_a$.
(*b*) Equation (7–19) using Table 7–5, returning k_b.
(*c*) Table 7–14, returning α, β, C, and $\bar{k}_c$.
(*d*) Equations (7–26) and (7–75), returning $\bar{k}_d$ and C_{kd}.

7–45 Write and test a computer subroutine or procedure that implements Eqs. (7–76) and (7–77), returning $\bar{q}$, $\hat{\sigma}_q$, and C_q.

7–46 Write and test a computer subroutine or procedure that implements Eq. (7–35) and Tables 7–8 and 7–18, returning $\sqrt{a}$, C_{Kf}, and $\bar{K}_f$.

Summary of Parts 1 and 2

The first recommendation is to reread Chap. 1. With the experience you have gathered so far, you will gain from doing it. With the meat you have added to the bare bones of the introductory chapter, it will have a greater meaning. In Sec. 1–3, there are over two dozen design considerations. We have addressed item 2 in detail, the question of the strength/stress relationship in a loss-of-function for ductile and brittle materials, for steady and fatigue loading, and for finite and indefinite life. We have also started on item 7, reliability, as it applies to stress/strength relationships. In investigating the stress/strength relations, the reader should now be prepared to

- Identify the critical location(s), either by inspection, or, if not obvious, by analyzing the several candidates, and identifying the "worst case."
- Identify the significant strength at that location.
- Identify the significant stress at that location.
- Address the question of whether the disparity between stress and strength is sufficient such that function will be preserved in the face of service loading.

This preparation took a long time because an extensive set of ideas and insights had to be identified in and among your prerequisite studies, and placed in a useful context.

The question of stiffness, distortion, and deflection, item 3, and their influence on loss of function has also been addressed. The reader should now be prepared to identify

- The level of distortion that risks loss of function.
- The location(s) at which loss-of-function due to distortion is possible.
- The level of distortion present.
- Whether the difference is sufficient.

Some other considerations will be touched on in Part 3, and those just noted will be further developed for the application at hand. As we proceed into Part 3 our focus becomes more specific as we consider particular machine elements and their applications.

For now, the reader should feel comfortable with a kit of tools from which an adequacy assessment is devised. Skill 1 will take on additional substance as applications unfold. In addition to focus on individual elements, design/synthesis ideas will appear more often, and skill 2 will take form and grow.